Theses and Dissertations--Pharmacy

College of Pharmacy

2013

PRECLINICAL AND CLINICAL DEVELOPMENT OF THE LIPOPHILIC CAMPTOTHECIN ANALOGUE AR-67

Eleftheria Tsakalozou
University of Kentucky, etsakal@gmail.com

Right click to open a feedback form in a new tab to let us know how this document benefits you.

PRECLINICAL AND CLINICAL DEVELOPMENT OF THE LIPOPHILIC
CAMPTOTHECIN ANALOGUE AR-67

DISSERTATION

A dissertation submitted in partial fulfillment of the
requirements for the degree of Doctor of Philosophy in the
College of Pharmacy at the University of Kentucky

By

Eleftheria Tsakalozou

Lexington, Kentucky

Co-Directors: Dr. Markos Leggas, Associate Professor of Pharmaceutical Sciences
and   Dr. Val Adams, Associate Professor of Pharmacy Practice

Lexington, Kentucky

2013

Copyright © Eleftheria Tsakalozou 2013

ABSTRACT OF DISSERTATION

PRECLINICAL AND CLINICAL DEVELOPMENT OF THE LIPOPHILIC
CAMPTOTHECIN ANALOGUE AR-67

AR-67 is a lipophilic third generation camptothecin analogue, currently under early stage clinical trials. It acts by targeting Topoisomerase 1 (Top1), a nuclear enzyme essential for DNA replication and transcription and is present in two forms, the pharmacologically active lipophilic lactone and the charged carboxylate. In oncology patients participating in a phase I clinical trial, AR-67 lactone was the predominant species in plasma. Similarly to other camptothecins, the identified dose-limiting toxicities for AR-67 were neutropenia, thrombocytopenia and fatigue. In addition, *in vitro* metabolism studies indicated AR-67 lactone as a substrate for CYP3A4/5 as well as the UGT1A7 and UGT1A8 enzymes localizing in the liver and the gut.

Numerous studies have demonstrated the over-expression of transporters in certain tumor types. Here, the effect of interactions between AR-67 and efflux or uptake transporters on the antitumor efficacy of AR-67 *in vitro* was studied. We showed that BCRP and MDR1 overexpression confers resistance to AR-67.

Moreover, we demonstrated the therapeutic superiority of protracted dosing over more intense dosing regimens of AR-67 using xenografts models. Our studies indicated the schedule-dependent expression of Top1 and the preferential partitioning of AR-67 in the tumor tissue. We reason that these are factors that need to be taken into consideration when designing dosing schedules aiming to maximize efficacy.

As most cytotoxic drugs, AR-67 has a narrow therapeutic window. Thus, it is essential to identify the variables influencing exposure to this camptothecin analogue. A thorough compartmental pharmacokinetic analysis was performed on the patient data obtained in a phase 1 clinical trial on AR-67. Moreover, sources of intersubject variability associated

with obtaining pharmacokinetic parameter estimates were identified and a population covariate pharmacokinetic model was developed.

In conclusion, the drug development of AR-67 is a work in process. Findings presented above provide an insight on the factors contributing to its efficacy and toxicity when given to cancer patients.

KEYWORDS: AR-67, Camptothecin, Transporter, Dosing Schedule, Population Pharmacokinetics

<div style="text-align:right;">

Eleftheria Tsakalozou

Student's Signature

05/10/13

Date

</div>

PRECLINICAL AND CLINICAL DEVELOPMENT OF THE LIPOPHILIC

CAMPTOTHECIN ANALOGUE AR-67

By

Eleftheria Tsakalozou

Markos Leggas
Director of Dissertation

Val Adams
Co-Director of Dissertation

Jim Pauly
Director of Graduate Studies

05/10/13
Date

ACKNOWLEDGMENTS

First and foremost, I would like to thank my family, my parents and my brother, for their love and continuous support.

I would like to extend thanks to my advisor, Dr. Mark Leggas, for his guidance and support while I was pursuing my doctoral degree. I would like to express my gratitude for being assigned extremely diverse and, at the same time, interesting projects that allowed me develop as a scientist. Undoubtedly, the difficulties and challenges faced during the last six year have turned me into a more mature individual. I value the support and guidance offered by Dr. Susanne Arnold and I am grateful to her for essential contributions on the clinical aspect of the AR-67 project. I would also like to thank my Advisory Committee Members, Drs. Patrick McNamara, Peter Wedlund and Val Adams for their helpful comments and guidance. I value the contribution of Dr. John McCarthy who agreed in serving as my Outside Examiner. Finally, I would like to acknowledge the collaboration with Dr. Younsoo Bae.

Drs. Horn and Goswami have played an essential role in introducing me to new laboratory techniques, help me think critically and conduct high quality research. I will always appreciate their achievements as research scientists and their ethical integrity.

I would also like to thank from the bottom of my heart all the Leggas and McNamara Lab members, Dr. Kuei-Ling Kuo, Dr. Tamer Ahmed, Dr. Eyob Adane, Marta Milewska, Yali Liang, Dr. Lipeng Wang, Dr. Zhiwei Liu and Dr. Dominique Talbert, for their support, help and guidance. Most importantly, I value their friendship.

I am grateful to Catina RossoII, the Graduate Program Student Affairs Coordinator at UK College of Pharmacy, who has played a pivotal role in supporting and facilitating administrative issues throughout the last six years.

Finally, my deepest thanks go to Dr. Maria Vertzoni for mentoring me during my first steps as a research scientist at the University of Athens in Greece and for encouraging me to pursue a doctoral degree. I am very fortunate to have met her and feel honored to call her my friend.

TABLE OF CONTENTS

LIST OF TABLES

LIST OF FIGURES

1. Chapter 1: Introduction.

1.1 Camptothecins.

20(S)-Camptothecin (CPT) (Figure 1-1, A) is the first alkaloid, among a number of natural alkaloids, extracted in the 1960s from the stem wood of the tree Camptotheca acuminate, Nyssaceae that showed potent anticancer activity [1, 2]. Since then, semi-synthetic camptothecin analogues were synthesized and tested in a variety of solid tumors and leukemias *in vitro* and *in vivo* producing encouraging results. The identification of the enzyme target of camptothecins, Topoisomerase 1 (Top1), the elucidation of the mechanism of action and the systematic study of the physicochemical properties of camptothecins contributed significantly to the successful development of camptothecin analogues with promising response profiles in the clinic.
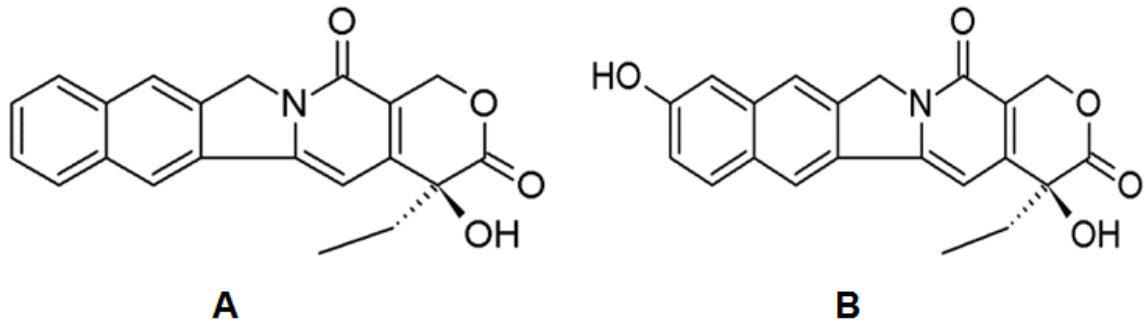
Figure 1-1. Alkaloids isolated from the Camptotheca acuminate, Nyssaceae.

Chemical structures of 20(S)-Camptothecin (CPT) (A) and 10-hydroxycamptothecin (B).

1.2 Mechanism of Action.

The increased susceptibility of S-phase specific cells to camptothecin exposure is attributed to the camptothecin mechanism of action. Studies [3-5] have shown that camptothecins target the nuclear enzyme Top1 which is responsible for the relaxation of supercoiled DNA during replication and transcription. Camptothecins stabilize the reversible complex that is formed between the DNA and Top1 by mimicking a DNA base pair and intercalating into the DNA. When the CPT-DNA-Top1 complex collides with the replication fork (replication) or RNA polymerase (transcription), the DNA religation process cannot be completed and double strand DNA breaks are formed [6, 7]. DNA repair mechanisms cannot balance the extensive drug-induced DNA damage and cells undergo apoptosis [8].

1.3 Resistance Mechanisms to Camptothecin Treatment.

Cancerous cells develop resistance to camptothecin analogues typically by decreasing their Top1 protein content [9, 10]. The nuclear enzyme is being sequestered from the nucleus and undergoes an ubiquitin-mediated degradation in the cytoplasm [11]. Interestingly, the Top1 protein levels return to basal levels in surviving cells when the drug is removed [9, 10]. Point mutations in the enzyme that prevent Top1 from interacting with the anticancer agent have resulted in resistance to CPT as well [12-14]. Finally, modulating the expression of transporters that are facilitating the intake or efflux of camptothecin analogues could lead to drug resistance [15].

1.4 Lactone-Carboxylate Interconversion.

Camptothecins are unique among anticancer agents for their physicochemical properties. They are typically present in biological matrices in two forms, the lipophilic lactone and the negatively charged carboxylate (Figure 1-2). The lactone form gives rise to the carboxylate by reversible hydrolysis of the α-hydroxy-δ-lactone pharmacophore

3

(ring E). The two major factors that have an impact on the equilibrium between lactone and carboxylate are protein binding and pH. Studies have indicated that albumin shows a higher affinity for the carboxylate than the lactone form which led to extensive lactone conversion to carboxylate [16, 17]. Additionally, acidic pH conditions were found to favor the formation of lactone by lactonization of the E-ring [18, 19].
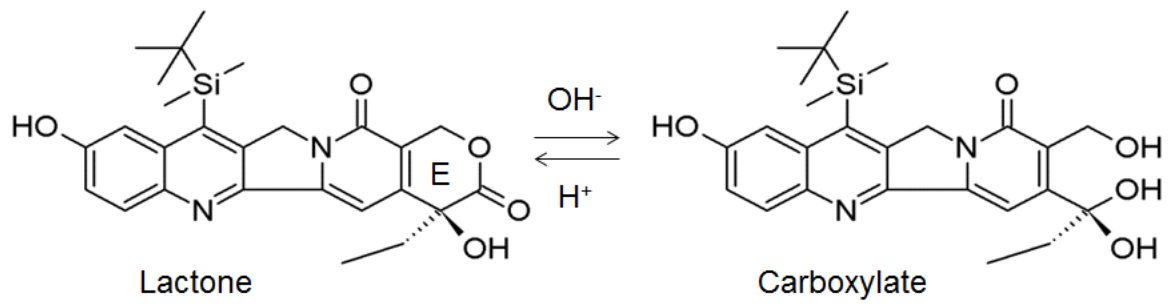
Figure 1-2. pH-dependent lactone-carboxylate interconversion.

1.5 Structure-Activity Relationships.

Camptothecin basic structure involves a 5-membered ring structure with a chiral center on position 20, presented on Figure 1-3. Structure-activity relationships have underlined the importance of the 20(S)-hydroxyl group for interaction with the Top1 active site and more specifically for the formation of a hydrogen bond with the amino acid Asp533 [3, 5, 7]. Contrary, the 20(R)-hydroxyl stereoisomer was found inactive while attempts to substitute the hydroxyl group with hydrogen or ethyl resulted in inactive analogues [5, 20]. Moreover, the planarity of the 5-membered ring system and the pyridine moiety in the D-ring are essential for antitumor activity [7, 21]. Holden et al and others showed that introduction of groups in positions 7, 10 and 11 led to more stable Top1-DNA-CPT complexes which increased the potential for colliding with the replication or transcription machinery [22-25]. Additionally, *in vitro* studies have indicated that substitution on positions 7, 9 and 10 are associated with decrease in the interaction of the carboxylate form of camptothecin analogues with albumin [16, 26, 27] and, therefore, increasing exposure to the pharmacologically active lactone form. Finally, substitution on carbon 12 prevented the analogue from interacting with Top1 [28].

Between the two camptothecin forms, the lipophilic lactone, through the α-hydroxy-δ-lactone pharmacophore (ring-E), has been traditionally considered to mediate the camptothecin cytotoxic activity [3]. However, crystalography studies have indicated that both the carboxylate and lactone form have the potential of interacting with Top1 [29].

6
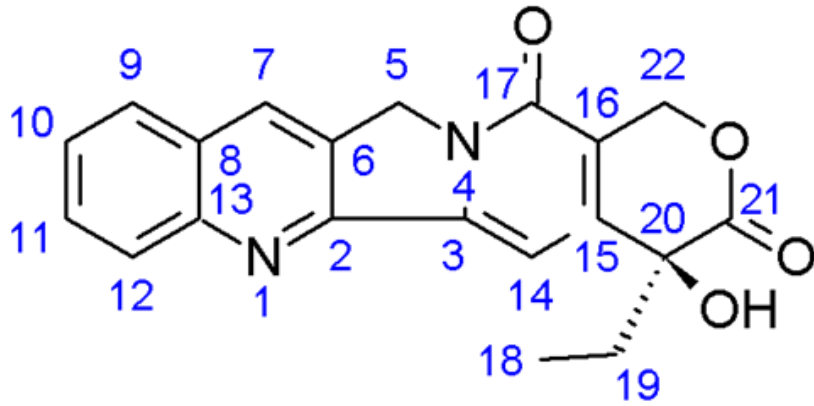
Figure 1-3. Camptothecin five-member ring structure.

1.6   2nd and 3rd generation Camptothecin Analogues.

In line with studies linking camptothecin cytotoxic activity with protein binding and lipophilicity, synthetic efforts aimed at producing derivatives with increased lactone stability which would lead to increased exposure to the pharmacologically active form (Figure 1-2). Initial efforts focused on synthesizing camptothecin analogues with low carboxylate affinity to human albumin. These 2nd generation water-soluble derivatives showed increased stability of the lactone pharmacophore in biological matrices [17] and were deemed superior to previously studied camptothecin derivatives. Two of those camptothecin analogues that showed significant activity preclinically as well as in the clinic are the FDA approved topotecan and irinotecan (Figure 1-4) [30, 31]. Additional water-insoluble 9-substituted (Figure 1-5) and water-soluble hexacyclic camptothecin analogues (Figure 1-6) are currently under early-stage development [32, 33].
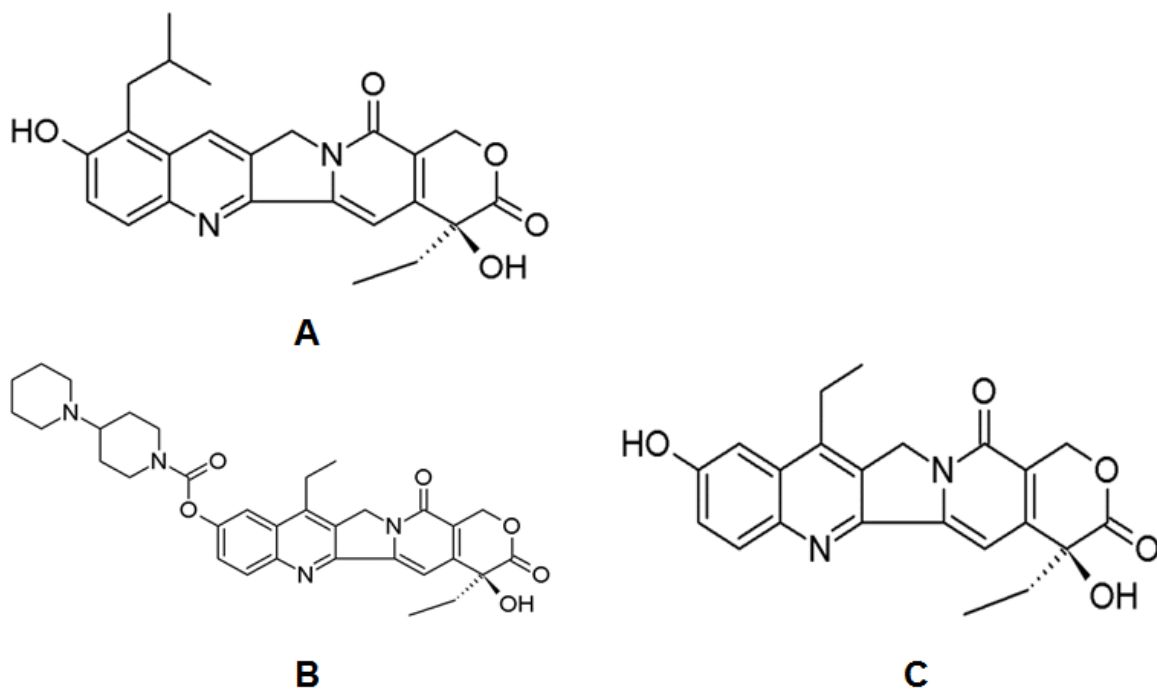
Figure 1-4. Second generation FDA approved and water-soluble camptothecin analogues.

Chemical structure of topotecan (TPT, Hycamtin, NSC 609669, SK&F 104864) (A), irinotecan (IRN, CPT-11, Camptosar) (B) and SN-38 (C), the active metabolite of irinotecan.
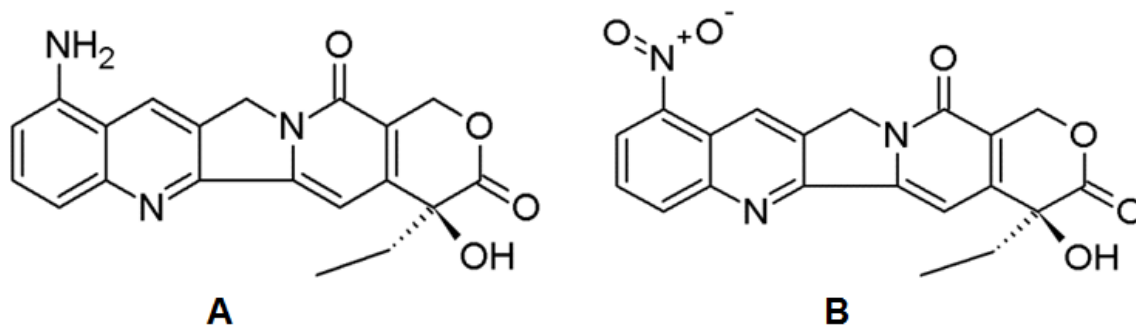
Figure 1-5. Second generation water-insoluble amino- and nitro-camptothecin analogues.

Chemical structure of 9-aminocamptothecin (9-AC, IDEC-132) (A) and 9-nitrocamptothecin (9-NC, Rubitecan, Orathecin) (B).
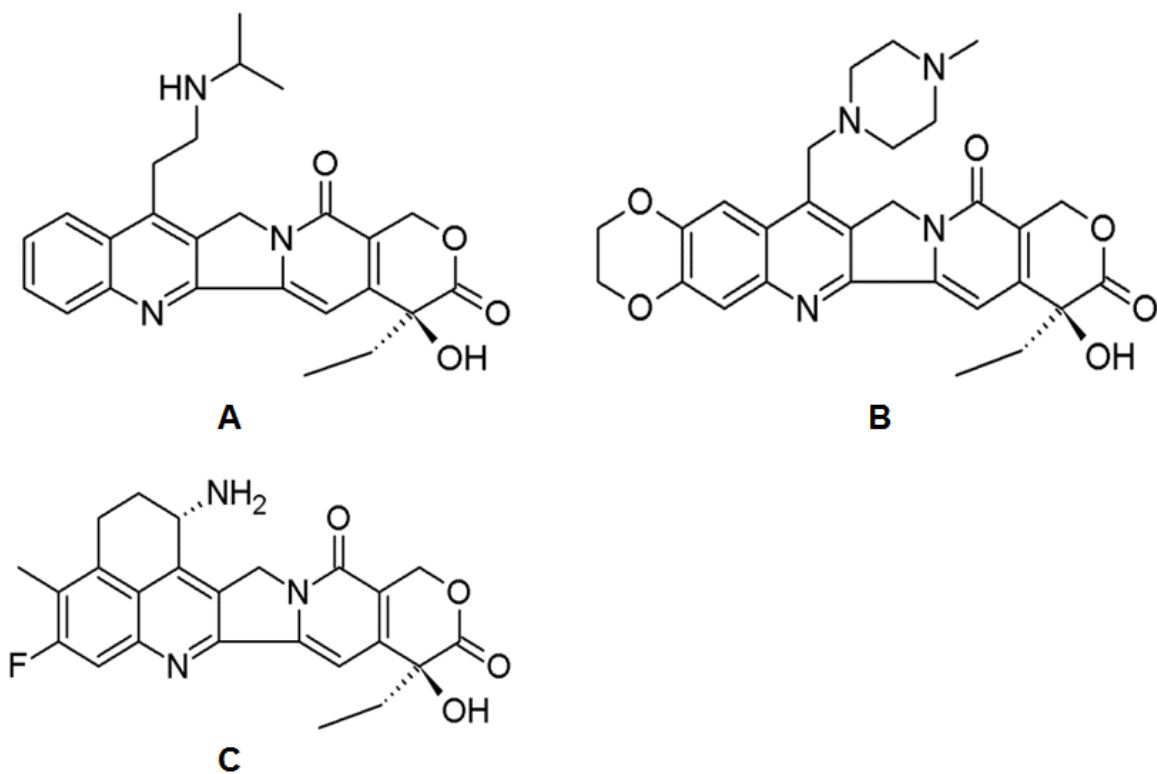
Figure 1-6. Second generation, water soluble, hexacyclic camptothecin analogues.

Chemical structure of belotecan (CKD-602, Camtobell) (A), lurtotecan (GI147211, GG211) (B) and exatecan (DX-8951) (C).

The 3rd generation camptothecin analogues (Figure 1-7) were characterized by low carboxylate hydrolysis rates and increased lipophilicity, which resulted in further stabilization of the lactone moiety potentially by extensive partitioning to lipid bilayers [32, 33]. In addition, replacement of the six- by a seven-membered α-hydroxy lactone pharmacophore gave rise to a new group of camptothecin derivatives, the homocamptothecins (Figure 1-7, D), with promising cytotoxic activity and reinforced lactone stability [32, 34-36].

Finally, substitution on position 7 (Figure 1-7, B, C and D) was explored further to achieve higher lipophilicity and antitumor activity. Those synthetic pathways produced analogues such as the silatecans [37, 38]. The 7-silyl group improved the lipophilic character of those analogues and further facilitated the interaction of silatecans with Top1 potentially by allowing the analogues to freely diffuse through membranes and access their enzyme-target [38].
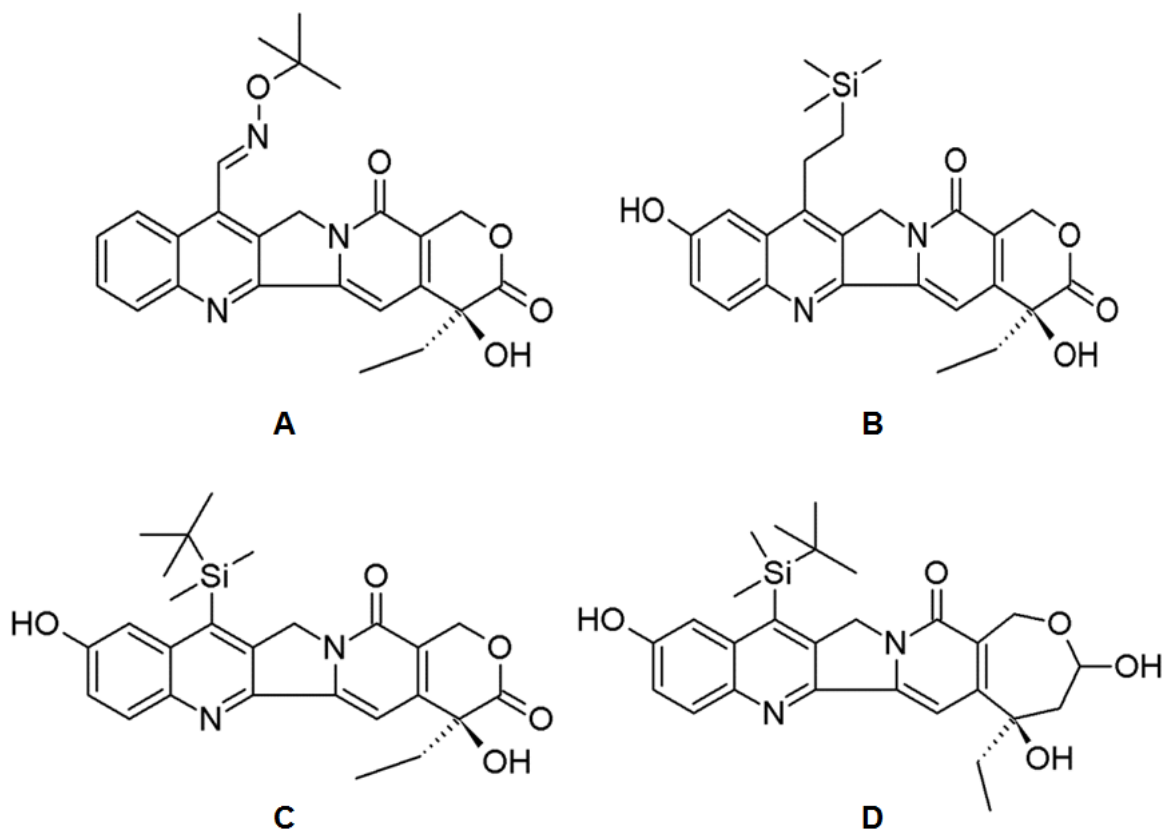
Figure 1-7. Third generation camptothecin analogues.

Chemical structure of gimatecan (ST14811) (A), karenitecin (B), AR-67 (DB-67) (C) and DB-91 (D).

1.7   Camptothecin Analogues in the Clinical Setting.

During one of the early clinical trials testing the activity and safety of CPT [39], the drug was administered in the carboxylate form due to solubility issues. Low response rates in combination with significant toxicity in the form of hemorrhagic cystitis were reported. As a result, the development of camptothecins was dropped and efforts were focused on the development of taxanes.

However, the interest in camptothecins was revived after a better understanding was obtained regarding its enzyme-target, Top1, the interaction taking place between Top1 and camptothecins and the factors that play a role on the equilibrium between the toxic carboxylate and the pharmacologically active lipophilic lactone form.

Two camptothecin analogues have emerged as promising candidates for clinical use after extensive *in vitro* and *in vivo* studies on their antitumor activity profile, topotecan and irinotecan. In addition to their very distinct pharmacokinetic properties, topotecan and irinotecan displayed noteworthy activity in the clinical setting.

1.7.1   Topotecan.

Topotecan (Figure 1-4, A) is a 2nd generation semisynthetic and water-soluble camptothecin that has received FDA approval for the treatment of recurrent cervical cancer in combination with cisplatin and for the treatment of ovarian and small-cell lung cancer after failure of first-line therapy [40, 41]. When compared to 20(S)-camptothecin, topotecan showed increased lactone stability *in vivo* and the lactone form accounted for about 25 % of the total drug in cancer patients [42, 43]. The kinetics of topotecan appeared to be linear over the dose range tested in clinical studies and its half-life was 1-2 hours [43, 44]. Topotecan was primarily eliminated through the kidneys as 30 % of the administered dose was quantified in the urine [44, 45]. The significance of renal

elimination was underlined in population analysis studies where indicators of renal function such as serum creatinine (SrCr), creatinine clearance (CRCL) or glomerular filtration rate (GFR) accounted for a large amount of intersubject variability accompanying drug clearance estimates [46-50] (Table 1-1). More importantly, dose adjustments were found necessary for patients with renal impairment to avoid life-threatening toxicities, primarily hematological such as neutropenia and thrombocytopenia [51, 52].

1.7.2 Irinotecan.

Irinotecan (Figure 1-4, B) belongs to the same group of camptothecin analogues as topotecan. The FDA has granted irinotecan approval for the treatment of metastatic carcinoma of the colon or rectum that is considered recurred or has progressed following 5-FU-based therapy [53]. Similarly to topotecan, the lactone to total drug ratio of irinotecan and SN-38, its active form *in vivo*, is improved compared to the first camptothecin analogues synthesized [54, 55], but its pharmacokinetic and toxicity profile are subtly different than the ones of topotecan.

Irinotecan is a prodrug that is biotransformed to its active form, SN-38, by carboxylesterases in the blood and the liver [56]. Irinotecan and SN-38 are further metabolized by CYP3A4 and UGT1A1/7 into products that are detected in the bile and feces (64 % of the dose) and to a much lesser extent in the urine [57, 58]. As a result of the enterohepatic circulation SN-38 undergoes [59, 60], patients treated with irinotecan experience diarrhea that often requires hospitalization. Half-lives for irinotecan and SN-38 have been estimated to be 14.6 h and 28.5 h, respectively [57] and SN-38 protein binding was 94.7 % [61]. Consistent with the involvement of the liver in the elimination of irinotecan and the solid exposure-toxicity relationship established for irinotecan/SN-38 with the development of population pharmacokinetic models (Table 1-1), patients with

liver impairment and patients UGT1A1*28 homozygous receive reduced doses of irinotecan and are being monitored closely for hematological and gastrointestinal toxicity [61-63]. Finally, a number of gastrointestinal and liver transporters have been implicated in the complex pathways of absorption, distribution and elimination for irinotecan and SN-38. The uptake transporters OATP1B1 and OATP1B3 facilitate the transfer of irinotecan and SN-38 into the hepatocytes [64, 65]. The glucuronides and other products of metabolic pathways are being effluxed into the bile by BCRP, MDR1 and MRP2 [64, 66, 67]. In the gut, irinotecan has the potential of being re-absorpted. It is expected that the BCRP and MDR1 efflux transporters localized on the apical side of the enterocytes would limit its oral bioavailability and potentially exacerbate gastrointestinal toxicity [66, 67]. Therefore, recent studies on irinotecan pharmacogenetics have focused on identifying sources of genetic variation in metabolic enzymes and transporters and on exploring correlations between polymorphisms of metabolic enzyme and transporter genes with toxicity [68, 69]. Naturally, the clinical relevance of those findings needs to be studied further.

Table 1-1. Topotecan and irinotecan population pharmacokinetic models.

Camptothecin, Species	Matrix	No Patients	Population pharmacokinetic parameter	Covariate	Reference
Topotecan, total drug	Plasma	82	CL	HT, WT, sex, SrCr	[49]
Topotecan, total drug	Plasma	31	CL	CRCL/SrCr+AGE*	[50]
Topotecan, total drug	Plasma	245	CL	CRCL, PS, WT	[48]
Topotecan, total drug	Plasma	190	CL	PS, CRCL	[47]
			V	WT	
Topotecan, lactone	Plasma	162	CL	GFR, AGE, TRIAL#, CONCOMINANT MEDICATION	[46]
			V	GFR, AGE, TRIAL#, CONCOMINANT MEDICATION	
Irinotecan, lactone and total drug	Plasma	70	CL	BSA	[70]
Irinotecan, total drug	Plasma		CL	AGE, PS	[71]
			V	WT	
SN38, total drug	Plasma	78	CL	T_{bil}, sex	
			V	T_{bil}, PS	
SN38G, total drug	Plasma		CL	PS	
			V	WT	
Irinotecan, total drug	Plasma	109	CL	BSA	[72]

Pharmacokinetic parameters, CL: population predicted clearance, V: population predicted volume of distribution
Patient Covariates, BSA: Body Surface Area, PS: Performance Status, WT: Weight, Tbil: serum total bilirubin, HT: Height, SrCr: Serun Creatinine, CRCL: Creatinine Clearance, GFR: Glomerular Filtration Rate, TRAIL#: phase I clinical trial number
SN-38G: SN-38 glucuronide
*Two models were proposed by the authors: CRCL (model 1) and SrCr and AGE (model 2)

1.8 AR-67 Preclinical Studies.

AR-67 (7-t-butyldimethylsilyl-10-hydroxycamptothecin, DB-67) (Figure 1-7, B) is a 3rd generation lipophilic camptothecin analogue that belongs to the family of silatecans (Figure 1-7) [37]. *In vitro* structure-activity studies have showed that the AR-67 fortified lipophilic properties should be attributed to the silyl group in position 7 while substitutions in positions 7 and 10 prevent the AR-67 carboxylate from interacting with albumin [38, 73]. It was originally hypothesized that the increased exposure to AR-67 lactone observed *in vitro* was the result of the lipophilic lactone moiety partitioning into erythrocytes and other membranous structures found in the bloodstream that could serve as a drug depot [74]. However, recent studies in animals have indicated that the carboxylate form is being eliminated at a higher rate than the lactone form [75]. Therefore, it is suggested that the lactone appears to be the predominant species *in vivo* and exhibits, essentially, high "apparent" blood stability [75].

The antitumor activity of AR-67 was evaluated in preclinical models both *in vitro* and *in vivo*. More specifically, AR-67 was tested against camptothecin and SN-38 for cytotoxicity using an array of established cancer cell lines (leukemia, melanoma, lung, colon, central nervous system, renal, prostate and breast cancer) [74]. Although, the lipophilic camptothecin analogue was more potent than 20(S)-camptothecin, the estimated GI50s for AR-67 were 10-fold lower than the respective ones for SN-38 [74]. Moreover, the antitumor activity of AR-67 was studied using colon cancer and glioma xenografts. AR-67 was proven to be more effective than irinotecan in decreasing relapse rates in animals that had resected metastatic liver tumors [76]. Additionally, U87 glioma xenografts showed high response rates to AR-67 treatment when compared to drug-vehicle treated animals. AR-67 treatment resulted in tumor growth inhibition and increase in survival while no toxicity was observed [77].

1.9 AR-67 Phase I Clinical Trial.

Preclinical studies demonstrating the potent antitumor activity of AR-67 were followed by a successful phase I clinical trial [78]. Patients with refractory or metastatic solid malignancies received AR-67 lactone as an 1-hour infusion daily for 5 days on a 21-day cycle and were monitored for safety and toxicity. The maximum tolerated dose (MTD) was estimated to be 7.5 mg/m^2/day. This dose administered daily for 5 days every 21 days is recommended for future phase II studies. Consistent with the toxicity profile of camptothecins [41], thrombocytopenia and febrile neutropenia were identified as dose limiting toxicities (DLT) in addition to fatigue. Changes in Absolute Neutrophil Counts (ANC) and Platelets (PLT) were used to establish correlations between AR-67 dose or exposure and hematological toxicity. Notably, no diarrhea was reported by any of the patients. This finding is in line with *in vitro* metabolism studies indicating AR-67 lactone as a good substrate for UGT1A7 and UGT1A8, enzymes localizing selectively in the gastrointestinal lumen [79]. Contrary to SN-38, AR-67 appeared to be a poor substrate for UGT1A1 [79] limiting the potential for life-threatening gastrointestinal toxicity in patients with the UGT1A1 7/7 genotype (homozygous for UGT1A1*28 allele) [60, 80]. Similarly to preclinical studies, AR-67 was present primarily in the lactone form in the blood. More specifically, the AR-67 lactone/total AUC ratio was estimated to be 85.7 % for patients in the MTD cohort contrary to the respective irinotecan and topotecan ratios ranging from 30 to 76 % [58]. As a result, exposure to the pharmacologically active lactone was higher with AR-67 than with the FDA-approved camptothecins irinotecan and topotecan. Notably, AR-67 administration resulted in clinical responses in patients with lung and duodenal cancer. This is a promising finding as irinotecan and topotecan have exhibited documented activity against gastrointestinal and lung cancer, respectively [40, 41, 53]. Finally, AR-67 followed linear kinetics over the administered dose range (1.2-12.4 mg/m^2/kg) and the estimated plasma half-life (noncompartmental

analysis) was ~1.5 h [78]. Additional studies on days 1 and 4 of cycle 1 showed that AR-67 is mostly protein bound. More specifically, overall protein binding was 95.4%±1.8 for lactone vs. 89.7%±3.2 for carboxylate [81].

1.10 Transporters.

1.10.1 ATP-Binding Cassette Multidrug Transporters.

The ATP-Binding Cassette (ABC) transporters are proteins responsible for the transport of chemical entities through lipid bilayers. They are typically expressed in the outer membrane of the eukaryotic cells as well as in membranes of organelles in the cytoplasm, and they require ATP hydrolysis to function. Breast Cancer Resistance Protein (BCRP) and Multidrug Reistance-associate Protein-1 (MDR1) belong to the ABC superfamily of transporter proteins [67].

1.10.1.1 BCRP.

ATP-Binding Cassette Subfamily G member 2 (ABCG2 gene) was originally found to be overexpressed in the MCF-7 breast cancer cell line and was associated with resistance to mitoxantrone, doxorubicin, and daunorubicin [82, 83]. Due to the type of tissue of origin, it was named Breast Cancer Resistance Protein (BCRP). It is a 72 kDa transporter that is believed to comprise of 2 or 4 dimers [84] each of which is comprised of 3 transmembrane (TM) segments and a Nucleotide Binding Domain (NBD) [67]. BCRP is expressed in normal tissues such as the placenta, adrenal glands, liver (bile ductules), blood-brain barrier, lung, prostate and gastrointestinal tract [85] and it facilitates the transfer of endogenous compounds such as flavonoids, aflatoxin A, drug and metabolite conjugates and porphyrins through membranes [67]. Moreover, anticancer agents, tyrosine kinase inhibitors, antiviral drugs and antibiotics have been reported to undergo BCRP-facilitated transport [67]. Depending on its localization, this

efflux transporter can protect the fetus or the brain from the toxic effects of xenobiotics [86] or mediate the transport of xenobiotics into the milk [87].

1.10.1.2 MDR1.

Multidrug Resistance-associated Protein 1 (MDR1, P-glycoprotein, P-gp) is a 170-kDa glycoprotein encoded by the MDR1/ABCC1 gene. It is a single polypeptide with 12 transmembrane (TM) domains and 2 nucleotide binding domains (NBD). Although originally cloned and extensively studied in cancer cells, MDR1 is expressed in the apical site of epithelial cells in the blood-brain barrier, gastrointestinal tract (small and large intestine), placenta, kidney (proximal tubule) and liver (bile ductules) [88-90] serving a protective/detoxifying role [67]. MDR1 substrates are typically amphiphatic, lipid-soluble compounds, with aromatic rings and high molecular weights (> 300) [67]. Steroid hormones, lipids (phospholipids), peptides and small cytokines are some of the most common endogenous MDR1 substrates. Xenobiotics readily transported by MDR1 include, but are not limited to, anticancer agents, HIV-protease inhibitors, antiarrhythmics, immunosuppressive agents, calcium channel blockers, tyrosine kinase inhibitors and cardiac glycosides.

1.10.2 Organic Anion Transporting Polypetides.

Organic Anion Transporting Polypeptides (OATPs) [65, 91] are expressed in multiple tissues mediating the infllux of amphipathic endogenous and exogenous compounds. They are sodium, ATP-independent transporters coded by the solute carrier gene SLC. The human OATP family comprises of 11 members: OATP1A2, 1B1, 1B3, 1C1, 2A1, 2B1, 3A1, 4A1, 4C1, 5A1 and 6A1 [65]. All members share a similar structure that includes 12 TM domains. Notably, SLCO1A6 [92, 93] (gene symbol SLC21A6, protein symbol LST-1, OATP-C, OATP2, OATP1B1) and SLCO1A8 [94, 95] (gene symbol SLC21A8, protein symbol LST-2, OATP8, OATP1B3) genes are expressed strictly in the

basolateral membrane (sinusoidal membrane) of human hepatocytes and their protein products share a broad spectrum of overlapping substrates. They facilitate the uptake of substrates from the portal blood to the hepatocytes and contribute to the vectorial transport of compounds from the blood to the bile. OATP substrates are anions with molecular weights higher than 300 kDa. OATP1B1 has been reported to transport conjugated and unconjugated bilirubin, bile acids, conjugated steroids, eicosanoids and thyroid hormones [65, 96]. Xenobiotics identified as OATP1B1 substrates include statins, methotrexate, SN-38, antibiotics and angiotensin II receptor antagonists [96]. Although OATP1B3 showed an 80 % amino acid homology with OATP1B1, cholecystokinin, docetaxel and paclitaxel and digoxin are selectively being transported by OATP1B3 and not by OATP1B1 [65, 96].

1.11 Multidrug Resistance and ABC-Transporters.

Multidrug resistance (MDR) is a phenomenon in which cancer cells simultaneously become resistant to structurally unrelated chemotherapeutic agents when exposed to a single chemotherapeutic drug [97]. MDR can be intrinsic or acquired as a result of exposure to anticancer agents. MDR is commonly mediated through one or more transporters that are protein structures localizing in the cell membrane and can interfere with the cytotoxic profile of chemotherapeutic agents. For instance, increase in the expression level of an efflux transporter or decrease in the expression level of an uptake transporter at the site of action, namely the tumor tissue, could result in lower exposure and, therefore, resistance. Two transporters frequently associated with multi-drug resistance are BCRP and MDR1.

1.11.1.1 MDR1 and BCRP Efflux Transporters.

A number of studies have shown increased expression of the efflux transporter BCRP in both solid tumors and leukemias [85]. Ross et al [98] showed BCRP mRNA levels

comparable to the ones quantified in the MCF-7 cell line in 33 % of the AML blasts in leukemic patients. Using immunohistochemistry and western blotting as a cross-reference method, high BCRP expression was observed in the digestive tract, endometrium, lung and melanoma tumor tissue samples obtained from untreated patients in a study by Diestra et al [99]. High mRNA levels of the same efflux transporter were quantified in 22 % of lung tumor tissue patient samples [100]. Interestingly, work by Candeil et all suggested that the observed increase on the mRNA levels of BCRP can be drug-induced [101]. Similarly to BCRP, MDR1 over-expression has been reported in primitive hematopoietic progenitor cells [102] and in human tumor tissues derived from the adrenal gland, colon and renal carcinomas, the testis and the brain [88, 89]. Detectable levels of MDR1 have been identified in osteosarcomas, ovarian and small-cell lung carcinomas, Ewing's sarcoma and breast cancer [15]. Guerci et al were able to demonstrate 33 % complete response rates among MDR-1+ in MDS-AML patients against a complete response rate as high as 78 % among patients that did not express MDR-1 in their blasts [103]. Additionally, MDR1 was introduced as a predictor of outcome in acute myeloid leukemia patients by Leith et al [104]. Finally, BCRP and MDR1 expression have been studied concurrently or alone in leukemic patients in a number of studies that propose a prognostic role for these transporters [105-107].

1.12 Chemosensitivity and the OATP1B3 Uptake Transporter.

Recent studies reported increased mRNA expression of OATP1B3 in human lung tumor tissue when compared to normal lung tissue [108]. Hormone-dependent cancers have been associated with OATP1B3 overexpression. The SLCO1B3 gene was found highly expressed in prostate tumor tissue [109] while the protein expression of the transporter correlated with prognosis in breast cancer patients [110]. Interestingly, OATP1B3

23

ارة للاستشارات

www.manaraa.com

overexpression has been reported in colorectal tumors [111-113] and a prognostic role in lower grade early stage colon cancer has been suggested for this transporter [112].

Therefore, increased cellular expression of OATP1B3 could benefit patients that are being treated with anticancer agents selectively transported by OATP1B3. As preclinical studies have demonstrated the OATP1B3-mediated uptake of paclitaxel [114], the impact of OATP1B3 overexpression at the tumor on paclitaxel tumor pharmacokinetics and on response to drug treatment warrants further exploration.

24

2. Chapter 2: Specific Aims.

2.1 Hypothesis 1.

The MDR1 and BCRP efflux transporters expressed in the tumor tissue confer resistance to AR-67 lactone and overexpression of the uptake transporter OATP1B3 at the tumor site is associated with increased sensitivity to the cytotoxic effect of AR-67 carboxylate *in vitro*.

2.1.1 Specific Aim 1a.

Validate the expression and function of the efflux MDR1 and BCRP and the uptake OATP1B1 and OATP1B3 transporters in *in vitro* models.

2.1.2 Specific Aim 1b.

Assess the MDR1 and BCRP-mediated efflux of AR-67 lactone and OATP1B1 and OATP1B3-mediated uptake of AR-67 carboxylate using the previously validated *in vitro* models.

2.1.3 Specific Aim 1c.

Evaluate the effect of the efflux transporters MDR1 and BCRP on the cytotoxic effect of AR-67 lactone and the effect of the uptake transporter OATP1B3 on the cytotoxic effect of AR-67 carboxylate using the previously validated *in vitro* models.

The expression level of transporters in tumor tissue obtained from cancer patients has been studied in the past. Interestingly, BCRP and MDR1 as well as OATP1B3 have been found to be over-expressed in breast, prostate, colon and leukemia cancer types and to correlate with response in certain cases [88, 89, 97-110, 112, 113, 115]. Moreover, previous studies have demonstrated the interaction between camptothecin analogues and certain efflux or uptake transporters [116-121]. Additionally, *in vivo*

studies in animals showed that the efflux MDR1 and BCRP transporters interfere with the absorption of AR-67 when administered orally [122]. Against this background, we hypothesized that efflux and uptake transporters could have an impact on the toxicity profile of AR-67 *in vitro*. To investigate the impact these transporters could have on the toxicity profile of AR-67, cell lines overexpressing the transporters of interest were used. These cell lines were initially validated using prototype substrates (Specific Aim 1a). After the transporter-mediated transfer of AR-67 species was demonstrated (Specific Aim 1b), the MDR1 or BCRP conferred resistance and the OATP1B3-mediated sensitivity to AR-67 was evaluated (Specific Aim 1c).

2.2 Hypothesis 2.

AR-67 protracted low-dose dosing schedules that do not result in depletion of Top1 at the tumor site are more efficacious than AR-67 given at the maximum tolerated dose.

2.2.1 Specific Aim 1a.

To determine the maximum tolerated dose of AR-67 in the xenografts model used, neutropenia was selected as an endpoint of AR-67-related toxicity.

2.2.2 Specific Aim 1b.

Demonstrate that low-dose protracted dosing of AR-67 is superior to more intense high-dose dosing schedules in xenografts.

2.2.3 Specific Aim 1c.

Study AR-67 pharmacokinetics and Top1 kinetics at the tumor tissue after administration of AR-67 and evaluate Top1 as a biomarker of AR-67 biological activity.

2.2.4 Specific Aim 1d.

Study the toxicity profile of AR-67 given to cancer patients intermittently and test the feasibility of obtaining a tumor biopsy from cancer patients twice within 24 hours after drug administration.

Camptothecins are S-phase specific anticancer agents. Therefore, they were anticipated to exert their maximum cytotoxic activity after continuous exposure [123, 124]. However, xenograft studies have demonstrated that protracted low-dose intermittent administration of camptothecins results in better response rates than more intense dosing schedules [125-128]. Moreover, Top1 expression appeared to decrease after exposure to camptothecin analogues in *in vitro* and *in vivo* studies [9, 10]. This established interaction between camptothecins and their enzyme-target is often characterized as a resistance mechanism of cells against this group of anticancer agents. Against this

27

background, we hypothesized that AR-67 antitumor activity can be enhanced when AR-67 is given intermittently at low doses to allow the expression of Top1 at detectable levels at the site of action, the tumor. To determine the maximum tolerated dose of AR-67 in our animal model, low white blood cells counts were used as an indicator of toxicity as hematological toxicity is typically observed after treatment with camptothecins [41, 78] (Specific Aim 1a). Following, the antitumor activity of AR-67 (Specific Aim 1b) and the kinetics of Top1 and AR-67 at the tumor tissue (Specific Aim 1c) were studied during AR-67 administration under differing dosing regimens. Finally, patients received AR-67 at the MTD determined during the recently completed phase I clinical trial over 15 instead of 5 days and were monitored for toxicity (Specific Aim 1d).

2.3   Hypothesis 3.

Identifying sources of intersubject variability when describing the population pharmacokinetics of AR-67 would render drug administration to cancer patients safer.

2.3.1   Specific Aim 1a.

Develop a population pharmacokinetic model for AR-67 from pharmacokinetic data collected in the AR-67 phase I clinical trial.

2.3.2   Specific Aim 1b.

Perform covariate analysis to include sources of intersubject variability in the previously developed population pharmacokinetic model that would lead in more accurate AR-67 population pharmacokinetic parameter estimates.

2.3.3   Specific Aim 1c.

Study the effect of smoking, tumor type, obesity and performance status on AR-67 clearance and the AR-67 toxicity profile based on data collected during the AR-67 phase I clinical trial.

2.3.4   Specific Aim 1d.

Determine whether or not body-size measures account for the intersubject variability observed in the total body clearance estimates of AR-67 obtained using the previously developed population pharmacokinetic model.

Study of the population pharmacokinetic and pharmacodynamic properties of anticancer agents, including camptothecins, has allowed clinicians to safely administer those agents to cancer patients [48, 50, 71, 72]. For instance, extensive studies on the pharmacokinetic properties of marketed camptothecins in different patient subpopulations have resulted in dose adjustments in patients with impaired kidney and liver function that receive topotecan and irinotecan, respectively to lower toxicity [52, 61,

29

63]. Therefore, the AR-67 population pharmacokinetics was studied using the non-linear mixed effects theory [129, 130] (Specific Aim 1a). Sources of intersubject variability were incorporated in the population pharmacokinetic model that was developed to increase its accuracy (Specific Aim 1b). As previous studies on AR-67 elimination have showed that it is primarily eliminated via metabolism [78, 79], factors that might interfere with the metabolic activity of enzymes in the liver and the gut were examined (Specific Aim 1c). Finally, the intersubject variability associated with AR-67 total body clearance was evaluated after normalization to body-size measures to decide whether or not flat or fixed dosing for AR-67 warrants further investigation (Specific Aim 1d).

3. Chapter 3: The effect of BCRP, MDR1 and OATP1B3 on the antitumor efficacy of the lipophilic camptothecin AR-67 *in vitro*

3.1 Introduction.

AR-67 is a third generation camptothecin analogue that belongs to the class of 7-silylcamptothecins [37]. Similar to other camptothecins, AR-67 undergoes pH dependent, but reversible, hydrolysis of the lipophilic lactone to the hydrophilic carboxylate [38]. Although both lactone and carboxylate forms interact with DNA [29], they have different transport characteristics. The lactone passively diffuses into the cell and is considered the pharmacologically active form. In contrast, the negatively charged carboxylate requires transporter-mediated uptake, and it is often considered an inactive form. Preclinical studies have demonstrated the high lipophilicity and an "apparent" blood stability of the lactone form of AR-67 compared to FDA-approved camptothecins [74, 75].

A common link between drug disposition and drug efficacy are transporter proteins, which could play a pivotal role in both the disposition and efficacy or toxicity of camptothecin analogs. As AR-67 exists in equilibrium between the hydrophobic lactone and hydrophilic carboxylate forms, both influx and efflux transporters could potentially play roles in both metabolic clearance and tumor sensitivity. Intracellular drug concentration will be influenced by the balance between cellular efflux, potentially resulting in resistance, and cellular uptake, potentially resulting in sensitivity. Metabolic clearance, on the other hand, may result from vectorial transport, where both influx and efflux transporters contribute to clearance in the same direction.

The effect of transporters on the pharmacokinetic and pharmacodynamic profile of the FDA approved camptothecins topotecan and irinotecan has been demonstrated in previous studies. Topotecan and the active irinotecan metabolite, SN-38, have been identified as BCRP substrates [116, 118] while MDR1-mediated transport has been reported for topotecan and irinotecan [116, 117]. Notably, expression of BCRP in established cancer cell lines and tumor biopsy samples has been associated with resistance to camptothecins [100, 101]. Among the uptake transporters, OATP1B1 has been implicated in the transport of irinotecan and SN-38, which has also been identified as an OATP1B3 substrate [119, 121]. However, little is known about the potential interactions between AR-67 and transporters and the implications of these interactions on the antitumor activity of AR-67 and its pharmacokinetic profile.

In this study we explored the interaction of AR-67 with BCRP and MDR1 and with OATP1B3 and OATP1B1. First we determined if expression of the efflux transporters BCRP and MDR1 would have an impact on the cytotoxic profile of the lipophilic AR-67 lactone *in vitro*. Additionally, we examined the effect of OATP1B3 expression on the intracellular amounts of AR-67 lactone and carboxylate. Based on recent studies reporting increased expression of OATP1B3 in tumor tissues [110, 113], we tested whether increased intracellular AR-67 uptake, facilitated by OATP1B3, would potentiate the antitumor activity of AR-67 *in vitro*. To address these questions, we used established cancer cell lines that expressed functional forms of the BCRP, MDR1, OATP1B3 and OATP1B1 transporters.

3.2   Materials and Methods.

3.2.1   Cell Lines and Reagents.

Madin-Darby canine kidney II (MDCKII) cells were obtained from the European Collection of Cell Cultures. Cells were mock transfected with pcDNA3.1 vector or with pcDNA3.1-ABCG2 [131]. OVCAR-8 and its derivative cell line expressing human MDR1 (NCI/ADR-RES) were from NCI Developmental Therapeutics. HeLa (cervical adenocarcinoma) cells were stably transfected with OATP1B3 cDNA and RKO (colon carcinoma) cells were stably transfected with OATP1B1 cDNA, inserted in the multiple cloning site of the pIRESneo2 vector (Clontech, Mountain View, CA) [108, 132]. MDCKII cells were cultured in Minimum Essential Media (MEM) supplemented with 5 % fetal bovine serum (FBS) and Geneticin (G418, 800 μg/mL) while OVCAR-8 and NCI/ADR-RES cells were cultured in Dulbecco's Modified Eagle Medium (DMEM) supplemented with 10 % FBS. The HeLa and RKO cell lines were grown in DMEM supplemented with 10 % FBS and Geneticin (G418, 800 μg/mL). Additionally, non-essential amino acids (1 %) were added to the RKO growth media. Penicillin (100 U/mL) and streptomycin (100 μg/mL) were added in the media. All of the aforementioned materials were supplied by Gibco, Invitrogen Corporation (Carlsbad, CA).

3.2.2   Validation of expression and functional activity of BCRP, MDR1, OATP1B3 and OATP1B1.

3.2.2.1   Immunoblot Analysis.

BCRP, MDR1 and Top1 protein expression in transfected cell lines was confirmed by Western blot analysis using standard procedures. Commercially available antibodies clone BXP-21 and clone F4 (Kamiya Biomedical Company, Seattle, WA) and Top1

(Abcam, Cambridge, MA) were used for detection of BCRP (1:100), MDR1 (1:1000) and Top1 (1:500). Actin (Sigma-Aldrich, St. Louis, MO) was used as a loading control.

3.2.2.2 *Hoechst 33342 and Resazurin Assays.*

BCRP functional activity were demonstrated by measuring intracellular accumulation of (2 µM) Hoechst 33342 (Invitrogen, Carlsbad, CA) [67] in the MDCKII-pcDNA and MDCKII-BCRP cells in the presence and absence of 4 µM GF120918 [133, 134] (a gift from GlaxoSmithKline) as previously described [87]. Fluorescence was measured in cell lysates using a microplate reader and values were normalized to protein concentration (Pierce BCA protein Kit, Fisher Scientific). MDR1 functional activity in OVCAR-8 and NCI/ADR-RES cell lines was evaluated using Vinblastine (Sigma-Aldrich, St. Louis, MO) and Vorinostat (SAHA) (Cayman Chemical Company, Ann Arbor, MI). The cell lines were incubated with either Vinblastine (10^{-9} – 1 µM) or SAHA (10^{-6} – 756 µM) for 72 hours and cell viability was assessed using a resazuring assay as described in section 3.2.8.

3.2.2.3 *RT-PCR Analysis.*

Hela-pIRES, Hela-OATP1B3, RKO-pIRES and RKO-OATP1B1 were grown to confluence in growth medium. RNA was isolated using RNeasy Kit (Qiagen) following manufacturer's protocol including on-column DNA digestion. cDNA synthesis was performed with High Capacity cDNA Reverse Transcription Kit (Applied Biosystems, Foster City, CA) according to the manufacturer's protocol. The PCR reaction was performed by SYBR Green-based qPCR using an iCycler Multicolor Real-Time PCR Detection System (Bio-Rad, Hercules, CA). The gene-specific primers for human SLCO1B3, SLCO1B1and 18s were as follows: SLCO1B3, 5'-GTCCAGTCATTGGCTTTGCA-3' (forward) and 5'-CAACCCAACGAGAGTCCTTAGG-3' (reverse), SLCO1B1, 5'-TGCTGTGATGTCATTGTCCTT-3' (forward) and 5'-

CATGACATGTGAGGTGCCTCCAAG-3' (reverse), 18s, 5'-CGCCGCTAGAGGTGAAATTCTT-3' (forward) and 5'-CGAACCTCCGACTTTCGTTCTT-3' (reverse). Amplification conditions were as follows: 95 °C (5 min), [95 °C (45 sec), 62 °C (1 min), 72 °C (1 min)] × 30 cycles, 95 °C (2 min). The PCR products were separated by 3 % agarose electrophoresis and visualized by UV in the presence of ethidium bromide.

3.2.2.4 ^{3}H-BQ-123 and ^{3}H-CCK-8 Intracellular Uptake Assay.

Stable clones of RKO cells with plasmids containing the transporter OATP1B1 or empty vector pIRESneo2, were seeded and allowed to reach confluency. BQ-123, a substrate for the OATP1B1 transporter [135], was obtained from GE Healthcare. Cells were incubated with 5 µM of BQ-123 in transport buffer for 30 min (37°C). To validate the function of the OATP1B3 transporter, stable clones of Hela cells with plasmids containing the transporter OATP1B3 or empty vector pIRESneo2, were seeded and allowed to reach confluency. CCK-8 (GE Healthcare), a substrate specific for only the OATP1B3 transporter [136], was incubated at a final concentration of 5 nM in transport buffer for 10 min (37°C). At the end of the incubation period, BQ-123 or CCK-8 was removed by aspiration, followed by three successive washes in PBS (4°C). Cells were then dried at 37°C and lysed by shaking at room temperature overnight in 0.2 N NaOH. Samples were neutralized with 0.2 N HCl. Intracellular radioactivity of the lysate was measured by a liquid scintillation counter from a lysate and scintillation cocktail mixture. Protein concentrations of lysates were measured using the Bio-Rad Protein Assay, allowing for normalization of samples in CPM/mg.

3.2.2.5 Immunohistochemistry.

Immunohistochemical analysis was used to verify the expression of OATP1B3 and OATP1B1 in the HeLa and RKO cell lines and liver tissue. Cell pellets and tissues were

processed with Histogel (Richard-Allan Scientific, Fisher Scientific) and fixed in 4 % formalin. Antigen retrieval was performed using citrate buffer (0.01M citrate buffer, 0.05 % Tween-20, pH 6.0) at 100 °C for 3 min. A 5 % hydrogen peroxide in PBS solution and an avidin/biotin blocking system were used for blocking of the endogenous peroxidase and the endogenous biotin. Following incubation with 5 % normal goat serum, slides were incubated with anti-OATP2 (OATP2, MDQ/2F260, Novus Biologicals, Littleton, CO) (1:100) overnight (4 °C). The secondary goat anti-mouse antibody (1:100, room temperature) was applied. Streptavidin-HRP conjugate (Dako, Carpinteria, CA) and the Vector NovaRED peroxidase substrate kit were used for visualization. Nuclei were counter-stained using hematoxylin. The expression of the aforementioned transporters was evaluated in human liver tissue. To exclude false positive results, slides were incubated with chromatographically purified mouse IgG (Zymed, San Francisco, CA). All supplies were obtained from Vector (Burlingame, CA) unless otherwise stated.

3.2.3 Preparation of Drug Stock and Working Solutions.

AR-67 (DB-67; Novartis) was solubilized in dimethylsulfoxide (DMSO) at a concentration of 1 mg/mL (AR-67 lactone stock solution) and stored at -80 °C. AR-67 carboxylate working solutions were prepared by dilution of one volume of lactone stock solution with 9 volumes of 0.005 N NaOH and were allowed to convert to carboxylate overnight at 4 °C (AR-67 carboxylate stock solution) [137]. Working solutions were stored at -80 °C after their preparation and at 4 °C during the experimental procedure.

3.2.4 Intracellular Amount of AR-67 in BCRP and MDR1 Expressing Cell Lines.

To examine the effect of ABC efflux transporters BCRP and MDR1 on the intracellular amount of AR-67, cells were seeded in six-well plates. The next day, medium was replaced and the cells were incubated in serum-free medium (Opti-MEM) with 0.125, 0.25, 0.5, 0.75 and 1 µM AR-67 lactone for 5 min at 37°C. The incubation time was

36

selected to ensure linearity in the transport process. At the end of the incubation, medium was aspirated and cells were washed twice with Opti-MEM (4 °C). Cells were lysed with 200 µL of 0.5 N NaOH and placed on a rocker (4 °C) for 10 min. Extraction and quantification of AR-67 was carried out as indicated in an HPLC-FL method under conditions that ensure system suitability [137]. Protein was quantified using the BCA Protein Assay Kit (Pierce, Thermo Fisher Scientific). In inhibition studies, cells were pre-incubated with GF120918 (5 µM) [133, 134] for 1 h prior to incubation with 1 µM AR-67 lactone (for 5 min).

3.2.5 Transepithelial Flux of AR-67.

MDCKII-pcDNA and MDCKII-BCRP cells were grown on Corning Transwell® 3414 membrane inserts (3.0-µm pore size, 24-mm diameter; Corning Glassworks, Corning, NY). When TEER exceeded 200 $\Omega \cdot cm^2$s in both cell lines, the medium was aspirated and replaced with 1.8 ml of serum-free Opti-MEM with or without GF120918 (5 µM) on both the apical and basolateral side. Cells were placed at 37°C in humidified 5 % CO_2 incubator for 1 h. When 0.2 ml of 50 µM AR-67 lactone was added to the donor side to a final concentration of 5 µM and 0.2 ml of medium was added to the receiver side. Cells were then placed on a rocker and incubated at 37 °C and 5 % CO_2. AR-67 amount was quantified in 50 µL samples using the HPLC method described previously [137].

The data collected when studying the BCRP-mediated transport of AR-67 lactone in polarized MDCKII transfected cells grown on Transwell® inserts (Fig. 3) were used to quantify the efflux activity of BCRP in the presence and absence of GF120918. Apparent permeability values and efflux ratios were estimated [138, 139]. Apparent permeability values ($P_{app,A>B}$ and $P_{app,B>A}$) were obtained for surface of the transwell membrane S=4.5cm^2 and after quantifying the AR-67 concentration at the donor side at t=0 h using

HPLC [137]. Efflux ratios were equal to $P_{app,B>A}/P_{app,A>B}$. Standard deviation values were calculated with the propagation error theory.

3.2.6 Intracellular Uptake of AR-67 Carboxylate.

The effect of the expression of OATP1B3 and OATP1B1 on the intracellular uptake of AR-67 was studied using the HeLa-pIRES/OATP1B3 and RKO-pIRES/OATP1B1 cell lines using serum-free medium (Opti-MEM). To evaluate the dose-dependent OATP-mediated uptake of AR-67, OATP transfected cell lines were incubated with 0.5, 1, 1.5, 2 and 3 µM AR-67 carboxylate for 1 min. The incubation time was selected to ensure linearity in the transport process as indicated by preliminary studies. The pH of carboxylate containing media was 7.2. In inhibition studies, Hela-pIRES/OATP1B3 and RKO-pIRES/OATP1B1 cells were incubated with 1 µM AR-67 carboxylate for 5 and 10 min, respectively. The inhibition of transporter-mediated uptake was studied by pre-incubation with bromosulfophthalein (BSP) (50 µM) [65, 140] for 10 min and keeping the concentration of BSP constant during substrate incubation.

At the end of the incubation period, cells were washed twice with Opti-MEM (4 °C) before being lysed and AR-67, calculated as the sum of the two forms, was extracted from the cell lysate and quantified as described above [137].

When quantification of each of the AR-67 forms separately was required, cells were incubated with AR-67 carboxylate or lactone (1 µM) for 0.083, 0.5, 1, 3, 6, 12, 24 and 48 h at 37 °C and washed twice with Opti-MEM (4 °C) at the end of the incubation period. PBS was added; cells were scrapped off and lysed by sonication. AR-67 lactone and carboxylate were extracted and quantified using HPLC [137].

3.2.7 Drug Stability in Culture Media.

AR-67 interconversion was studied in cell culture media at pH 7.4 (37 °C) and humidified atmosphere of 5 % CO_2. AR-67 carboxylate (1 μM) or lactone (1 μM) were added in the media at t=0 h. AR-67 carboxylate and lactone concentrations were quantified at 0, 0.5, 1, 2, 4 and 6 h using HPLC [137].

3.2.8 Cytotoxicity Assays.

Cells were seeded in 96-well plates at initial densities that ensured their exponential growth for the duration of the experiment. To study the effect of AR-67 lactone and AR-67 carboxylate on cell viability, cells were seeded and allowed to adhere overnight. Twenty-four hours later, the cell culture medium was replaced with drug-containing medium. The final concentration of DMSO in cell culture media never exceeded 1 %. Cells expressing BCRP and MDR1 were exposed to AR-67 lactone for 72 h. The effect of BCRP and MDR1 on AR-67 lactone-induced cytotoxicity was studied in the presence of the dual BCRP/MDR1 inhibitor GF120918. MDCKII-pcDNA/BCRP cells were pretreated for 30 min with GF120918 (1 μM) followed by co-treatment with GF120918 (1 μM) and AR-67 lactone. OVCAR-8 and NCI/ADR-RES cells were pretreated for 30 min with GF120918 (5 μM) followed by co-treatment with GF120918 (5 μM) and AR-67 lactone. The cytotoxic effect of AR-67 carboxylate on the OATP expressing cell lines after various exposure times was also evaluated. In these cases, cells were treated with AR-67 carboxylate for 5 and 30 min, 1 and 3 h. At the end of the incubation period, the drug-containing media was removed and the cells were washed once with ice cold PBS. Following, drug-free media was added in the wells and cells were allowed to grow for 48 h at which point their viability was assessed.

Cell viability was assessed with the CellTiter 96® AQeous Non-Radioactive Cell Proliferation Assay kit (Promega, Fisher Scientific) following the manufacturer's

instructions. The viability of the HeLa- and RKO-OATP transfected cell lines was evaluated by using a resazurin assay (RSZ, Alamar Blue).

3.2.9 γH2AX activation in HeLa-pIRES and HeLa-OATP1B3 cells.

Western blot analysis was used to assess the phosphorylation of Histone 2AX (γH2AX) in HeLa-pIRES and HeLa-OATP1B3 cells as a result of exposure to AR-67 carboxylate (20 μM) for 5 min. At the end of the treatment period, AR-67 was removed and cells were allowed to grow in drug-free media for 3 hr. Cell lysate preparation and western blot analysis were performed following standard procedures. Anti-Phospho-Histone H2AX (Cell Signaling, Danvers, MA) (1:500) was used for γH2AX detection. Protein expression was quantified performing densitometry analysis using the Molecular Imaging Software (version 4.04, Eastman, Kodak, New Haven, CT) and Actin (Sigma-Aldrich, St. Louis, MO) was used as a loading control.

3.2.10 Data Analysis and Statistics.

GraphPad Prism (version 5.02 for Windows, GraphPad Software Inc., San Diego, USA) was employed for the graphical representation of the results, data analyses and statistical comparisons.

To calculate the kinetic parameters for the OATP1B3 and OATP1B1 transporters, AR-67 intracellular uptake was determined as described above. Transporter mediated uptake was corrected by subtracting intracellular amount in mock transfected cells and error propagation was applied. Data were modeled using the Michaelis-Menten equation which provided us with a satisfactory fitting:

$$V = V_{max} \times C/(K_m + C)$$

where V (ng of total AR-67/μg protein/min) was the rate of transport of AR-67 lactone or carboxylate, C (μM) is the concentration of AR-67 carboxylate added in the well and K_m

(μM) was the concentration of AR-67 lactone or carboxylate at which the transporter activity was equal to its half maximum value (V_{max}).

Dose-response data were also fitted using non-linear regression analysis. The viability of the treated cells was normalized with the viability of untreated (control) cells. IC_{50} values were estimated as the dose of the cytotoxic drug that induces response equal to half of the maximum response observed.

3.3 Results.

3.3.1 AR-67 Lactone Is a Substrate of BCRP and MDR1.

BCRP and MDR1-expressing cell lines with validated expression and function (Figure 7-1 and 7-2 for BCRP and MDR1, respectively) were used to assess the interaction of AR-67 lactone with these efflux transporters. Initial studies demonstrated a time-dependent increase in intracellular amounts within the first 10 minutes. The intracellular amount of total AR-67 was then measured following 5 min incubation with a range of AR-67 lactone concentrations. Intracellular AR-67 amounts in MDCKII-BCRP (Figure 3-1, A) and NCI/ADR-RES cell lines (Figure 3-1, B) were lower than those in MDCKII-pcDNA and OVCAR-8 cells, respectively. The transporter effect was reversed when cells were pretreated with GF120918 (Figure 3-1, C and D), which is known to inhibit the drug efflux mediated by the ABCG2 and ABCB1 gene products [133, 134]. BCRP-mediated efflux of AR-67 lactone, in the presence and absence of GF120918, was also evaluated using polarized MDCKII transfected cells grown on Transwell® inserts. GF120918 had no effect on drug transfer from the apical to the basolateral side in MDCKII-pcDNA cells (Figure 3-2, A), but increased the transfer in MDCKII-BCRP cells (Figure 3-2, B). This is consistent with the apical expression of BCRP in polarized MDCKII cells [131]. GF120918 also attenuated AR-67 transfer from the basolateral to the apical side in MDCKII-pcDNA (Figure 3-2, C). However, the effect of GF120918 treatment on MDCKII-BCRP cells was more significant (Figure 3-2, D) when compared to the effect of GF on the MDCKII-pcDNA cells (Figure 3-2, C). This is consistent with the determination of the apparent permeability and efflux ratio values estimated (Table 7-1) for transport across BCRP expressing cell monolayers. Collectively, these data suggest that AR-67 lactone is a substrate for MDR1 and BCRP.

Our attempt to perform similar studies with AR-67 carboxylate yielded insignificant intracellular AR-67 amounts in monolayers and drug transfer across polarized cells (data not shown).
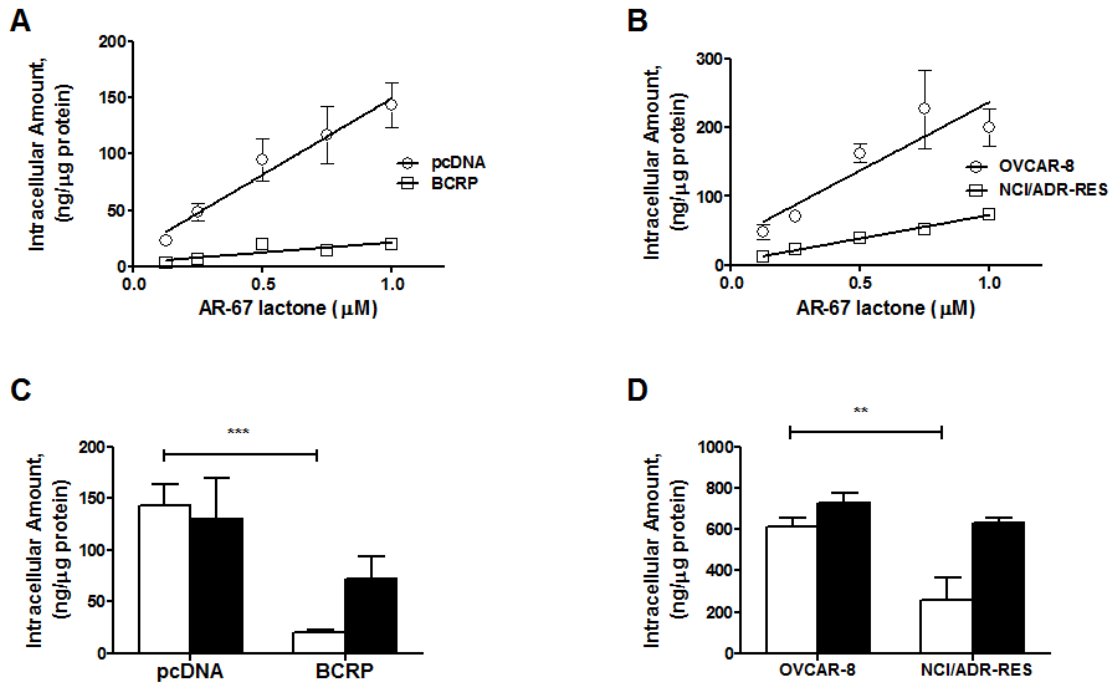
Figure 3-1. Effect of BCRP and MDR1 expression on the intracellular AR-67 amounts in MDCKII-pcDNA/BCRP and OVCAR-8/NCI/ADR-RES cells.

(A) MDCKII-pcDNA/BCRP and (B) OVCAR-8/NCI/ADR-RES cells were incubated with 0.125, 0.25, 0.5, 0.75 and 1 µM of AR-67 lactone for 5 min and the AR-67 intracellular amount was evaluated. The effect of the dual BCRP/MDR1 inhibitor GF120918 was tested by treating (C) MDCKII-pcDNA/BCRP and (D) OVCAR-8/NCI/ADR-RES cells without (open bars) and with (solid bars) GF120918 (5 µM for 1 h) prior to incubating with 1 µM AR-67 lactone for 5 min. At the end of the incubation periods, the cells were lysed and the intracellular AR-67 was quantified using HPLC as mentioned in the Materials and Methods section. Data are represented as mean (n=3) ± SD. Statistical analysis was performed using unpaired t-test, statistical significance for ** $p < 0.01$ and *** $p < 0.001$.
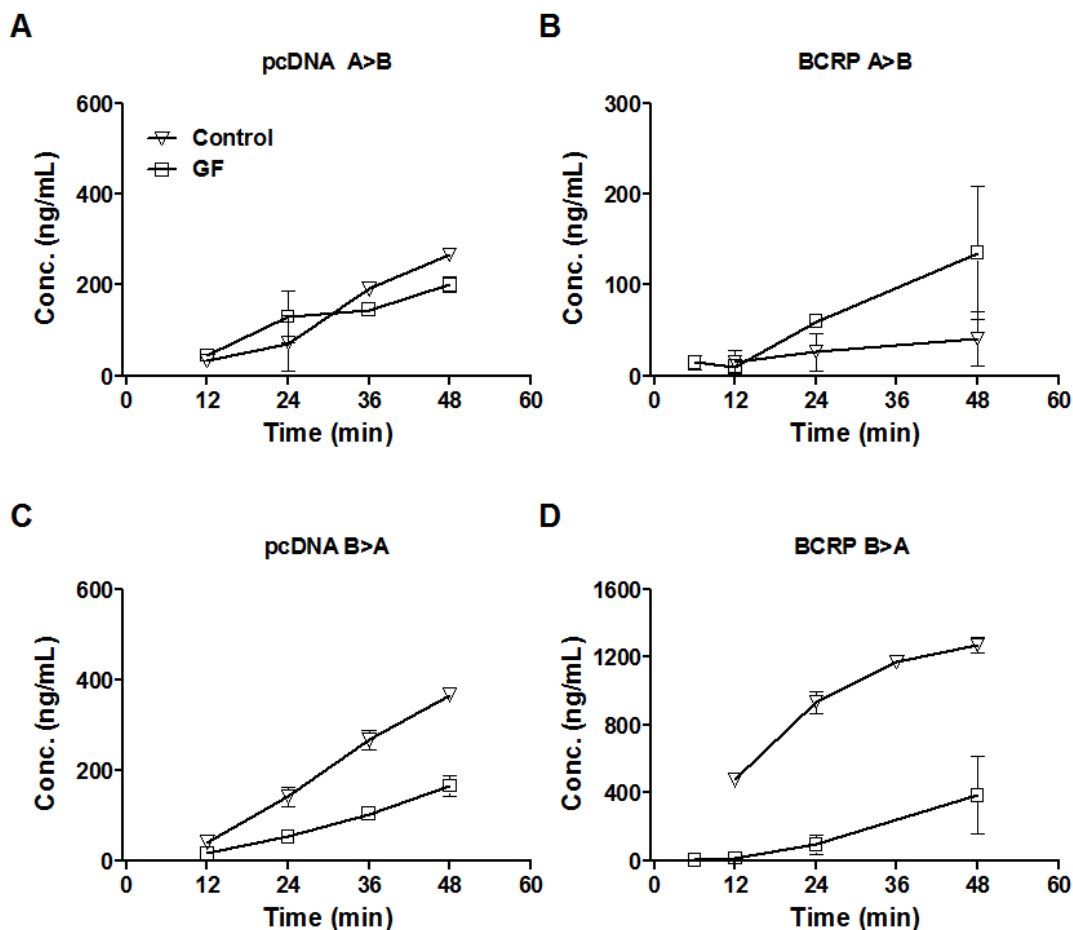
Figure 3-2. Effect of BCRP on the vectorial transport of AR-67 in MDCKII-pcDNA/BCRP cells.

Transepithelial transport of 5 µM AR-67 lactone in MDCKII-pcDNA and MDCKII-BCRP cells apical to basolateral (A, B) and basolateral to apical (C, D) in the presence and absence of the inhibitor GF120918 (5 µM). AR-67 was quantified using HPLC as determined in the Materials and Methods section. Data are represented as mean (n=3) ± SD.

45

www.manaraa.com

3.3.2 AR-67 Carboxylate is Transported by OATP1B1 and OATP1B3.

Previous *in vivo* pharmacokinetic studies demonstrated that AR-67 carboxylate has a relatively higher clearance than the lactone form [75]. Given the anionic nature of the carboxylate, we reasoned that rapid clearance may be through its increased uptake in the liver by organic anion transporters. Here, we assessed the uptake of AR-67 carboxylate in cells transfected with either SLCO1B1 or SLCO1B3. The expression of the OATP1B1 and OATP1B3 transporters was validated using RT-PCR analysis and immunohistochemistry while their function was evaluated using prototype substrates (Figure 7-3). Initial time-dependent studies showed rapid uptake of AR-67 carboxylate in both transporter expressing cell lines, but not in the mock transfected cells (data not shown). Subsequently, concentration-dependent uptake studies were conducted after incubation with AR-67 carboxylate for 1 min. The intracellular amount of total AR-67 was significantly higher in the OATP1B3 (HeLa-OATP1B3) and OATP1B1 (RKO-OATP1B1) expressing cells than that in the mock-transfected ones (Figure 3-3, A and B, respectively). The concentration-dependent uptake of AR-67 carboxylate by OATP1B3 (Figure 3-3, A) is consistent with saturable kinetics. The transporter mediated uptake was diminished by the addition of BSP (Figure 3-3, C and D) [65, 140]. Kinetic analysis also demonstrated higher affinity of AR-67 carboxylate for OATP1B3, than OATP1B1, with estimated K_m values of 0.32 μM and 2.58 μM, respectively. Additionally, incubation with the AR-67 lactone form did not result in significant uptake differences between OATP1B3 or OATP1B1 and mock transfected cells (data not shown).
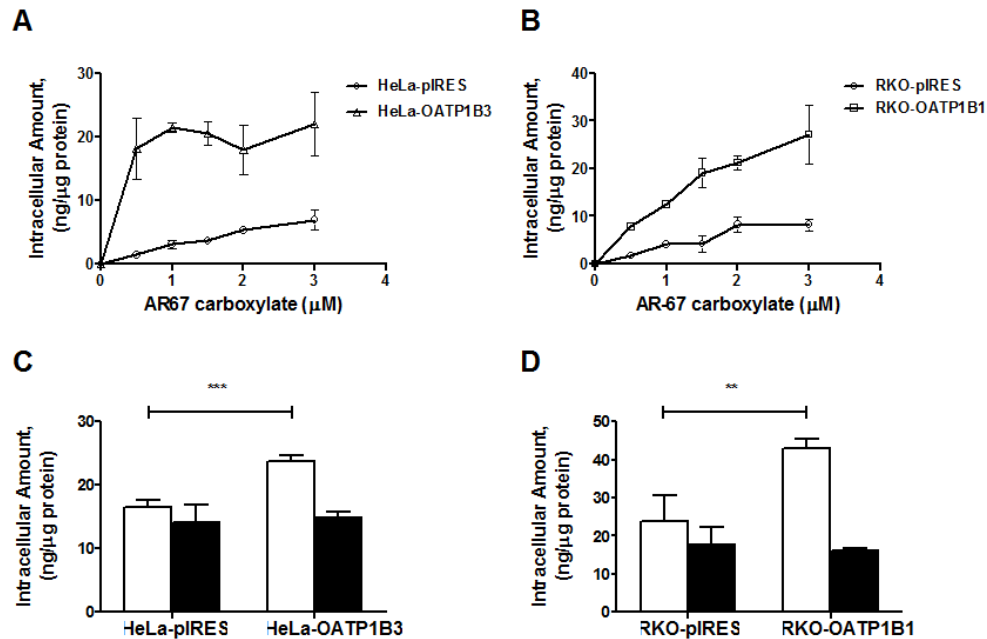
Figure 3-3. Effect of OATP1B3 and OATP1B1 expression on the intracellular AR-67 amounts in HeLa-pIRES/OATP1B3 and RKO-pIRES/OATP1B1 cells.

(A) HeLa-pIRES/OATP1B3 and (B) RKO-pIRES/OATP1B1 cells were incubated with 0.5, 1, 1.5, 2 and 3 μM of AR67 carboxylate for 1 min to study the dose-dependent uptake of the carboxylate form. The estimated K_m values for OATP1B3 and OATP1B1 were 0.32 (0.0-0.8316) μM and 2.58 (0.0-6.253) μM, respectively. They were obtained by using the Michaelis-Menten equation to fit the transporter mediated uptake of AR-67 as described in the Materials and Methods section and are reported as mean (95 % confidence interval). (C) HeLa-pIRES/OATP1B3 and (D) RKO-pIRES/OATP1B1 cells were incubated with 1 μM of AR-67 carboxylate for 5 and 10 min, respectively (open bars). The inhibitory effect of BSP (50 μM) was studied by pretreating for 10 min prior to exposure to AR-67 carboxylate as described previously for all cell lines (solid bars). Intracellular AR-67 was quantified using HPLC as determined in the Materials and Methods section. Data are represented as mean (n=3) ± SD. Statistical analysis was performed using unpaired t-test, statistical significance for ** $p<0.01$ and *** $p<0.001$.

3.3.3 BCRP and MDR1 Confer Resistance to AR-67 Lactone.

To evaluate the significance of the interaction between AR-67 lactone and the efflux transporters BCRP and MDR1, we assessed their potential for conferring drug resistance in the context of *in vitro* cytotoxicity studies. We found that BCRP confers a 10-fold resistance as measured by the differences in the estimated IC_{50} values between MDCKII-pcDNA and MDCKII-BCRP cells (Figure 3-4, A). The BCRP effect was negated in the presence of the transporter inhibitor GF120918 (Figure 3-4, B). Similarly, AR-67 lactone was significantly more cytotoxic to the OVCAR-8 than the NCI/ADR-RES cells as demonstrated by a 100-fold lower IC_{50} values (Figure 3-4, C). The transporter effect on the cytotoxic profile of AR-67 lactone was eliminated in the presence of GF120918 (Figure 3-4, D). To determine if sensitivity differences between transporter expressing and non-expressing cells were due to variability in the expression of the Top1 enzyme, we assessed its expression in the MDCKII-pcDNA/BCRP and OVCAR-8/NCI/ADR-RES cell lines (Figure 7-4). Our results indicated comparable Top1 protein expression between the control and transporter-expressing cell lines.
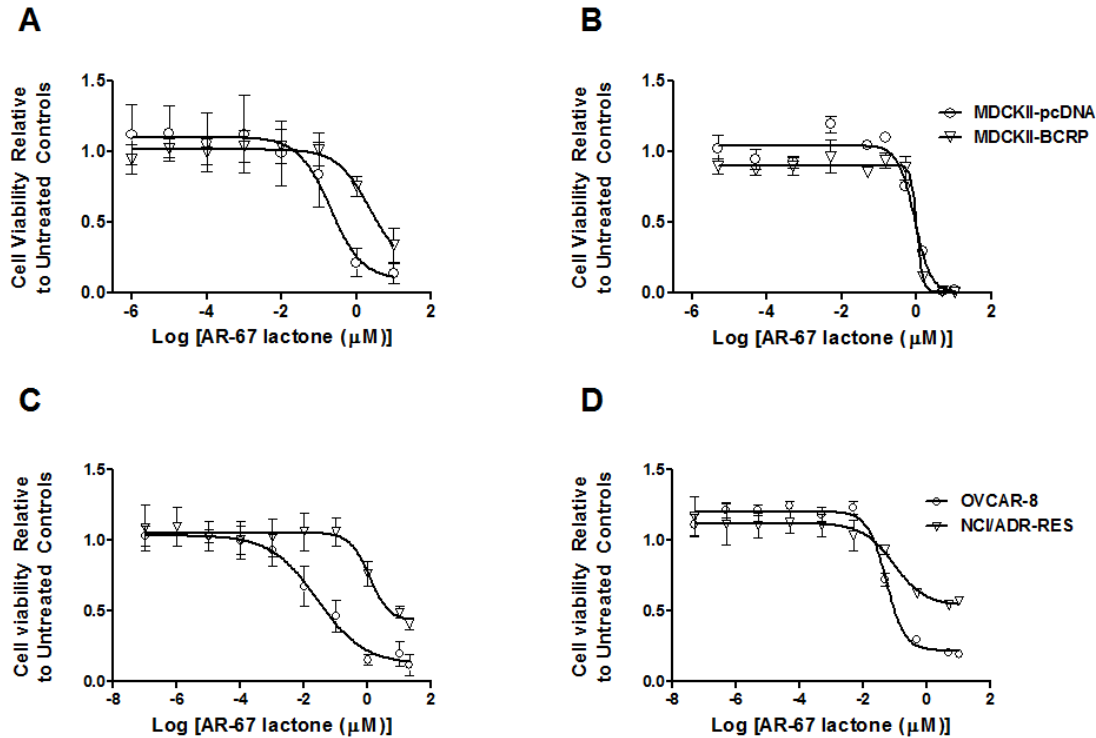
Figure 3-4. BCRP and MDR1 decrease the cytotoxicity of AR-67 lactone.

(A) Following 72 h drug incubation, IC_{50} values were estimated in MDCKII-pcDNA (0.21 µM, [0.11-0.40], Hill slope -1.269) and MDCKII-BCRP (2.37 µM, [1.41-4.00], Hill slope -0.0324), ** $p<0.01$, unpaired Student t-test). (B) After pretreatment (30 min) and in the presence of GF120918 and AR-67 lactone (72 h), IC_{50} values were obtained in MDCKII-pcDNA (0.88 µM, [0.72-1.09], Hill slope -1.979) and MDCKII-BCRP (1.02 µM, [0.79-1.32], Hill slope -5.357). (C) Similarly, IC_{50} values were estimated in OVCAR-8 (0.027 µM, [0.018-0.043], Hill slope -0.5908) and NCI/ADR-RES (1.16 µM, [0.79-1.70], Hill slope -1.399), *** $p<0.0001$, unpaired Student t-test). (D) After pretreatment (30 min) and in the presence of GF120918 and AR-67 lactone (72 h), IC_{50} values were obtained in OVCAR-8 (0.053 µM, [0.044-0.064], Hill slope -1.497) and NCI/ADR-RES cells (0.095 µM, [0.044-0.21], Hill slope -0.8837). The AR-67 lactone doses ranged from 10^{-7} to 21 µM. IC_{50} parameters and best fit lines were estimated by nonlinear regression analysis. Data are plotted as mean ± SD (n=3) and IC_{50} values (µM) are reported as (mean, [95 % confidence interval]).

3.3.4   OATP1B3 Expression Does Not Sensitize Cells to AR-67 Carboxylate.

Our study showed that OATP1B3 and OATP1B1, which are highly expressed in the liver [92-95], have the potential of transporting AR-67 carboxylate (Figure 3-3). However, several recent studies have reported that OATP1B3 is also expressed in tumor tissues [110-113]. To determine whether active uptake of the carboxylate could sensitize OATP1B3 expressing cells, we conducted cytotoxicity studies (Figure 3-5). The equivalent Top1 expression in HeLa-pIRES and HeLa-OATP1B3 was verified by Western blot (Figure 7-4). Initially the cytotoxicity of AR-67 carboxylate was assessed after 48 h of continuous drug exposure (Figure 3-5, D), but due to the reformation of the lactone upon incubation (Figure 3-6) we also determined the cytotoxicity after 0.5, 1, and 3 h (Figure 3-5, A-C) of drug treatment, which allows for relatively greater carboxylate exposure. As expected by the action of camptothecins during S-phase, longer incubation resulted in lower IC_{50} values (Figure 3-5, E). However, OATP1B3 expressing cells were not more sensitive than mock transfected cells.
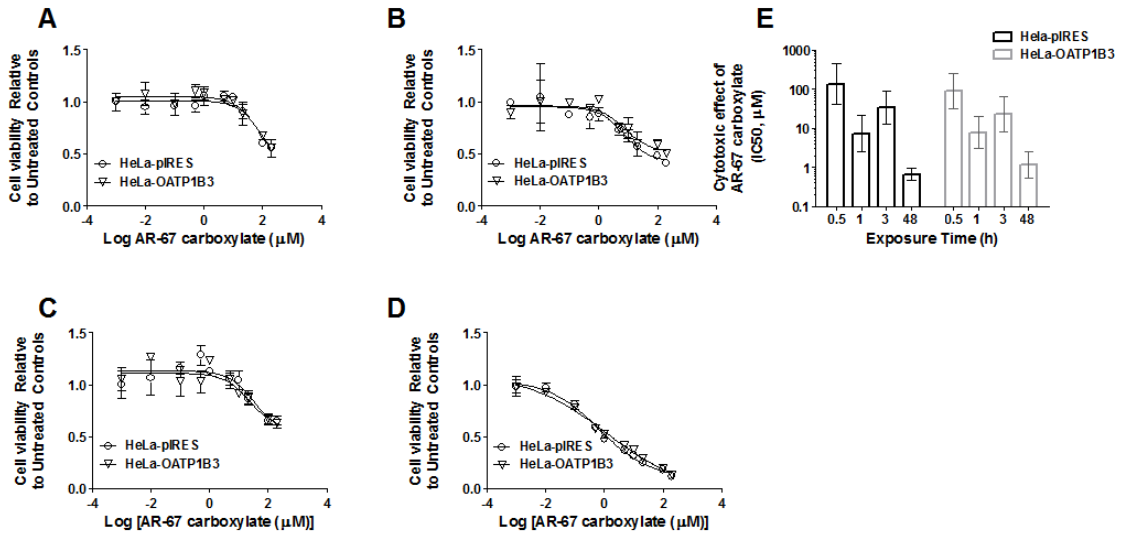
Figure 3-5. Time-dependent cytotoxic effect of AR-67 carboxylate on HeLa-pIRES and HeLa-OATP1B3 cell lines.

(A-D) HeLa-pIRES and HeLa-OATP1B3 cell lines were exposed to AR-67 carboxylate for 30 min (A), 1 (B), 3 (C) and 48 (D) h, as described in the Materials and Methods section. The AR-67 carboxylate doses ranged from 10^{-3} to 210 µM. (E) Summary of the cytotoxicity of AR-67 carboxylate on HeLa-pIRES and HeLa-OATP1B3 cells studied under the experimental conditions described in panels A to D. IC_{50} values to reflect the effect of AR-67 on cell viability were used. Cell viability was assessed at the end of the treatment as described in the Materials and Methods section. Nonlinear regression analysis was performed to model the data (solid line). Hill slopes for estimated HeLa-pIRES and HeLa-OATP1B3 IC_{50} values after 48 h incubation were -0.5053 and -0.3207, respectively. Data points on the graphs are reported as mean (n=3) ± SD and IC_{50} values (µM) are reported as mean, (95 % confidence interval).

A
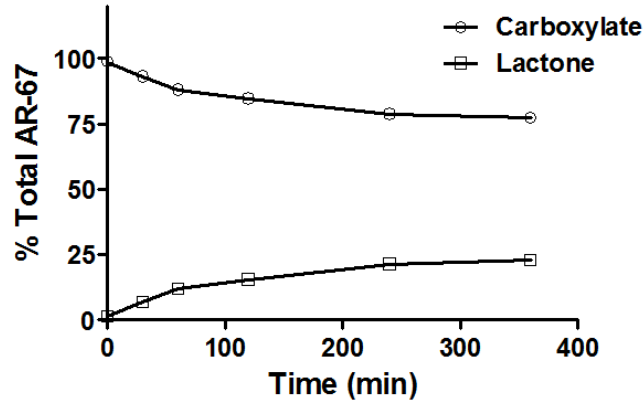
B
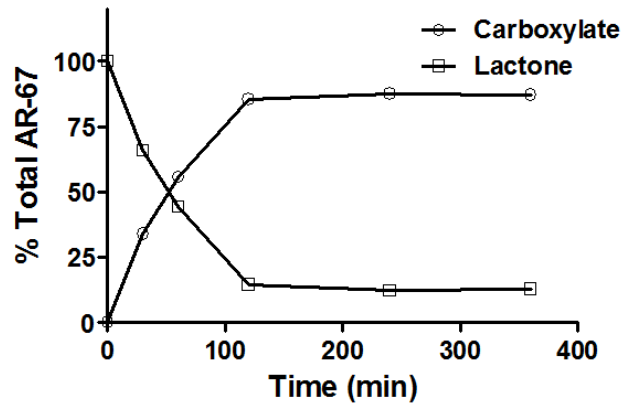
Figure 3-6. Stability of AR-67 in cell culture media.

The time course of AR-67 interconversion was studied in cell culture media (pH 7.4, 37 ºC, 5 % CO_2) after the addition of 1 µM of AR-67 carboxylate (A) or 1 µM of AR-67 lactone (B). Data are represented as the % ratio concentration of carboxylate or lactone over total drug.

3.3.5 Time-Dependent Intracellular AR-67 Uptake after Exposure to Lactone and Carboxylate.

To gain a better understanding of the apparent lack of sensitivity of OATP1B3 cells to AR-67 carboxylate (Figure 3-5), we determined the intracellular exposure to each AR-67 form. The intracellular uptake of AR-67 was assessed over 48 h after exposing cells to carboxylate (1 µM, Figure 3-7, A) or lactone (1 µM, Figure 3-7, B). The lactone form was found to dominate the intracellular compartment regardless of which form was added in the cell culture media (Figure 3-7). As expected, the intracellular AR-67 carboxylate amount was higher in the HeLa-OATP1B3 cells than in the HeLa-pIRES cells at all times and irrespective of the extracellular AR-67 form. However, the intracellular lactone amount was not different between the two cell lines, but it was significantly higher than the respective carboxylate one. The ratio of lactone to carboxylate increased from about 1, at 5 min, to 34 in the HeLa-pIRES and to 24 in the HeLa-OATP1B3 cell line after 48 h of incubation with AR-67 carboxylate (Figure 3-7, A). As expected, when AR-67 lactone was added in the cell culture media, it diffused rapidly into both cell lines and was about 100 times higher than the intracellular carboxylate at the 5-min time point (Figure 3-7, B). Although the amount of the intracellular carboxylate increased by almost 5 fold during the 48 h incubation, lactone dominated and lactone amounts were significantly higher than the carboxylate respective ones (Figure 3-7, B). Importantly, at steady state the intracellular lactone and carboxylate reached the same ratio regardless of which form was added in the cell culture media (Figure 3-7). Although carboxylate is the form that prevails in cell culture medium, after carboxylate (Figure 3-6, A) or lactone addition (Figure 3-6, B), this study demonstrates that the cells are exposed to significantly higher lactone amounts.

Notably, after 5 min of incubation with AR-67 carboxylate, intracellular AR-67 carboxylate accounted for 42 % and 55 % of the total drug in HeLa-pIRES and HeLa1B3 cells, respectively. This is the only time point with high intracellular AR-67 carboxylate amounts in the OATP1B3 cells compared to the respective lactone ones (Figure 3-7, A). To determine if this difference would be adequate to sensitize the OATP1B3 cells to carboxylate, we studied the cytotoxic effect of AR-67 carboxylate in Hela-pIRES and HeLa-OATP1B3 after drug exposure for 5 min, which was followed by 48 h growth. Although the IC_{50} values of carboxylate and lactone were lower in HeLa-OATP1B3 cells, as compared to HeLa-pIRES transfected cells, the differences were not statistically significant. As shown in Figure 3-8, A, the relatively increased exposure of OATP1B3 expressing cells to AR-67 carboxylate over the 5 min drug exposure did not result in significant sensitization. To verify this result we then assessed the effect of drug exposure on DNA damage by the induction of γ-H2AX [141-143]. In accordance with the lack of a transporter effect on cell viability (Figure 3-8, A), the degree of γ-H2AX activation after treatment with AR-67 carboxylate (Figure 7-5) did not differ between the HeLa-pIRES and the HeLa-OATP1B3 transfected cells. For comparison, the cytotoxic effect of lactone was also studied under the same experimental conditions with similar results in both cell lines (Figure 3-8, B). Overall, HeLa-pIRES and HeLa-OATP1B3 were more sensitive to the lactone rather than the carboxylate when the IC_{50} values were used to evaluate the cytotoxic effect of AR-67 (Figure 3-8).

54
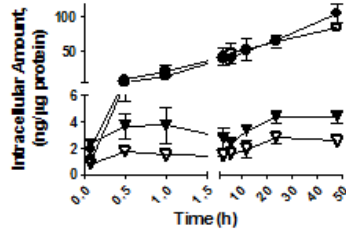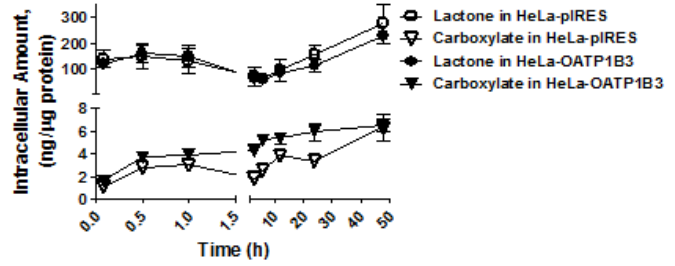
Figure 3-7. Time course of AR-67 carboxylate and lactone intracellular amount in HeLa-pIRES and HeLa-OATP1B3 cells after incubation with AR-67 carboxylate or lactone.

HeLa-pIRES and HeLa-OATP1B3 cells were incubated with 1 μM of the AR-67 forms, carboxylate (A) and lactone (B). AR-67 forms intracellularly were quantified by HPLC as described in the Materials and Methods section. Data are represented as mean (n=3) ± SD.
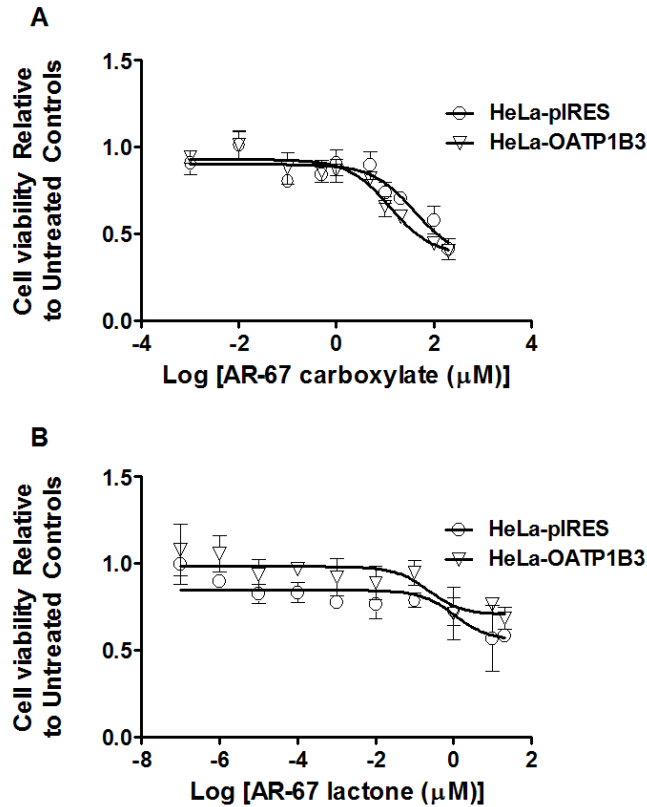
Figure 3-8. Effect of AR-67 carboxylate and lactone on HeLa-pIRES and HeLa-OATP1B3 cell lines.

(A) HeLa-pIRES and HeLa-OATP1B3 cells were treated with AR-67 carboxylate for 5 min, cells were washed, drug-free media was added in the wells and cells were allowed to grow for 48 h before assessing cell viability. The estimated IC_{50} values were 40.32 μM (16.36-99.33) and 13.08 μM (8.29-20.62) for HeLa-pIRES and HeLa-OATP1B3 cells, respectively. (B) HeLa-pIRES and HeLa-OATP1B3 cells were treated with AR-67 lactone for 5 min, cells were washed and drug-free media was added in the wells. The estimated IC_{50} values were 1.08 μM (0.20-5.70) and 0.23 μM (0.028-1.93) for HeLa-pIRES and HeLa-OATP1B3 cells, respectively. Data analysis to obtain IC_{50} values was performed using nonlinear regression (solid line). Data are presented as mean (n=3) ± SD and IC_{50} values (μM) are reported as mean (95 % confidence interval).

3.4 Discussion.

In this study, we demonstrated that BCRP and MDR1 transport AR-67 lactone. The MDCKII-BCRP cell line was found to be more resistant to AR-67 lactone treatment than the mock-transfected cells and MDR1 expression conferred resistance to the same anticancer agent using OVCAR-8 and NCI/ADR-RES cells. Additionally, we studied the interaction between AR-67 carboxylate with the uptake transporters OATP1B3 and OATP1B1 and showed that these transporters mediate its transport. However, the OATP1B3-expressing cell line did not show increased sensitivity to AR-67 carboxylate in validated *in vitro* systems. In an effort to study the factors that play a role on the antitumor activity of AR-67 *in vitro*, we quantified both AR-67 forms intracellularly after treatment with either AR-67 lactone or carboxylate. Interestingly, our intracellular uptake data indicated that the AR-67 lactone was favored intracellularly and overcame the OATP1B3-mediated increased intracellular uptake of AR-67 carboxylate by fifty-fold. This may explain why the uptake of AR-67 carboxylate does not sensitize OATP1B3 expressing cells.

Based on the physicochemical properties of the AR-67 lactone and carboxylate, we expected that both efflux and uptake transporters would interact with AR-67. Studies have shown that MDR1, and possibly BCRP, transport substrates that have the potential for partitioning into the lipid bilayer and are mostly lipid-soluble moieties with planar aromatic rings [67], like AR-67 lactone. Conversely, OATP1B1 and OATP1B3 proteins selectively transport anions [65], such as AR-67 carboxylate. Therefore, in our studies we adjusted the pH to ensure the exposure of cells to AR-67 lactone or carboxylate, as needed. Furthermore, the exposure and incubation times for transport and cell viability assays were considered in the context of lactone/carboxylate conversion kinetics.

Our studies showed that AR-67 lactone is a substrate of BCRP and MDR1 (Figure 3-1). This is in accord with previous publications showing similar results with topotecan [67, 116]. Other camptothecin analogs have also been shown to be substrates of BCRP, which was reported to transport irinotecan, SN-38 and SN-38 glucuronide [117, 118, 144]. Our studies also showed that AR-67 carboxylate is transported by OATP1B1 and OATP1B3 (Figure 3-3). Previous studies have shown that irinotecan and its metabolite SN-38 are substrates of OATP1B1 [119]. However, Yamaguchi et al showed that SN-38, but not irinotecan, can be taken up by OATP1B3 [121]. Finally, *in vitro* studies have shown that among the lipophilic camptothecins, gimatecan and karenitecin, but not lurtotecan, are substrates of OATP1B1 [120]. However, the authors did not indicate which form was transported.

After identifying AR-67 lactone as a BCRP substrate, we used the MDCKII-pcDNA/BCRP cell lines to demonstrate that BCRP expression confers resistance to treatment with the lactone form (Figure 3-4, A). Our findings agree with findings from other studies on camptothecins. BCRP expressing lung cancer cell lines appeared to be more resistant to SN-38, than the parent cell line [145]. Moreover, studies in metastatic hepatic tumor tissue indicated that BCRP might be implicated in the development of resistance specifically to irinotecan-based chemotherapy *in vivo* [101]. Despite the significant expression of BCRP in certain cancer types and especially in a small subpopulation of primitive stem cells [115], definitive clinical relevance of BCRP expression in tumor tissues has yet to be proven. Additionally, as a result of the MDR1-mediated efflux of AR-67 in NCI/ADR-RES cells (Figure 3-1, B and D), as compared to OVCAR-8 cells, a resistance phenotype was observed (Figure 3-4, C). Previous studies have been suggestive of the prognostic role of MDR1 in leukemia patients treated with anthracyclines [102, 103], established substrates of MDR1. However, further studies are

required to evaluate the impact of an MDR1-AR-67 interaction on clinical response in cancer patients.

Both *in vitro* and clinical studies have indicated that OATP1B3 facilitates the cytotoxic effect of paclitaxel [146, 147]. Here, we tested if OATP1B3 would sensitize cells after exposure to the anionic AR-67 carboxylate. Our studies showed that the observed cytotoxic effect was not different between HeLa-pIRES and HeLa-OATP1B3 cells irrespective of the exposure time to the carboxylate (Figure 3-5). However, the cytotoxic effect of AR-67 carboxylate increased in a time-dependent manner consistent with its mechanism of action targeting cells primarily in their S-phase. In addition, comparable activation of the DNA damage marker γ-H2AX (Figure 7-5) in HeLa-pIRES and HeLa-OATP1B3 cells after 5 min exposure to AR-67 carboxylate was consistent with the absence of OATP1B3 effect on cell viability (Figure 3-8, A). The quantification of the intracellular levels of both AR-67 forms suggest that the lipophilic lactone diffused freely in the cell while the transfer of the carboxylate form into the cytoplasm was a slow and transporter-mediated process, limited by saturable kinetics (Figure 3-7). Ultimately, the intracellular lactone/carboxylate steady state amounts, independent of the extracellular lactone/carboxylate kinetics (Figure 3-6), suggested that the AR-67 carboxylate-induced cytotoxic effect was restricted due to its physicochemical properties. Notably, the same intracellular lactone-carboxylate amount ratio was observed when cells were exposed to either lactone or carboxylate suggesting that the interconversion between the two forms depended strictly on intracellular factors (Figure 3-7). Rapid conversion of carboxylate to the lactone form in the cytoplasm due to protein-binding cannot be excluded. Moreover, although the intracellular pH would favor carboxylate formation, the AR-67 intracellular distribution pattern could be similar to the one observed for third generation lipophilic

59

camptothecin gimatecan, which partitions into lysosomes where the lactone form is favored due to low pH conditions [148].

The microenvironment of solid tumors is characterized by hypoxia and low pH as a result of disorganized vasculature and underdeveloped lymphatic system [149, 150]. Previous studies have shown increased transport activity of BCRP and MDR1 at acidic conditions [151, 152] and pH-sensitive transport activity of OATP1B3 [153]. Therefore, further studies on the AR-67 cytotoxic effect under low pH conditions are necessary.

The first-in-human study showed that approximately 87 % of total AR-67 quantified in the blood was in the lactone form and that AR-67 is primarily eliminated through the liver [78]. However, pharmacokinetic modeling of preclinical data demonstrated that the apparent stability was due to increased carboxylate clearance [75]. Our findings suggest that OATP1B1 and OATP1B3 hepatic expression is the likely mechanism for this clearance and thus it may play a key role in the disposition of AR-67. These studies, therefore, demonstrate how transporters can play a key role in drug disposition without having a significant role in cellular uptake and tumor responsiveness.

Multiple studies have underlined the importance of efflux and uptake transporters in the disposition of anticancer agents. Furthermore, genetic polymorphisms in ABCG2 and ABCB1 that were identified in patients receiving irinotecan and diflomotecan, respectively, resulted in altered pharmacokinetics and pharmacodynamics [154-157]. Additionally, SLCO1B1 polymorphisms possibly related with the toxicity profile of irinotecan and other cytotoxic agents have been reported [69, 158, 159]. Similarly, the clinical impact of *in vitro* identified OATP1B3 polymorphisms need to be explored further in well-designed large-scale human trials [146, 160]. In line with these studies and our

results, future studies should explore further the potential role of BCRP, MDR1, OATP1B1 and OATP1B3 polymorphisms on the transport of AR-67.

In conclusion, our study demonstrated that AR-67 lactone is a substrate of the ATP-binding cassette transporters MDR1 and BCRP. Additionally, both BCRP- and MDR1-mediated efflux of AR-67 lactone conferred resistance using validated *in vitro* models. The clinical significance of these findings need to be explored further. Although our *in vitro* work suggests that OATP1B3 expression might not increase the efficacy of AR-67 given to cancer patients expressing the transporter in the tumor tissue, we demonstrated that AR-67 carboxylate can be transported by the OATP1B1 and OATP1B3 transporters. Taking into consideration the liver-specific expression of these uptake transporters [92, 93, 95] and the impact of carboxylate clearance on exposure to AR-67 [75], we reason that they may be playing a key role in the elimination of AR-67.

61

4. Chapter 4: Protracted dosing of the lipophilic analogue AR-67 in non-small cell lung cancer xenografts and humans

4.1 Introduction.

AR-67 [37] is a novel, lipophilic camptothecin analog of the silatecan group. Camptothecin analogs are anticancer agents that confer their anticancer effect via interaction with the DNA/Top1 complex, primarily during replication [4, 161]. As with many cytotoxic anticancer agents, the camptothecin analogue dose range that separates optimum response and the onset of toxicity can be narrow [41, 162, 163] and much effort has been expended to increase the anticancer effect while minimizing toxicity [33].

Given that not all cells within a tumor mass are undergoing replication at any given time, it was reasoned that more frequent camptothecin dosing would facilitate increased efficacy. Indeed, studies in xenograft models clearly demonstrated that protracted dosing schedules were more efficacious than shorter courses of therapy with higher doses [125-128, 164]. However, when protracted low-dose schedules were tested in the clinic, response rates were lower than expected [123, 124]. In part, this may have reflected species differences in pharmacokinetics as well as differences in tolerating therapy considering the generally poor performance status of patients enrolled in early phase clinical trials [123, 165]. Further studies showed that efficacy could be improved when the therapeutically active drug exposure seen in animals could also be achieved in humans [166]. Although, these approaches increased the reliability and accuracy of the preclinical models, the goal of identifying the optimal dosing schedule for camptothecins in humans has not yet been determined.

Here we sought to assess the efficacy and toxicity of AR-67 by considering its pharmacokinetics and biodistribution in non-small cell lung cancer xenografts (NSCLC), the dose dependent degradation of Top1 in tumor tissue and the expression of protein markers that are indicative of camptothecin-induced DNA damage. First, we determined the MTD of AR-67 in mice using the clinically relevant endpoint of hematologic toxicity. Subsequently, we evaluated the survival of NSCLC xenografts that received AR-67 at a dose cumulatively equal to the previously determined MTD, but administered at protracted dosing schedules. Moreover, we assessed the effect of different dosing schedules of AR-67 on the expression of Top1 and other apoptosis proteins to determine the optimal dose. Finally, to define the most appropriate dosing schedule in the clinic, we determined the tumor biodistribution of AR-67 in a pilot clinical study. Not unlike targeted therapies, our studies suggest that camptothecin analogues should be developed by considering not only their maximum tolerated dose, but also their effect on the molecular target, Top1.

4.2 Materials and Methods.

4.2.1 Chemicals and Reagents.

Magnesium- and calcium-free Dulbecco's phosphate buffered saline (PBS) was purchased from Gibco Invitrogen (Carlsband, CA). 5% Dextrose in water (D5W) was from Baxter Healthcare Corporation (Deerfiled, IL). AR-67 for preclinical studies was obtained from Novartis (East Hanover, NJ). Arno Therapeutics (Flemington, NJ) provided AR-67 for clinical use. The solid compound was stored at $-80^{\circ}C$. AR-67 lactone solutions were prepared by reconstituting lyophilized AR-67 with 5% Dextrose in water (D5W) and stored at $-20°C$ protected from light until ready for use in *in vivo* studies.

4.2.2 Preclinical Studies.

4.2.2.1 Cell Lines.

Non-small cell lung cancer NCI-H460 (ATCC, Manassas, VA) were grown and subcultured in Dulbecco's Modified Eagle Medium (Fisher Scientific, Fair Lawn, NJ) supplemented with Fetal Bovine Serum (Gibco, Invitrogen Corporation, Carlsbad, CA), in the absence of antibiotics. Cells were maintained at 37°C in a humidified atmosphere containing 5 % CO_2. No further cell line authentication in addition to the one offered by ATCC (Mycoplasma testing and Short Tandem Repeat profiling) was performed as cells were used within 6 months after purchase from the vendor.

4.2.2.2 Animal Studies.

Maximum tolerated dose, pharmacokinetics and antitumor efficacy studies were conducted using female athymic nude mice (nu/nu, Harlan Laboratories). All experiments were approved and conducted following the guidelines set by the University of Kentucky's Institutional Animal Care and Use Committee. In all studies AR-67 was administered through the tail vein as an intravenous (iv) bolus. In tumor bearing mice,

the tumor volume (V) was calculated by using the formula: $V = (D1 \times (D2)^2 \times \pi) / 6$ where D1 and D2 are the length and width of the tumor mass, respectively, and D1>D2. Tumor dimensions were measured using a Vernier caliper.

To determine the MTD, non-tumor bearing mice were administered various dosages (n=3/dosage) of AR-67 daily for five consecutive days and white blood cell (WBC) counts were measured using a Heska Vet Blood analyzer on days 5, 9, 12, and 22. A WBC count below 500/μL was selected as indicative of neutropenia and to signify life-threatening therapy-induced toxicity. Tolerability to camptothecin toxicity was also evaluated by calculating the percentage change of body weight from day 1. Body weight loss exceeding 10% signified toxicity.

The antitumor activity of AR-67 lactone administered following differing dosing schedules was assessed using NCI-H460 xenografts. AR-67 lactone was administered as presented on Figure 7-6, A. Control animals received D5W. Animals (n=5-8/treatment) were monitored individually for tumor volume and survival. Mice were euthanized when their tumor volume exceeded 1500 mm^3, which was used as a surrogate point for mortality.

To assess the effect of exposure to AR-67 lactone on protein expression at the tumor tissue, NCI-H460 tumor bearing animals were used. They received AR-67 lactone as described on Figure 7-6, B. Control animals were treated with the drug vehicle. Tumor tissues from control- and drug-treated animals were collected 6 hours after AR-67 administration on the last treatment day. The tumor tissue was snap-frozen in liquid nitrogen and stored at -80°C in cryopreservation vials until processed for protein isolation and western blot analysis.

65

Finally, to study the plasma pharmacokinetics and tumor biodistribution of AR-67, animals bearing tumors >50 mm^3 were randomized into groups (n=3 animals/time point) that received 1 or 5 mg/kg of AR-67 lactone. Non-tumor bearing nu/nu mice were used to study the normal tissue biodistribution of AR-67. Blood samples and tissues were collected at select time points. AR-67 concentrations were quantified using a validated bioanalytical method [137].

4.2.3 Clinical Study.

4.2.3.1 Patients.

Patients (ages ≥ 18 y, n=3) with refractory and metastatic solid tumors were eligible to participate in this study. Eligibility and exclusion criteria were similar to those of the previously reported phase I clinical trial [78], with the exception of the exclusion of strong CYP3A4 substrates, inhibitors and inducers.

4.2.3.2 Drugs and Study Design.

The present study was approved by the Markey Cancer Center Protocol Review Committee and the University of Kentucky Institutional Review Board. Patients provided written informed consent before participating in the trial.

AR-67 was prepared by reconstituting lyophilized AR-67 with D5W to a final concentration between 0.05 mg/mL and 0.5 mg/mL. Within four hours of reconstitution, the total volume of AR-67 was infused iv over one hour via an infusion pump using non-polyvinyl chloride (PVC) bags and tubing, as previously reported [78].

In this pilot trial, patients were to receive AR-67 (7.5 mg/m^2/day) on days 1, 4, 8, 12 and 15 of a 21-day cycle. This was equivalent to the cumulative MTD determined during the previous phase I study in which patients were treated with the same dosage on days 1-5 of a 21-day cycle [78]. However, the first participant experienced grade 4 hematological

toxicities and as determined in the study protocol, dose de-escalation was performed and the two remaining patients received 5.5 mg/m^2/day on days 1, 4, 8, 12 and 15.

The pharmacokinetic profile of AR-67 was studied on day 1 of cycle 1 in all patients. Blood samples were collected pre-dose, 5, 45 and 65 minutes, 1.5, 2, 4, 6 and 24 hours after the start of the infusion. AR-67 was quantified in the extracted plasma using an HPLC method [137]. Additionally, two core-needle biopsies of primary tumor or metastasis were obtained from each patient. The biopsies were performed between 3 and 24 hours after the beginning of the infusion on day 1 of cycle 1 and were at least 3 hours apart. Core-needle tumor biopsies were obtained under ultrasound/computed tomography (CT) guidance or direct visualization. The tissue was snap-frozen to avoid protein and AR-67 degradation. Expression levels of Top1 and γH2AX were evaluated in the tumor tissue using western blot analysis. A portion of the tumor tissue was also used to measure AR-67 concentrations. Standard (calibration) curves and quality control samples were prepared in xenograft tumor tissue and AR-67 was quantified by HPLC, as previously described [137].

4.2.3.3 Assessment, Follow-up and Monitoring.

Toxicity was graded using the National Cancer Institute Common Toxicity Criteria 4.0 (CTCAE 4.0). DLT was defined as any of the following that are possibly, probably or definitely related to AR-67 (during the first course of therapy): any grade 5 toxicity, grade 4 neutropenia of > 7 days duration, or grade 4 neutropenia with fever (>101^{0}F) or infection of any duration, grade 4 thrombocytopenia, any grade 3 or 4 non-hematologic toxicity with the exception of grade 3 nausea and/or vomiting, grade 3 diarrhea of brief duration, grade 3 fever (with or without neutropenia) or any grade alopecia). Patients were considered evaluable for a DLT if they received at least 3 planned doses of AR-67 in cycle 1 and had either: proceeded to cycle 2 of therapy, or been followed for at least

28 days and met criteria for starting cycle 2. Tumor response was assessed every two cycles of therapy based on the Response Evaluation Criteria in Solid Tumors (RECIST) (version 1.1) [167]. Tumor volume was measured by computer tomography scan or magnetic resonance imaging. In the case of complete or partial response or stable disease, patients were allowed to receive AR-67 for up to 6 cycles.

4.2.4   Immunoblot Analysis.

Tumor tissue was removed from the -80°C storage and allowed to thaw at 4°C. Tissue homogenate was prepared as described previously and in the presence of protein inhibitors (Complete Mini, Roche Diagnostics GmbH, Manheim, Germany). Protein content was determined using a colorimetric assay as per the manufacturer's protocol (BCA Protein Assay, Thermo-Fisher Scientific, PA). The samples were electrophoresed using standard procedures; membranes were incubated with anti-Top1 (Abcam, Cambridge, MA), anti-γH2AX, anti-cl-caspase 3 and anti-caspase 3, anti-PARP and anti-cl-PARP (dilution 1:1000) (Cell Signaling, Danvers, MA) and anti-actin (dilution 1:2000) (clone AC-15, Sigma-Aldrich, St. Louis, MO) overnight at 4°C. Actin was used as loading control. Protein expression was quantified by performing densitometry analysis and using the Molecular Imaging Software (version 4.04, Eastman, Kodak, New Haven, CT)

4.2.5   Pharmacokinetic and Statistical Analysis.

AR-67 pharmacokinetic parameter estimates were obtained by performing non-compartmental analysis using Phoenix WinNonLin 6.2 (Pharsight, CA). GraphPad Prism (version 5.01, GraphPad Software Inc., San Diego, CA) was used for statistical analyses and graphical data representation. Exposure to AR-67 was evaluated by calculating the Area Under the Curve (AUC) of the plasma or tissue concentration versus time graphs (0 to 6 h) (GraphPad Prism) using the trapezoidal rule. Effects of AR-67 dosing schedules on survival of xenograft bearing mice was assessed using Kaplan-Meier

survival analysis. Median survival times were compared using one-way ANOVA and the

Tukey test for multiple comparisons, $p<0.05$ for statistical significance. Animals removed

from the study were no longer plotted in the tumor growth curves. Data are presented as

[mean; error bars, SD].

4.3 Results.

4.3.1 Toxicity Profile of AR-67 in Nude Mice.

Historically, body weight has been used as a marker of drug-induced toxicity in animal models. However, in the clinical setting neutropenia is one of the major DLT associated with exposure to camptothecins [41, 78]. Therefore, animals that received AR-67 were monitored for both weight loss and hematological toxicity. Notably, the WBC counts of the drug-treated animals decreased in a dose-dependent manner (Figure 4-1, A). On day 5, animals that received 10 and 15 mg/kg AR-67 had WBC counts indicative of neutropenia, but these counts returned to normal within 4 days after the end of the treatment (Figure 4-1, A). Percent change in body weight is shown in Figure 4-1, B. The most pronounced decrease in body weight was 6.8 and 7.3 % in animals that received 10 and 15 mg/kg AR-67, respectively. Treated animals regained weight after treatment cessation. Comparatively, monitoring the WBC counts was a better marker of drug-related toxicity than tracking changes in body weight. In view of these findings, the MTD of AR-67 lactone was 7.5 mg/kg given daily as an iv bolus for 5 consecutive days.
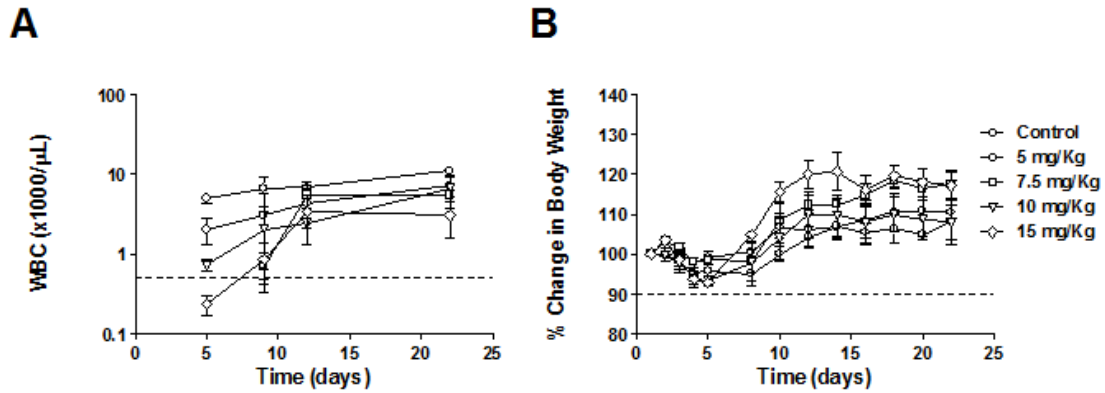
Figure 4-1. Effect of AR-67 treatment on white blood cell count and body weight in non-tumor bearing nude mice.

Animals received AR-67 lactone daily for five consecutive days at doses equal to 5, 7.5, 10 and 15 mg/kg as indicated by arrows. White blood cell counts (A) were obtained on days 5, 9, 12 and 22 and body weight (B) was monitored daily during the treatment period and on days 8, 10, 12, 14, 16, 18, 20 and 22. Dashed lines (at Y=0.5 for panel A and at Y=90 for panel B) signify AR-67-induced toxicity associated with decrease of the white blood cell population at levels indicative of neutropenia (500/µL) (A) or with 10% loss of body weight (B). Data points consist of 3 mice per time point; bars, SD.

4.3.2 Antitumor Activity of AR-67 In NSCLC Xenografts.

Previous studies have indicated schedule-dependent antitumor activity for camptothecins [125-128]. To replicate those findings with AR-67, NSCLC xenografts received AR-67 at differing dosing schedules. Tumor volume and survival curves of NSCLC xenografts are depicted in Figure 4-2. Treatment with AR-67 lactone inhibited tumor growth in NCI-H460 NSCLC tumor bearing mice (Figure 4-2, A). Contrary to the more intense dosing schedule (7.5 mg/kg, Dx5), the AR-67 protracted dosing schedules (3.75 mg/kg, Dx5x2 and 2.5 mg/kg, Dx5x3) resulted in longer survival time (p<0.05) than vehicle treated animals. However, survival was comparable between the animals being treated with the 3.75 mg/kg, Dx5x2 and 2.5 mg/kg, Dx5x3 dosing schedules (p>0.05).
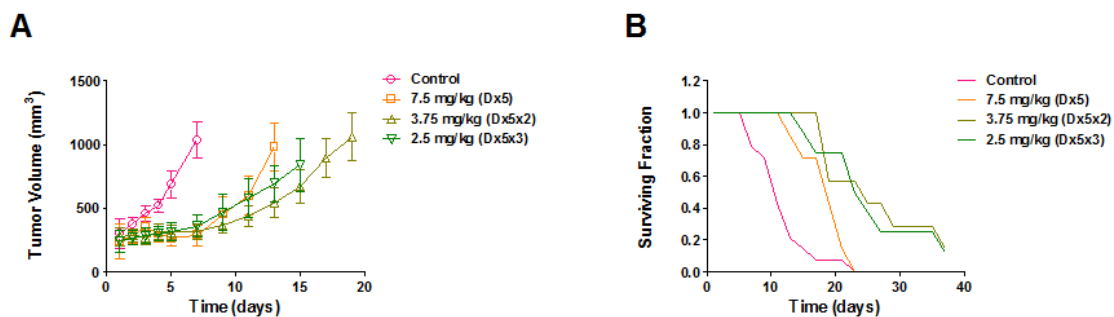
Figure 4-2. Antitumor effect of AR-67 in NSCLC xenografts.

Tumor growth (A) and survival curves of nude mice bearing NCI-H460 tumors (B). NCI-H460 tumor-bearing nude mice received AR-67 lactone or D5W as an iv bolus following varying dosing schedules. Groups consisted of 7-8 mice per treatment; bars, SD.

4.3.3 Schedule-dependent Biological Effects of AR-67 In Tumor Tissue Obtained From NSCLC Xenografts.

Previous studies have demonstrated a reversible decrease in the expression of Top1 as a resistance mechanism used by cancer cells treated with camptothecins, including AR-67 [9, 168]. Here we assessed the effect of different dosing schedules on the expression level of Top1 and other proteins implicated in the mechanism of action of AR-67. As presented in Figure 4-3, western blot analysis showed that Top1 expression is inversely related to the dose administered and is maintained at higher levels when AR-67 is given intermittently at low doses. Subsequently, we evaluated if the sustained expression of Top1 correlated with DNA damage. Previous studies have indicated that phosphorylation of H2AX (γH2AX) is directly associated with camptothecin-induced DNA damage leading to its evaluation as a biomarker of response to camptothecins [141-143]. In our study, γH2AX expression appeared to be schedule-dependent with highest protein levels being detected in tissue samples obtained from the low-dose 3.75 mg/kg, Dx5x2 and 2.5 mg/kg, Dx5x3 treatment groups (Figure 4-3). We then probed further for the effect of DNA damage by assessing cleaved PARP (cl-PARP). Typically, cleavage of total PARP after exposure to cytotoxic agents is suggestive of cellular disassembly and apoptosis [169, 170] and is mediated by cleaved caspase 3 (cl-caspase 3), the active form of caspase 3 [171]. Specific to camptothecin analogue treatment, PARP cleavage was detected in tumor biopsies obtained from colon cancer patients before and after irinotecan administration [172]. In our xenograft model, western blot analysis showed expression levels of cl-caspase 3 and cl-PARP in the animals of the 2.5 mg/kg, Dx5x3 and 3.75 mg/kg, Dx5x2 treatment groups. On the contrary, the animals of the 7.5 mg/kg, Dx5 treatment group had non-detectable levels of cl-caspase 3 and cl-PARP (Figure 4-3).
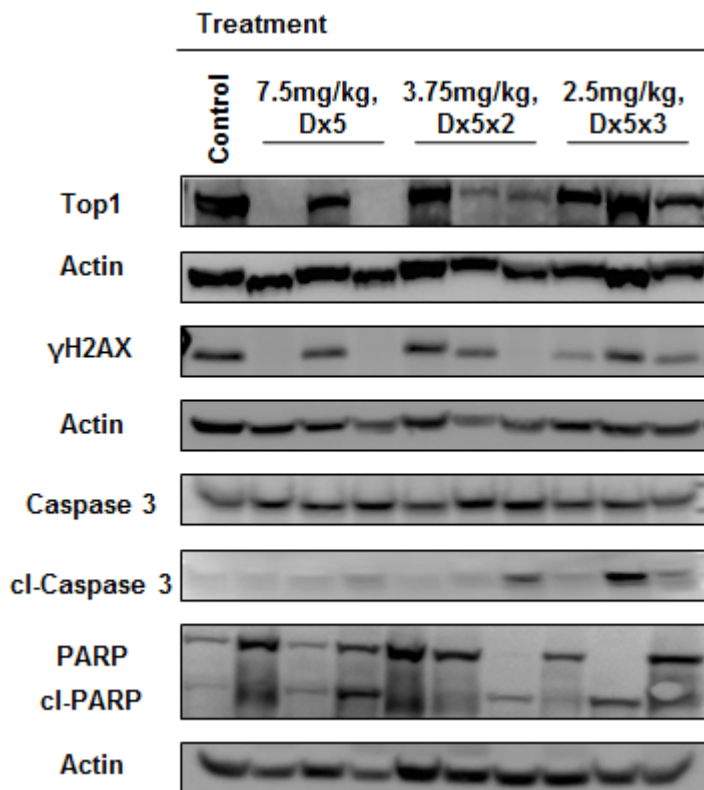
Figure 4-3. Biological activity of AR-67 lactone in NSCLC xenografts.

Evaluation of the expression level of Top1, γH2AX, cl-caspase 3, caspase-3, cl-PARP and PARP in tumor tissue obtained from NCI-H460 xenografts using western blot analysis. Actin was used as a loading control. Groups consisted of 3 mice per treatment; bars, SD.

4.3.4   AR-67 Plasma And Tumor Pharmacokinetics In NSCLC Xenografts.

Drug partitioning and achieving pharmacologically relevant concentrations at the tumor tissue are essential for antitumor activity [173, 174]. In addition, considering the high lipophilicity of AR-67 lactone, we sought to determine its tumor and tissue biodistribution so that we could facilitate the design of an optimal dosing schedule. Plasma and tumor concentration profiles of total (lactone and carboxylate) AR-67 in NCI-H460 tumor bearing nude mice after the intravenous administration of 1 and 5 mg/kg of lactone are presented in Figure 4-4, A and B, respectively. Following administration, the plasma concentration of total AR-67 rapidly decreased bi-exponentially. AR-67 partitioned into the tumor tissue and maximum concentrations were observed at 5 min and 45 min after doses 1 and 5 mg/kg of AR-67, respectively. The elimination half-life ($t_{1/2}$) (mean (±SD)) of AR-67 in plasma was 1.4 h (± 0.4) and 1.4 h (± 0.3) after administration of 1 and 5 mg/kg of lactone, respectively. Interestingly, the half-life at the tumor tissue was 4.0 h (± 1.8) and 16.1 h (± 7.9) after administration of 1 and 5 mg/kg of AR-67, respectively. Collectively, these data suggest that the elimination of AR-67 takes place at a slower rate from the tumor compared to the plasma compartment.

Dose-normalized systemic and tumor exposures are depicted in Figure 4-4, C. The dose normalized AR-67 AUC was equivalent for the 1 and 5 mg/kg dosages suggesting linear pharmacokinetics in plasma, which is consistent with the previous observation in the first in man study [78]. On the contrary, in the tumor tissue the dose normalized AUC of the 5 mg/kg dose was more than 3 times higher than that of the 1 mg/kg dose. These results suggest non-linear kinetics of AR-67 at the tumor tissue. To determine whether this was a tumor-specific phenomenon, we also measured AR-67 in lung, heart, liver, kidney and brain after dosing animals with 1 mg/kg (data not shown) and 5 mg/kg (Figure 4-4, D). AR-67 partitioned in all organs, with highest amount identified in the liver. Interestingly,

AR-67 appears to be eliminated faster from normal tissues, than from tumor tissue, with $t_{1/2}$ ranging from 1.0 h ($\pm$ 0.1) to 1.4 h ($\pm$ 0.4) in the liver, kidney, brain, and lung of animals receiving the 5 mg/kg dosage (Figure 4-4, D).
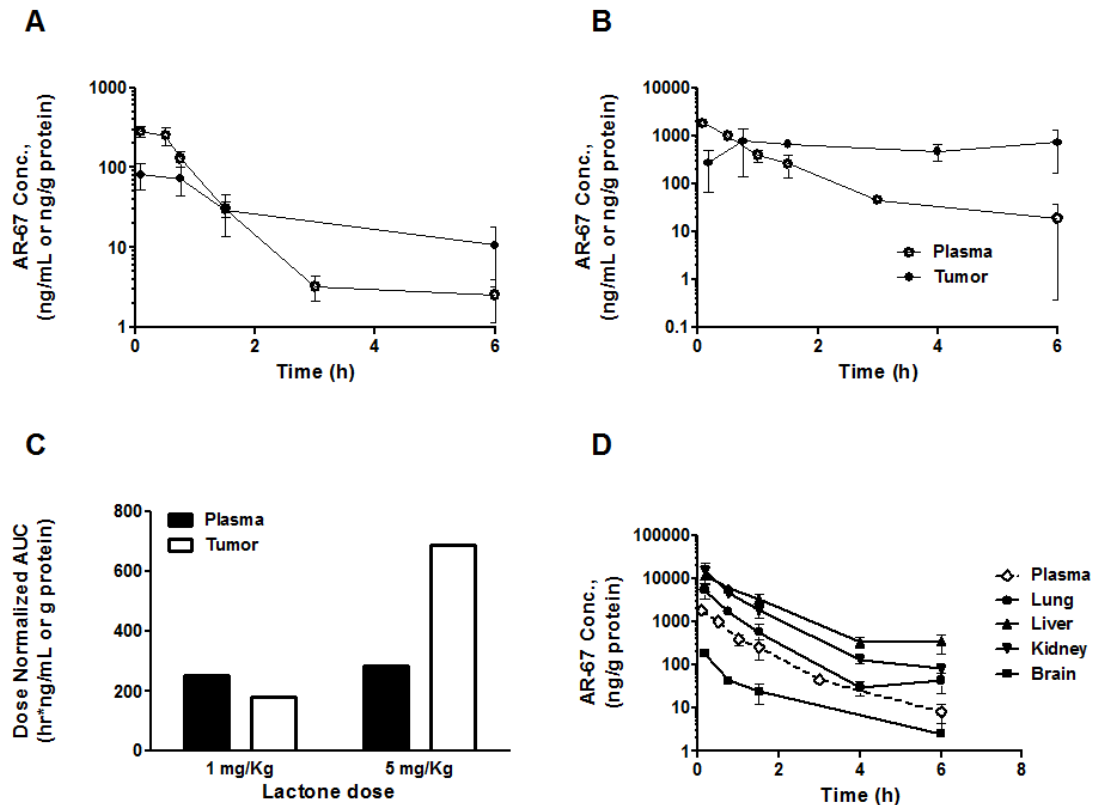
Figure 4-4. AR-67 pharmacokinetics in NSCLC xenografts.

Pharmacokinetic profile of total AR-67 in plasma (open symbols) and tumor tissue (solid symbols) after intravenous bolus administration of 1 (A) and 5 (B) mg/kg of AR-67 lactone in NCI-H460 xenografts. Plasma (solid bars) and tumor (open bars) dose normalized $AUC_{0\rightarrow6h}$ of total AR-67 levels (C) after iv administration of 1 and 5 mg/kg of AR-67 lactone in NCI-H460 xenografts. (D) AR-67 biodistribution in nu/nu mice. Pharmacokinetic profile of total AR-67 in lung, liver, kidney and brain tissue after intravenous bolus administration of 5 mg/kg of AR-67 lactone in nude mice. Data consists of 3 mice per time point group; bars, SD.

78

4.3.5 Clinical Summary.

Our preclinical data in NSCLC xenografts demonstrated the superiority of protracted dosing of AR-67 (Figure 4-2) and a long half-life in tumor tissue (Figure 4-4, B). To test the validity of the latter finding in humans, we designed a pilot clinical trial. AR-67 was given at 7.5 mg/m^2/day, which is the MTD determined in a previous phase I clinical trial [78]. In the present study, however, the same cumulative AR-67 dose was given intermittently over 15 instead of 5 days. To design the protracted dosing schedule for AR-67, the estimated tumor half-life (~16 hours) in NSCLC xenografts (Figure 4-4, B) was taken into consideration and a 96-hour dosing interval was selected in this proof-of-principle trial. Moreover, the schedule-dependent expression of Top1 was suggestive of its value as a biomarker of biological response. Therefore, based on our preclinical studies, Top1 expression profile appears to be a factor that needs to be taken into consideration when designing dosing schedules of camptothecins that aim to optimize efficacy.

Patients were enrolled between October 2010 and June 2011. Participants had previously received standard therapy and showed progressive disease. Metastatic disease was present in all participants. Patient demographics are presented on Table 4-1.

As this was the first time AR-67 was given following a protracted dosing schedule, patients were followed closely for toxicity and response. The first recruited patient developed DLTs of grade 3 fatigue and grade 4 neutropenia. Therefore, the 7.5 mg/m^2/day dose level was not considered tolerable and dose reduction was introduced per study protocol. Overall, AR-67 exhibited the same toxicity profile as previously reported [78]. Namely, hematological toxicities and fatigue were identified as dose limiting. AR-67 dose of 5.5 mg/m^2/day of AR-67 was well tolerated by the remaining

study participants. Interestingly, although stable disease was observed with one of the study participants that received AR-67 at the 5.5 mg/m^2/day dose, the patient was taken off the study protocol due to fatigue and symptomatic deterioration. A summary of toxicities and responses is presented on Table 4-1.

Table 4-1. Patient characteristics, dose to escalation scheme, clinical responses and DLTs.

Patients	Gender	Age (yrs)	AR-67		Clinical Response	Dose-limiting Toxicities
			Dose $(mg/m^2/d)$	Treatment Cycles Completed		
#1	Male	55	7.5	1	PD	Fatigue, neutropenia
#2	Male	37	5.5	1	PD	Anemia
#3	Female	61	5.5	4	SD	Fatigue, anemia
All patients were Caucasians, PD: Progressive Disease, SD: Stable Disease						

4.3.6 AR-67 Plasma And Tumor Pharmacokinetics In Cancer Patients.

As stated previously, the major objective of this pilot clinical study was to characterize the pharmacokinetics of AR-67 at the tumor site. Based on the tumor pharmacokinetics of AR-67 in NSCLC xenografts (Figure 4-4, A and B), the half-life of AR-67 in the tumor was estimated to be significantly higher than its plasma half-life. Therefore, we obtained serial tumor biopsies from patients at the presumed terminal phase in order to assess the half-life and relative concentrations compared to plasma. The first biopsy was obtained at 4-6 hours and the second at 22-25 hours after the beginning of the infusion. The amount of tissue collected varied significantly between patients (0.8 - 55.2 mg) and adequate amounts for quantifying AR-67 were only collected from one patient with a skin lesion. The plasma pharmacokinetic profiles of all patients as well as the measured tumor concentrations from a single patient are presented in Figure 4-5. Interestingly, as previously demonstrated in the NSCLC xenografts (Figure 4-4, A and B), tumor concentrations in tumor tissue at ~4.5 hours were higher than plasma and still measurable at ~24 hours. In contrast, plasma concentrations were minimal by 6 hours and undetectable at 24 hours, in all patients.
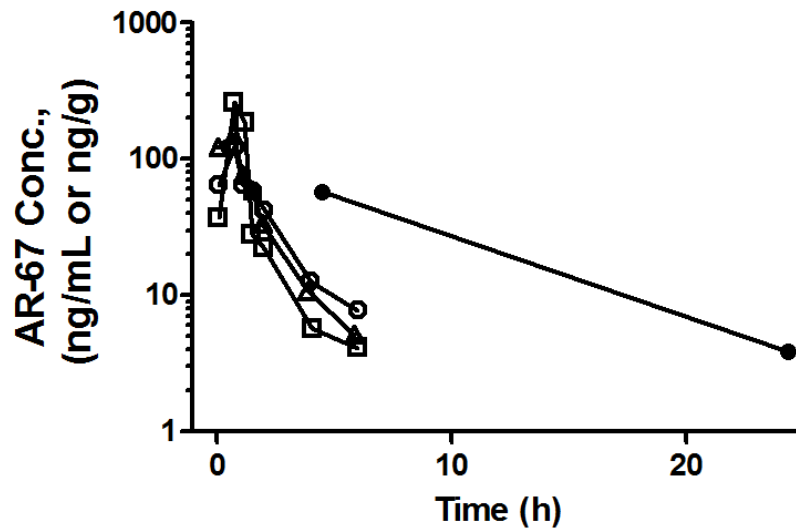
Figure 4-5. AR-67 plasma and tumor pharmacokinetic profile in patients with solid tumors.

Total AR-67 concentrations in plasma (open symbols) and tumor (closed symbols) after intravenous administration of AR-67 lactone as an 1-hour infusion on day 1 of cycle 1. Plasma samples were collected at predose and 0.1, 0.8, 1.1, 1.5, 2, 4, 6 and 24 hours after the start of the infusion on day 1 of cycle 1. Biopsies (skin lesion) were collected at 4.5 and 23.4 h after the start of the infusion.

4.3.7 Pharmacodynamic Analysis In Tumor Tissue Obtained From Cancer Patients.

Our studies using NSCLC xenografts (Figure 4-3) revealed the schedule-dependent expression of Top1 and support its further evaluation as a biomarker of biological response. Having demonstrated sustained concentrations of AR-67 in tumor tissue for 24 hours we proceeded in studying the effect of drug exposure on Top1 and γH2AX in the tumor tissue collected from the study participants. Interestingly, Top1 protein expression increased in the majority of patients. However, drug exposure had contradictory effects on the expression profile of γH2AX in the only two patients with γH2AX detectable levels in this study (Figure 7-7).

4.4 Discussion.

We have demonstrated that the antitumor activity of AR-67 in NSCLC xenografts is schedule-dependent and low doses given over a protracted schedule were more efficacious than a high dose administered over 5 consecutive days. In view of these results, we examined the expression profile of proteins implicated in the camptothecin mechanism of action. Our analysis clearly showed that the expression pattern of Top1, the enzyme-target of AR-67, was schedule-dependent and sustained Top1 expression correlated with molecular markers of DNA damage as well as with improved efficacy in a xenograft model. Our studies also demonstrated that AR-67 accumulates in tumor tissue and, contrary to the plasma compartment, displays non-linear kinetics. Camptothecin analogues are thought of as cytotoxic drugs. However, Top1 undergoes proteasome mediated degradation following exposure to increased drug concentrations [11]. Here we also observed dose dependent Top1 degradation *in vivo* and these data (Figure 4-3) provide evidence that suggests camptothecin development should also be considered in the context of sustained Top1 expression.

As reported with other camptothecins [125, 127, 128, 164], the AR-67 antitumor activity was schedule-dependent (Figure 4-2), with low-dose protracted dosing schedule found superior. Protracted dosing maximizes the number of S-phase cells being exposed to AR-67 rendering the camptothecin highly toxic and efficacious. Survival of NSCLC xenografts indicated that AR-67 exhibits superior antitumor efficacy when given intermittently at low doses. Our data suggest that prolonged low-dose schedules, which do not eradicate Top1 (Figure 4-3), facilitate marked therapeutic behavior. On the basis of these findings, Top1 expression appeared to be a critical requirement for drug efficacy and could be a predictive marker of efficacy in future clinical trials. *In vitro* and *in vivo* studies [9, 10] have described the reversible proteasome-mediated degradation [11] of

Top1 in the presence of the drug. Because of the interplay between camptothecins and Top1, as well as dependence on the expression of the protein-target for exhibiting anticancer activity [175], camptothecins appear to share traits of molecularly targeted agents. Although AR-67 is considered a cytotoxic agent, verification of biological activity, through identification of targets of interaction and biomarkers of biological activity is essential to the success of effective drug development [176-178].

The pharmacokinetics of AR-67 were non-linear at the tumor tissue (Figure 4-4, A and B). We hypothesize that this is potentially the result of increased partitioning of the lipophilic AR-67 lactone [179] which is favored in the acidic tumor microenvironment and of increased protein binding in the tumor tissue [149, 180]. Regardless of the underlying mechanism, the non-linear kinetics of AR-67 in tumor tissue (Figure 4-4, C) suggests that the plasma concentrations alone should not be considered when deciding on a dosing schedule.

In view of our preclinical studies, a pilot clinical trial was undertaken to demonstrate feasibility and to assess toxicity. The study did meet its objective to test the feasibility of obtaining two serial tumor biopsies from the participants within 24 h after the beginning of the infusion on Day 1 of Cycle 1. As in the NSCLC xenografts, differing AR-67 kinetics between the plasma and the tumor was observed in one of the study participants (Figure 4-5). The undetectable AR-67 amounts in the rest of the patients can be attributed to the small tissue amount collected for biopsy and the lower dose (5.5 mg/m^2/d) these patients received (Table 4-1). These limiting factors should be taken into consideration when designing future trials. In addition, the MTD at the protracted schedule should be evaluated, but in the context of Top1 expression.

In conclusion, in xenograft studies, AR-67 appeared to be more efficacious when administered following a low-dose protracted dosing schedule rather than a high-dose short dosing schedule (daily x 5) and this resulted in sustained Top1 expression, which correlated with prolonged survival. Furthermore, we demonstrated that AR-67 follows non-linear kinetics in NSCLC xenografts. Future studies will need to carefully evaluate surrogate tissues for the expression of Top1 and other markers (e.g., γH2AX, cl-PARP) as a way to optimize the dosing schedule of AR-67.

5. Chapter 5: Population Pharmacokinetic Analysis of the Lipophilic Camptothecin Analogue AR-67 in Phase I Oncology Patients

5.1 Introduction.

Camptothecins are considered basic components of clinical oncology today. They interact with Top1, a nuclear enzyme responsible for relieving DNA torsional stress and induce cell death by stabilizing the DNA-enzyme-drug complex [3, 4]. Moreover, camptothecin analogues are present in two forms, the charged carboxylate and the lipophilic lactone that are engaged into a pH- and protein-binding-dependent equilibrium [16, 18]. However, it is believed that their cytotoxic action is mediated via the lactone species [3].

Similarly to most anticancer agents, camptothecins have a relatively narrow therapeutic index and their administration has been associated with life-threatening toxicities [40, 41, 163]. Identifying sources of intersubject variability allows the establishment of an accurate dose-exposure-response relationship that could lead to enhanced efficacy and reduction of toxicity. For those reasons, the pharmacokinetic profile of camptothecins has been studied extensively and covariates have been included in population pharmacokinetic models to increase their predictive value [46-48, 70, 72, 181, 182]. Studies introduced renal function as the most important determinant of topotecan clearance [46-50, 52]. Contrary, impaired liver function, UGT1A1*28 homozygosity and co-administration of metabolic enzyme inducers or inhibitors were found to correlate with chemotherapy-related toxicity in patients treated with irinotecan [63, 71, 183, 184].

AR-67 [38, 74, 76, 77] is a novel camptothecin analogue, currently undergoing early-stage clinical trials. Its pharmacokinetic and pharmacodynamic profile was studied for the first time in humans during a phase I clinical trial [78]. Notably, exposure to AR-67 correlated well with hematological toxicity experienced by the study participants. Subsequent *in vitro* studies on the metabolic profile of AR-67 suggested elimination via extensive metabolism by uridinoglucuronosyltransferases (UGT) and CYP450 enzymes localizing in the gut and the liver [79]. As AR-67 is currently being evaluated in phase 2 clinical trials, it is necessary to concentrate our efforts on determining the patient characteristics that contribute to the high intersubject variability associated with estimates of pharmacokinetic parameters. Determining sources of inter-individual variability with clinical relevance will allow us to identify the patients that could benefit the most from being treated with this novel camptothecin analogue.

In this study, the pharmacokinetic and pharmacodynamic data collected during the phase I clinical trial were analyzed to describe the distribution and elimination profile of AR-67. Covariates contributing to intersubject variability were included in the developed population pharmacokinetic model and estimates for the AR-67 population pharmacokinetic parameters were obtained. Additionally, the effect of smoking, obesity and performance status on AR-67 pharmacokinetic and toxicity profile was studied. Finally, the lactone clearance was normalized to body-size measures in an effort to decrease the intersubject variability associated with this clinically important pharmacokinetic parameter.

5.2 Materials and Methods.

5.2.1 Patient Population.

The analysis performed included AR-67 plasma concentration versus time data from patients with solid tumors that participated in a phase I clinical trial [78]. The aims of the study were to determine the maximum tolerated dose and to identify the dose-limiting toxicities for this novel camptothecin analogue. AR-67 was administered as a 1-hr infusion daily for first 5 days of a 21-day cycle. Patient eligibility criteria have been described elsewhere [78]. Briefly, patients were ≥18 yrs of age, ECOG performance status ≤2, normal hematological tests and adequate renal and liver function, no prior chemotherapy, radiation (within 2 weeks) or surgery (within 3 weeks) was allowed. Patients allergic to other camptothecins or cremophor-EL and patients receiving anticonvulsants or any other strong enzyme inducers were excluded from the study. The study was approved by the Institution Review Board of the University of Kentucky and written informed consent was obtained from patients before entering the clinical trial.

Of the 26 patients that participated in the phase I clinical trial, only those with a complete covariate profile (n=19) were considered for the development of the base and covariate models for lactone and total AR-67 in plasma and when testing for inter-occasion variability. The demographics and clinical characteristics of the patients at study entry [78] are summarized on Table 5-1.

Table 5-1. Patient demographics and clinical characteristics.

Patient Characteristic		N	Mean	Median (range)
Age, yrs		19	55.9	61 (30-72)
BSA, m^2		19	1.91	1.87 (1.48-2.44)
Sex	Female	10		
	Male	9		
CRCL, mL/min		19	109.4	105 (50.4-162.7)
BUN, mg/dL		19	12.7	12 (4-22)
Alb, g/dL		19	2.9	3 (1.2-3.7)
T_{bil}, mg/dL		19	0.7	0.6 (0.4-2.3)
ALP, U/L		19	127.2	104 (45-281)
ALT, U/L		19	20.1	17 (7-38)
AST, U/L		19	29.3	28 (12-51)
LDH, U/L		19	256.7	181 (101-469)
DOSELEV, mg/m^2/day		1.2 (n=1), 1.6 (n=1), 2.34 (n=2), 3.23 (n=3), 4.5 (n=1), 6.3 (n=1), 12.4 (n=1), 8.9 (n=2), 7.5 (n=5)		
HCT, %		19	34.5	34.4 (26.7-44.0)
Tobacco	Yes	5		
	No	17		
Liver tumor (primary, metastatic)	Yes	11		
	No	14		
Gastrointestinal tract tumor (primary, metastatic)	Yes	8		
	No	17		

Table 5-1: continued

BMI, kg/m^2	<25	7	20.6	20.6 (16.8-24.3)
	25-30	11	27.6	27.8 (25.3-29.1)
	>30	7	40.4	34.2 (30.2-73.6)
PS	0	7		
	1	3		
	2	15		
Edema	Yes	13		
	No	12		
BSA: Body surface area, CRCL: creatinine clearance, BUN: blood urea nitrogen, Alb: albumin, T$_{bil}$: total bilirubin, ALP: alkaline phosphatase, ALT: alanine transaminase, AST: aspartate transaminase, LDH: liver dehydrogenase, DOSELEV: AR-67 dose level that patients were assigned to, HCT: hematocrit, BMI: Body Mass Index, PS: Performance Status.				

Moreover, body weight (WT, kg) and height (HT, m) measurements from the study participants were used to estimate body-size measures such as Body Surface Area (BSA, m^2), Lean Body Weight (LBW, kg), Ideal Body Weight (IBW, kg), Adjusted Ideal Body Weight (AIBW, kg) and Body Mass Index (BMI, kg/m^2) using the following equations [185, 186]:

$$BSA = 0.007184 \times WT^{0.425} \times HT^{0.725} \quad (1)$$

$$LBW \text{ (male)} = (1.1 \times WT) - 1.28 \times (WT/HT)^2 \quad (2)$$

$$LBW \text{ (female)} = (1.07 \times WT) - 1.48 \times (WT/HT)^2 \quad (3)$$

$$IBW \text{ (male)} = 50 + 2.9 \times (HT \text{ in inches} - 60) \quad (4)$$

$$IBW \text{ (female)} = 45.5 + 2.3 \times (HT \text{ in inches} - 60) \quad (5)$$

$$AIBW = IBW + 0.25 \times (WT - IBW) \quad (6)$$

$$BMI = WT/[HT(\text{in m})]^2 \quad (7)$$

In our study, individuals with BMI<25 were considered of normal weight while the BMI of overweight individuals ranged from 25 to 30. Individuals with BMI>30 were considered obese.

Patients were closely monitored for hematological toxicity. Measurements of the absolute neutrophil count (ANC, 10^3/uL), white blood cell counts (WBC, 10^3/mm^3), hemoglobin levels (Hb, g/dL) and platelet counts (PLT, 10^3/mm^3) were taken on day 1 (baseline), 8, 15 and 21 of cycle 1. The lowest value among the collected measurements per individual during cycle 1 was declared as the nadir. The %ANC, WBC, Hb and PLT decrease baseline-normalized was calculated as the % absolute difference between the baseline and the nadir measurements divided by the baseline measurement.

5.2.2 Drug Administration.

AR-67 was supplied by the National Cancer Institute (Rapid Access to Intervention Development program) and prepared for administration as described by Arnold et al. [78]. The investigational agent was administered at 9 dose levels ranging from 1.2 to 12.4 mg/m^2/day (Table 5-1).

5.2.3 Pharmacokinetic Sampling And AR-67 Quantitation In Plasma.

Blood samples were collected from each patient at predose, 5, 45, 65 min and 1, 5, 2, 4, 6, 8 and 24 h after the start of the infusion on days 1 and 4 of cycle 1 and AR-67 lactone and carboxylate were quantified in the extracted plasma using a validated HPLC method, as described previously [137]. Lactone concentrations lower than 2.5 ng/mL and carboxylate concentrations lower than 1.0 ng/mL were not considered for the pharmacokinetic analysis as they were lower than the lower limit of quantification. The mean number of samples per patient included in the analysis was 13.

5.2.4 Nonlinear Mixed Effects Modeling Analysis.

Population pharmacokinetic analysis was performed following the nonlinear mixed effects theory as implemented in NONMEM (version 7.2.0, Icon Development Solutions, Ellicott City, MD, USA) integrated with PDx-POP (version 5.0, Icon Development Solutions, Ellicott City, MD, USA). Model development was performed as described in Bonate, 2011 [187] as well as the NONMEM User's Guide [130, 188].

The Expectation-Maximization (EM) method offered by NONMEM was used for the pharmacokinetic population analysis. Studies [129] have shown that the EM methods exhibit low running times and perform well with categorical data (non-normal) and complex pharmacokinetic/pharmacodynamic models. In our analysis, we obtained good initial parameter estimates using the Iterative Two Stage (ITS) method. Those initials

94

estimates were used by the Stochastic Approximation Expectation Maximization (SAEM) method to obtain maximum likelihood estimates for population parameters. The analysis was completed with the use of the Important Sampling (IMP) method where only the expectation step was performed to improve the objective function and the standard error estimates. As the Expectation-maximization methods perform better with MU referencing, the latter was implemented into the model.

5.2.5   Base Model.

Visual inspection of the log transformed lactone (Figure 7-8) and total AR-67 (Figure 7-9) plasma concentration data versus time and previously published work on camptothecins [46] led to the selection of a two-compartment pharmacokinetic model with first-order elimination from the central compartment to fit the concentration-time data (ADVAN 3, TRANS 4 subroutine in NONMEM). Estimates were obtained for the population parameters: clearance (CL) from the central compartment, volume of the central compartment (V1), inter-compartmental clearance (Q) and volume of the peripheral compartment (V2).

The intersubject variability (η, Eta) on the population estimate (P_{pop}, θ, Theta) of the pharmacokinetic parameter P for subject (i) (P_i) was modeled as an exponential term equal to:

$P_i = P_{pop} \times \exp(\eta_i)$ (8)

The residual error (ε, Epsilon), the difference between the observed (Cobs) and the predicted (C_{pred}) concentration values constitutes an important component of population analysis. Error introduced to measurements due to intrasubject/interoccasion variability (IOV), assay and sample handling/processing is designated as residual error. Different residual error models (additive, proportional, power, exponential and combination) were

tested. However, the exponential residual error model satisfied the criteria outlined in the Selection Model section:

$$C_{obs,i} = C_{pred,i} \times \exp(\varepsilon_i) \quad (9)$$

The distributions of the η and ε parameters were assumed to be normal with zero as mean and variances equal to ω (omega) and σ (sigma), respectively.

The area under the curve (AUC) was calculated as the ratio of the amount of AR-67 lactone administered over the individual population predicted clearance estimate.

5.2.6 Inter-occasion Variability.

The study design of the phase I clinical trial involved pharmacokinetic assessment on days 1 and 4. Intra-individual variability or inter-occasion variability (IOV) introduced into the model on these two occasions (day 1 - occasion 1 and day 4 - occasion 2) was tested on all pharmacokinetic parameters for statistical significance. IOV was studied on the base model before the inclusion of covariates to avoid attributing changes on pharmacokinetic parameters between occasions to individual characteristics. IOV was modeled as described by Karlsson et al. [189]. Briefly; IOV was included in the model as an exponential term (η_{IOV}):

$$P_i = P_{pop} \times \exp(\eta_i) \times \exp(\eta_{IOV,1}) \quad (10)$$

$$\text{and } P_i = P_{pop} \times \exp(\eta_i) \times \exp(\eta_{IOV,2}) \quad (11),$$

where P_i is the estimate for the pharmacokinetic parameter P for subject (i), P_{pop} is the population estimate for the pharmacokinetic parameter P, η_i is the intersubject variability for subject (i) in regards to the pharmacokinetic parameter P and $\eta_{IOV,1}$ and $\eta_{IOV,2}$ are the inter-occasion variability for subject (i) on occasion 1 (day 1) and on occasion 2 (day 4), respectively.

5.2.7 Covariate Model.

The two-compartment pharmacokinetic structural model presented in the base model section was selected as a base model for the covariate model building process (ADVAN 6 subroutine in NONMEM). The covariates tested were both continuous and categorical (Table 5-1). Body surface area (BSA, m^2), creatinine clearance (CRCL, mL/min), age (AGE, yrs), sex, blood urea nitrogen (BUN, mg/dL), albumin (Alb, g/dL), total bilirubin (T_{bil}, mg/dL), alkaline phosphatase (ALP, U/L), alanine transaminase (ALT, U/L), aspartate transaminase (AST, U/L), liver dehydrogenase (LDH, U/L), AR-67 dose level that patients were assigned to (DOSELEV, $mg/m^2/day$) and hematocrit (HCT, %). Continuous covariates entered in the model were either centered to their mean values or normalized to their mean values or standardized to improve model fitting. CRCL was calculated using the Cockcroft-Gault equation (12) [190]:

CRCL (mL/min) = [(140 - Age) x WT x A] / [72 x SrCr] (12),

where Age is inserted in the equation in years, WT is body weight (kg), A is a constant that equals 1 for males and 0.85 for females and SrCr is serum creatinine (mg/dL).

Covariates were tested for co-linearity by performing linear regression analysis (Table 7-2). Co-linear covariates were not included in the model as they have been shown to inflate the error model [187, 191].

Covariates were inserted in the model manually [187, 192]. Patient attributes were initially evaluated graphically for relationships with V1Eta (intersubject variability associated with V1) and CLEta (intersubject variability associated with CL) because these two population parameters are of clinical significance and candidate covariates were added into the model. Following, covariate relationships with QEta (intersubject variability associated with Q) and V2Eta (intersubject variability associated with V2) were

explored graphically and additional covariates were added to the model. Only covariates that satisfied the criteria described in the Model Selection section were included in the model.

5.2.8 Model Selection.

Goodness of fit plots, decrease in the objective function value (OFV, -2Log Likehood, -2LL), satisfactory precision of parameter estimates and model stability (confidence intervals of parameter estimates not-including zero) were used to decide model superiority. Plots of individual or population predicted versus observed drug concentrations were analyzed for closeness to the line of unity and plots of weighted or conditional weighted residuals versus individual population predicted drug concentrations were analyzed for randomness. Decrease by 3.84 units (for 1 degree of freedom) of the OFV was considered statistically significant ($p<0.05$). In the development of the covariate model, decrease in the intersubject variability (ω), in addition to the criteria mentioned above, was required for covariate inclusion into the model. The IOV is lumped with the residual error (ε) of the model in NONMEM [189]. Therefore, IOV was included in the model when a decrease of the sigma was observed and all the aforementioned criteria for model acceptance were met. Finally, precision was expressed as RSE%, which is produced by the standard error over the parameter value Both RSE% and Interindividual variability (IIV) are provided by NONMEM (ref).

5.2.9 Statistical Analysis.

Statistical analysis and graphical representation were performed using GraphPad Prism, version 5.01 (GraphPad Software Inc., San Diego, USA).

The unpaired t-test was used to detect statistically significant differences between two subject groups (F-test, $p>0.05$). The non-parametric Mann-Whitney test was used

otherwise. Comparisons of more than 2 group means were performed with one-way Analysis of Variance (one-way ANOVA) with Bonferroni correction. $p < 0.05$ was selected for statistical significance unless otherwise stated. Linearity was tested by performing linear regression analysis and the p value indicated whether the slope was statistically significantly different from zero ($p < 0.05$).

Pharmacokinetic parameter estimates were reported as mean ± SD or median (range) unless indicated differently.

5.3   Results.

5.3.1   Population Pharmacokinetic Analysis of AR-67 In Plasma.

This study used pharmacokinetic and pharmacodynamic data on the novel camptothecin analogue AR-67 collected in a first-in-humans clinical study [78] to describe the population pharmacokinetics of AR-67. Patient characteristics (Table 5-1) were incorporated into the model to achieve more accurate estimates of the model parameters.

5.3.1.1   Base Model.

Similarly to other camptothecin analogues [46], a two-compartment model with first order elimination from the central compartment was found to sufficiently describe the plasma concentration versus time data for both AR-67 lactone (Figure 7-8) and total drug (Figure 7-9). Moreover, the lowest value for the OFV function was obtained when the residual error was modeled as an exponential term to account for the differences between the observed and the predicted concentration data points. Population pharmacokinetic analysis for total AR-67 resulted in comparable population parameter estimates as the ones obtained previously for the lactone form.

More specifically, the AR-67 lactone population CL, V1, Q and V2 parameter estimates were 25 L/h, 3.7 L, 29.7 L/h and 38.1 L, respectively (Table 5-2). Although these estimates were obtained with satisfactory precision (RSE<5.75%), they were accompanied by significant intersubject variability. Namely, the coefficients of variation of interindividual variability for CL and V1 were 58.6 % and 106 %, respectively. Residual variability was estimated to be 32.7 %.

Table 5-2. Population pharmacokinetic parameter estimates for the lactone AR-67 base model obtained by performing population pharmacokinetic analysis.

	Population pharmacokinetic parameter	Mean (RSE,%)	IIV (RSE,%)	CV(%)*
Base Model	CLPOP, θ_1 (L/h)	25.0 (3.79)	0.343 (39.1)	58.6
	V1POP, θ_2 (L)	3.7 (1.86)	1.13 (30.0)	106.0
	QPOP, θ_3 (L/h)	29.7 (5.75)	0.498 (35.5)	70.6
	V2POP, θ_4 (L)	38.1 (4.92)	0.415 (22.0)	64.4
	Residual variability, ε		0.107 (16.7)	32.7
* Coefficient of variation for interindividual variability of the population pharmacokinetic parameter,# change in the objective function value after the addition of the relevant covariate , IIV: Inter-individual variability, OFV: Objective function value, POP: population pharmacokinetic parameter				

Additionally, clearance, V1, Q and V2 for total AR-67 were found to be 25.8 L/h, 2.9 L, 32.5 L/h and 28.8 L, respectively (Table 5-3). Clearance was the population parameter with the lowest intersubject variability (28.6 %) while V1 was the population parameter with the highest intersubject variability (119 %) among the studied population parameters. Residual variability (27.7 %) was of the same magnitude as the ε estimated for the lactone.

Table 5-3. Population pharmacokinetic parameter estimates for the total AR-67 base model obtained by performing population pharmacokinetic analysis.

	Population pharmacokinetic parameter	Mean (RSE,%)	IIV (RSE,%)	CV(%)*
Base Model	CLPOP, θ1 (L/h)	25.8 (2.2)	0.082 (30.6)	28.6
	V1POP, θ2 (L)	2.9 (27.0)	1.42 (28.9)	119.0
	QPOP, θ3 (L/h)	32.5 (5.3)	0.34 (40.3)	58.3
	V2POP, θ4 (L)	28.8 (3.6)	0.156 (32.2)	39.5
	Residual variability, ε		0.077 (12.7)	27.7
* Coefficient of variation for interindividual variability of the population pharmacokinetic parameter,# change in the objective function value after the addition of the relevant covariate , IIV: Inter-individual variability, OFV: Objective function value, POP: population pharmacokinetic parameter				

Diagnostic plots showed a symmetrical distribution around the line of unity when individual predicted or population predicted concentration values were plotted against observed concentration values for either lactone or total AR-67 (Figure 5-1, A and B, respectively). Additionally, the conditional weighted residuals were randomly distributed when plotted versus individual population predicted lactone or predicted total drug concentration (Figure 7-8).

Figure 5-1. Diagnostic plots of population pharmacokinetic base models developed for AR-67 lactone and total AR-67.

AR-67 lactone (A) and total AR-67 (B) individual (IPRE, circle) or population (PPRE, asterisk) predicted versus observed concentration in plasma. Individual and population predicted concentration values were obtained by studying the population pharmacokinetics of AR-67 administered in cancer patients (n=19) with solid tumors using a two-compartment structural model to fit the data and are presented in panels A and B for lactone and total AR-67, respectively. The line of Unity and the LOWESS curves for IPRE and PPRE were added for evaluation of goodness of fit. AR-67 plasma concentrations are given in ng/mL.

5.3.1.2 Inter-occasion Variability.

To avoid allergic reactions to the cremophor-EL-containing formulation of AR-67, patients were co-administered the CYP3A inducer dexamethasone [78, 193]. Additionally, *in vitro* studies have demonstrated the CYP3A4/5-mediated biotransformation of AR-67 lactone [79]. Therefore, the contribution of the potentially dexamethasone-induced clearance of AR-67 to the residual variability was evaluated by modeling IOV. However, no decrease on the OFV, CLEta or ε was observed when IOV on CL was studied (data not shown). Additionally, model instability was observed when IOV on V1, Q and V2 was included in the model (data not shown). Thus, IOV was not included in the model developed for either lactone or total AR-67.

5.3.1.3 Covariate Model.

As indicated in the materials and methods section, covariates that correlated with either CLEta or V1Eta were given priority and were incorporated into the model first.

AR-67 Lactone Covariate Model (Table 5-4). More specifically, although dose-levels as a covariate showed a weak correlation with CLEta and V1Eta of the lactone form, it did not meet the criteria of statistical significance (ΔOFV>3.84) and was not included in the model. Among BUN, age, AST and sex, only BUN incorporation into the model describing the population pharmacokinetics of the lactone form was successful (ΔOFV=-5.16, p<0.05) and resulted in decrease of the intersubject variability of V1 by 23.3 %. Interestingly, incorporation of BUN appeared to account for differences on population parameter estimates of V1 between men and women (*p=0.0043) although BUN values did not differ significantly (p=0.48) between the two groups in our study (data not shown). Following, BSA was identified as an important determinant of V2 (ΔOFV=-5.26, p<0.05) and accounted for 10.6 % of intersubject variability of V2. Considering sex as a

covariate, on either Q or V2, resulted in model instability and was not pursued further. To evaluate the developed lactone covariate model, the V1 and V2 pharmacokinetic parameters were calculated for a typical patient (BUN=15 mg/dL, BSA=1.86m^2) using the model derived equations (Table 5-4). The V1 population estimate for a typical patient was found 4.9 L which is included in the 95 % confidence interval of the base model V1 population estimate (2.4 - 6.1 L) and the V2 population parameter estimate (37.6 L) approximated the V2 estimate obtained with the base model (38.1 L).

Table 5-4. Population pharmacokinetic parameter estimates for the lactone AR-67 covariate model obtained by performing population pharmacokinetic analysis.

	Population pharmacokinetic parameter	Mean (RSE,%)	IIV (RSE,%)	CV(%)*	Change in OFV#	p value
Covariate Model	CLPOP, θ1 (L/h)	25.0 (3.85)	0.339 (39.8)	58.2		
	V1, θ2	1.35 (17.3)	0.684 (25.9)	82.7		
	V1POP (L)	EXP(θ2 x (BUN/12.7))			-5.16	<0.05
	QPOP, θ3 (L/h)	30.0 (5.85)	0.49 (35.5)	70.0		
	V2, θ4	5.2 (23.8)	0.289 (21.8)	53.8		
	θ5	1.08 (30.6)				
	V2POP (L)	θ4 x EXP((BSA)^θ5)			-5.26	<0.05
	Residual variability, ε		0.107 (17.0)	32.7		

* Coefficient of variation for interindividual variability of the population pharmacokinetic parameter,# change in the objective function value after the addition of the relevant covariate , IIV: Inter-individual variability, OFV: Objective function value, POP: population pharmacokinetic parameter

108

Total AR-67 Covariate Model (Table 5-5). Covariates were considered for the development of a total AR-67 covariate model. The only covariate that showed a noticeable relationship with CLEta was BSA. Although incorporation of BSA into the model was justified based on the model superiority criteria (ΔOFV=-4.69, *p<0.05), it accounted for only 3.5 % of intersubject variability of CL. Age, BUN and sex were selected for further testing when investigating for patient attributes to explain the high (119 %) intersubject variability of V1. Age and BUN were incorporated in the model and led to a statistically significant decrease of the OFV. However, they were also associated with model instability and, therefore, were abandoned. Contrary, sex was evaluated as a significant determinant of V1 because it resulted in a statistically significant decrease of OFV (ΔOFV=-4.29, *p<0.05) and explained 24.3 % of the V1 intersubject variability. Interestingly, addition of BSA and sex in the model, revealed a relationship between V1Eta and CRCL. However, the latter was not incorporated into the model because of co-linearity with BSA (Table 7-2). Finally, although dose-levels and sex appeared to correlate with QEta and V2Eta, boundary issues on estimates of population parameters prohibited inclusion of additional covariates in the final model. The total AR-67 pharmacokinetic parameters for a typical patient were calculated using the covariate model documented on Table 5-5. Clearance was estimated to be 25.2 L/h (BSA=1.86m^2) while V1 was 2.0 L for women and 5.8 L for men as a result of including sex into the model as a covariate.

Table 5-5. Population pharmacokinetic parameter estimates for the total AR-67 covariate model obtained by performing population pharmacokinetic analysis.

	Population pharmacokinetic parameter	Mean (RSE,%)	IIV (RSE,%)	CV(%)*	Change in OFV#	p value
Covariate Model	CL, θ1	10.8 (16.3)	0.063 (26.6)	25.1		
	θ2	0.456 (43.6)				
	CPOPL, (L/h)	Θ1 x EXP((BSA) x θ2)			-4.69	<0.05
	V1POP,F, θ3 (L), Female V1POP,M, θ4 (L), Male	2.0 (48.4) 5.8 (18.5)	0.897 (38.2)	94.7	-4.29	<0.05
	QPOP, θ5 (L/h)	31.5 (5.3)	0.305 (42.6)	55.2		
	V2POP, θ6 (L)	28.5 (3.55)	0.146 (32.7)	38.2		
	Residual variability, ε		0.077 (13.2)	27.8		

* Coefficient of variation for interindividual variability of the population pharmacokinetic parameter,# change in the objective function value after the addition of the relevant covariate , IIV: Inter-individual variability, OFV: Objective function value, POP: population pharmacokinetic parameter

Diagnostic plots (Figure 5-2, A and B, for lactone and total AR-67, respectively) of individual predicted or population predicted concentration values plotted against observed concentration values showed distribution around the line of unity. However, only subtle improvements were observed in the generated plots when compared to the respective base model ones (Figure 5-1, A and B, for lactone and total AR-67, respectively).
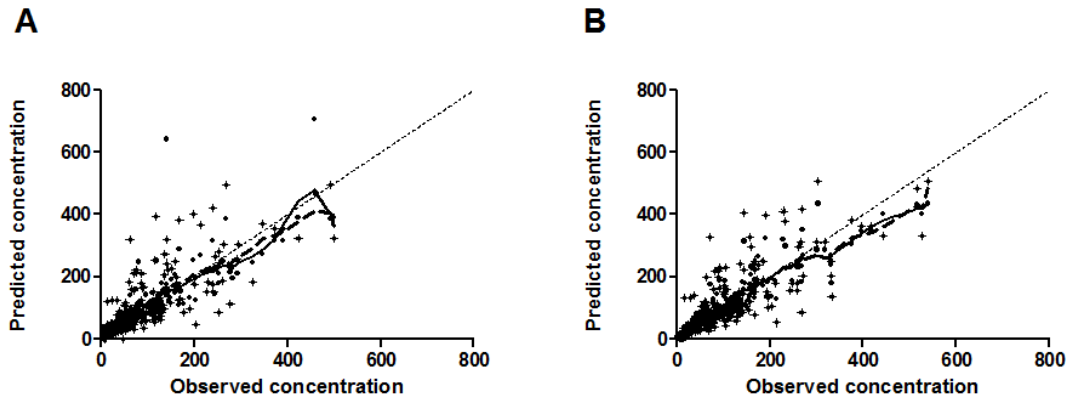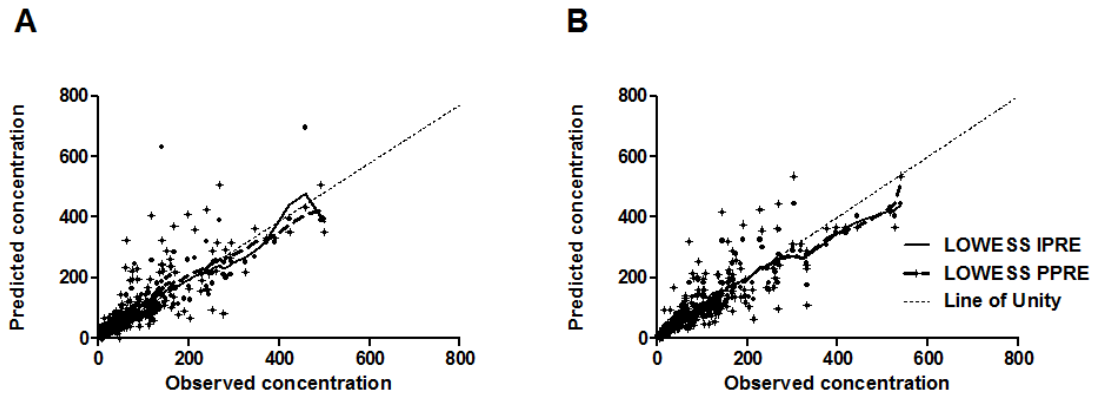
Figure 5-2. Diagnostic plots of population pharmacokinetic covariate models developed for AR-67 lactone and total AR-67.

AR-67 lactone (A) and total AR-67 (B) individual (IPRE, circle) or population (PPRE, asterisk) predicted versus observed concentration in plasma. Individual and population predicted concentration values were obtained by studying the population pharmacokinetics of AR-67 administered in cancer patients (n=19) with solid tumors using a two-compartment structural model to fit the data and are presented in panels A and B for lactone and total AR-67, respectively. The line of Unity and the LOWESS curves for IPRE and PPRE were added for evaluation of goodness of fit. AR-67 plasma concentrations are given in ng/mL.

5.3.2 Clinical Determinants of AR-67 Clearance And Toxicity.

Clearance is a pharmacokinetic parameter of clinical relevance as it is directly related to exposure and, therefore, efficacy and toxicity. *In vitro* studies and clinical data [78] strongly suggest that AR-67 is eliminated via metabolism by the CYP1A1, 3A4, 3A5, UGT1A1, UGT1A3, UGT1A7 and UGT1A8 metabolic enzymes localizing in the liver and the gut [79]. Therefore, factors that could have an impact on the activity of the aforementioned metabolic enzymes in the phase I oncology patients were studied here with the use of the previously developed covariate-free population pharmacokinetic models.

5.3.2.1 Smoking, Obesity And Tumor Type.

Smoking has been reported to alter the disposition and elimination profile of xenobiotics by inducing the metabolic activity of CYP and UGTs [194]. Against this background, the effect of smoking on exposure to lactone was tested, but no differences were detected between study groups (434.2 ng*h/mL ± 259.0 vs 415.8 ng*h/mL ± 361.6, p=0.90) (Figure 5-3). Similar results were obtained when clearances of total AR-67 between non-smokers and smokers were compared (data not shown).

113
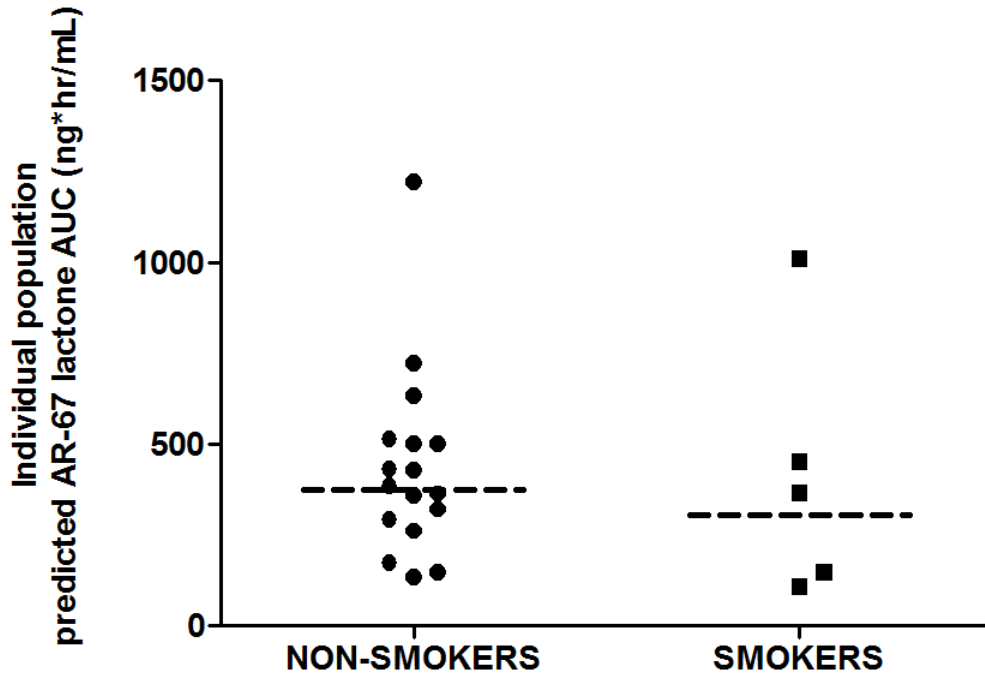
Figure 5-3. Scatter plots depicting the relationships between exposure to AR-67 lactone expressed as AUC and smoking status.

The AUC values were calculated as described in the materials and methods section. Statistically significant differences between subject groups were detected by performing the Unpaired t-test/Mann-Whitney test (NON-SMOKERS Vs SMOKERS). P<0.05 was considered statistically significant (*p<0.05). Only statistically significant differences are indicated. AUC values are given as ng*hr/mL. Broken line, geometric mean. AUC: Area Under the Curve.

Although numerous studies have shown an interaction between obesity and metabolism, high body fat has been reported to either induce or inhibit the metabolic activity of CYP and UGTs [195]. We attempted to identify differences in the elimination profile of AR-67 among groups of normal weight, overweight and obese patients. One-way ANOVA showed that lactone clearances did not differ among the three study groups ($p=0.09$) (Figure 5-4). Notably, the lactone clearance of a severely obese patient (BMI=73.6 kg/m^2) was 31.3 L/h, within the range of clearances of normal weight patients (23-39 L/h).
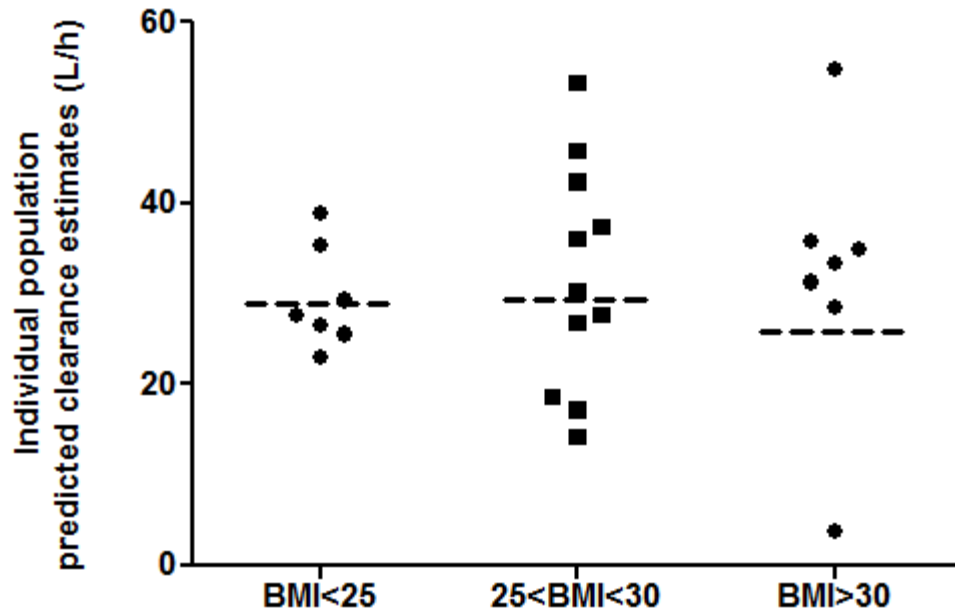
Figure 5-4. Scatter plots depicting the relationship between individual population predicted clearance estimates of AR-67 lactone and BMI as an obesity index.

The individual population clearance estimates were obtained after performing population analysis on pharmacokinetic data collected during the AR-67 phase I clinical trial (n=25) as described in the materials and methods section. Patients were divided into 3 groups based on their BMI: normal weight (BMI<25), overweight (25<BMI<30) and obese (BMI>30). Statistically significant differences between the 3 groups were detected by performing one-way Analysis of Variance (Bonferroni correction for multiple comparisons). $p < 0.05$ was considered statistically significant (*$p < 0.05$). Only statistically significant differences are indicated. Clearance and BMI values are given as L/h and kg/m^2, respectively. Broken line, geometric mean. BMI: Body Mass Index.

Finally, the potential of the elimination of AR-67 being compromised due to the presence of tumor in liver or gut was tested. Neither the lactone (p=0.17) nor the total AR-67 (p=0.71) clearance differed significantly between patient groups positive and negative for liver tumor (Figure 7-9). The same result was obtained when patients were arranged into groups based on presence or absence of gut tumor (Figure 7-9).

5.3.2.2 Effect Of Performance Status On AR-67 Clearance And Toxicity.

Population pharmacokinetic analyses have indicated performance status as an important covariate of camptothecin clearance (Table 1-1). In our study, patient groups of different performance statuses (PS=0 vs PS=1 vs PS=2) were not statistically significantly different in regard to their lactone clearances (data not shown, p=0.80).

Additionally, the effect of the performance status on toxicity was studied (Figure 5-5). As hematological toxicities, including neutropenia and thrombocytopenia prevented dose escalation in the AR-67 phase I clinical trial, % decreases of ANC, WBC, Hb and PLT were selected as toxicity endpoints. Our analysis showed that patients with worst performance status at baseline (PS=2) had statistically (*$p<0.05$) higher decreases in ANC, WBC and PLTs when compared to patients of PS=0 (Figure 5-5, A, B and D) increasing the potential of experiencing severe hematological toxicity.
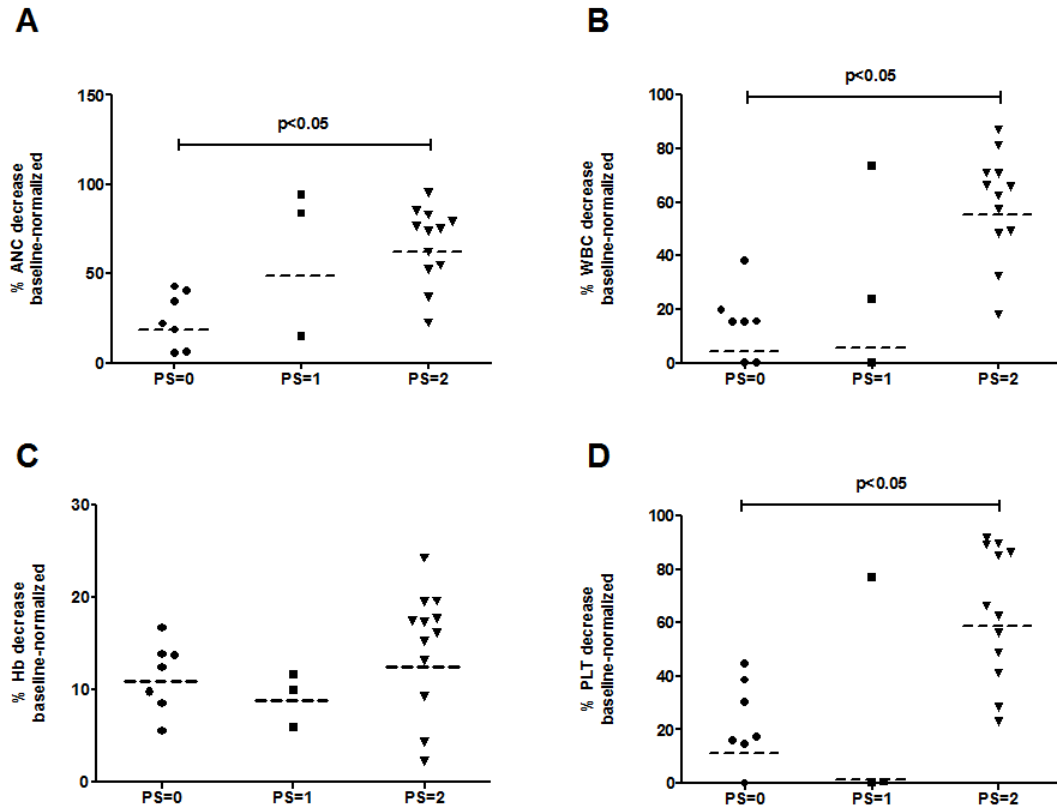
Figure 5-5. Scatter plots of the effect of performance status on the AR-67 toxicity profile.

Performance status (PS) is presented versus the %decrease from baseline of ANC (A), WBC (B), Hb (C) and PLT (D). The pharmacodynamic data (ANC, WBC, Hb and PLT) were collected on days 1, 8, 15 and 21 of cycle 1 from patients (n=25) participating in the AR-67 phase I clinical trial. Statistically significant differences between groups (PS=0, PS=1 and PS=2) were detected by performing one-way Analysis of Variance (Bonferroni correction for multiple comparisons). P<0.05 was considered statistically significant (*p<0.05). Only statistically significant differences are indicated. ANC and Hb values are presented in 10^3/uL and g/dL, respectively while PLT and WBC values are 10^3/mm^3. Broken line, geometric mean. PS: Performance Status, ANC: Absolute Neutrophil Count, WBC: White Blood Cells, Hb: Hemoglobin, PLT: Platelets.

5.3.2.3 Effect Of Body-size Measures On AR-67 Clearance.

Anticancer agents are typically dosed based on the patients' somatometric characteristics to account for the intersubject variability on the disposition and elimination of the drug [181]. Notably, no relationship was established between lactone clearance and any of the tested body-size measures, namely BSA, LBW, IBW, AIBW and BMI, using linear regression analysis (Figure 5-6). Additionally, when the previously mentioned clearance estimates were corrected with body-size measures, no improvement of the intersubject variability associated with CL was observed (Table 7-3).
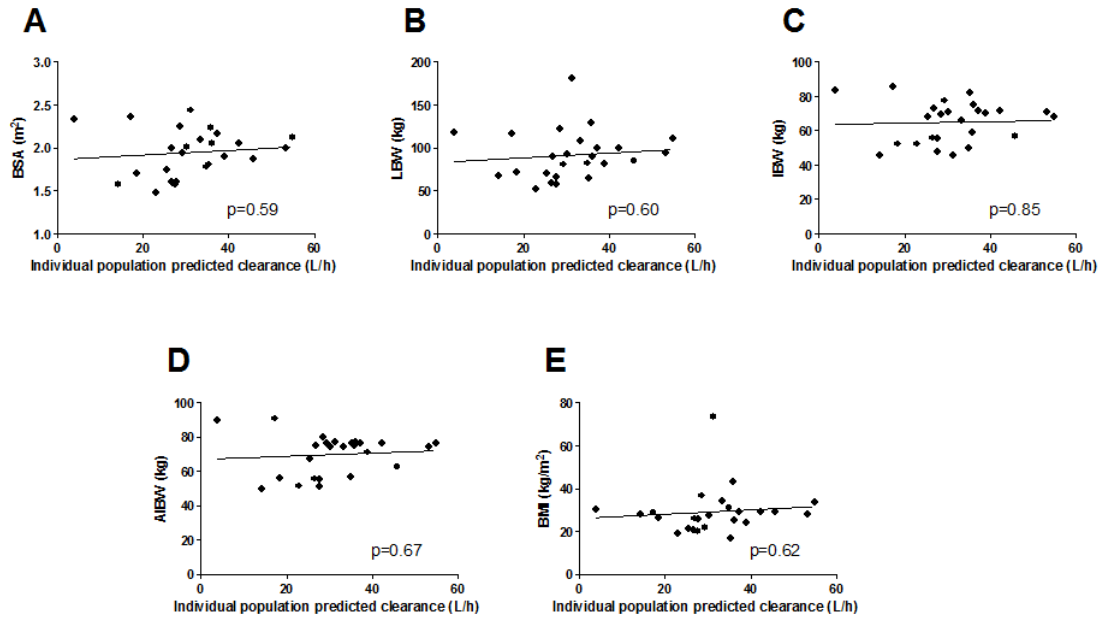
Figure 5-6. Relationship of individual population lactone clearance estimates and body-size measures.

Clearance estimates were obtained using a covariate-free population pharmacokinetic model described previously (n=25) and the body-size measures, namely BSA (A), LBW (B), IBM (C), AIBW (D) and BMI (E), were calculated as described in the materials and methods section. $P < 0.05$ is indicative of slope significantly different from zero. Clearance, BSA, LBW, IBW, AIBW and BMI values are given as L/h, m^2, kg, kg, kg and kg/m^2, respectively. BSA: Body Surface Area, LBW: Lean Body Weight, IBW: Ideal Body Weight, AIBW: Adjusted Ideal Body Weight, BMI: Body Mass Index.

5.4 Discussion.

Here, we studied the population pharmacokinetics of lactone and total AR-67 in plasma obtained from patients participating in a phase I clinical trial. Covariates were tested with the intent of decreasing the intersubject variability associated with the population parameter estimates. Our analysis showed that BUN and BSA accounted for 23.3 % and 10.6 % of interindividual variability of V1 and V2 in the lactone model, respectively. Moreover, BSA and sex were identified as determinants of total AR-67 CL and V1, respectively, and were incorporated in the total AR-67 model. Smoking and obesity had no effect on the pharmacokinetic profile of AR-67. Additionally, although performance status did not impact drug clearance, it did correlate with increased hematological toxicity. Finally, our analysis showed that normalization of AR-67 clearance to different body-measures, including BSA, did not result in decreased intersubject variability for this population parameter.

As AR-67 is undergoing clinical development, it is useful to establish a pharmacokinetic model to describe the AR-67 disposition and elimination as well as potential sources of intersubject variability. A two-compartment structural model was used in the population analysis of lactone and total AR-67. Since, similar pharmacokinetic parameter estimates were obtained using both models for either lactone or total AR-67 (Table 5-2 and 5-3), these models can be used interchangeably to describe AR-67 population pharmacokinetics. The total body clearance for total AR-67 was 14.4 L/h/m^2 ± 3.3 (Table 5-3) which is comparable to clearance values obtained previously (non-compartmental analysis, 14.5 L/h/m^2 ± 3.1 on day 1 and 17.4 L/h/m^2 ± 5.2 on day 4) [78].

In vitro studies and clinical data have suggested that AR-67 lactone could undergo metabolism in the liver and the gastrointestinal tract [78, 79]. Thus, the effect of liver enzymes and other indicators of liver function, such as albumin and bilirubin, were tested

121

as covariates on lactone CL. However, their inclusion in the model was not justified as they did not explain the observed high variability (58.6 %). Surprisingly, incorporation of BUN, an indicator of renal function, into the lactone covariate population model accounted for a significant percentage (23.3 %) of intersubject variability associated with V1 (Table 5-4). We attempted to attribute this finding to fluid retention, as some patients were clinically diagnosed with edema at study entry and were being treated with diuretics. However, BUN values were not statistically significantly different between patients with and without edema (p=0.47) (Table 5-1). Additionally, although the difference in BUN values between men and women was not statistically significant (p=0.48), incorporation of BUN eliminated gender differences on V1 (base model: *p=0.03 vs covariate model: p=0.08). This is a very interesting finding as BUN has not been assessed in previous camptothecin covariate analyses and, therefore, requires further investigation.

Moreover, BSA was considered for V2 (Table 5-4) potentially reflecting differences in body size and, therefore, differences in the extent of distribution of lipophilic AR-67 lactone possibly in adipose tissue. However, the difference in V2 estimates between obese (BMI>25) and non-obese (BMI<25) patients was not statistically significant (p=0.80), which indicated that AR-67 lactone was not distributing preferentially into fat tissues. Interestingly, V2 estimates differed between sexes (female vs male, 25.2 L ± 9.0 vs 34.9 L ± 10.8, *p=0.02). Taking into consideration that AR-67 is primarily eliminated through the liver and the liver volume, which is higher in men than in women, has been found to correlate with BSA [196, 197], we hypothesize that the association between BSA and V2 observed in our study is suggestive of AR-67 partitioning preferentially in the liver tissue from where it is being cleared efficiently.

122

BSA was also identified as a determinant of total body clearance of total AR-67 (ΔOFV=-4.69, $p<0.05$) (Table 5-5). Similar results have been reported for topotecan in pediatric patients [46] and irinotecan [70, 72]. However, Klein et al. failed to observe a relationship between BSA and irinotecan CLEta [71]. Moreover, Mathijseen et al., 2002 demonstrated that normalizing irinotecan clearance to body-size measures did not decrease the observed intersubject variability of this pharmacokinetic parameter introducing the concept of flat or fixed dosing for irinotecan [185]. In our study, normalization of lactone and total AR-67 total body clearance to BSA, LBW, IBW, AIBW and BMI did not have any effect on the variability observed with this pharmacokinetic parameter (Table 7-3). Additionally, when included in the covariate model, BSA accounted for only a small portion (3.5 %) of the intersubject variability observed with total body clearance (Table 5-5). These findings considered together question the inclusion of BSA on CL into the covariate model as well as dosing AR-67 based on BSA.

Previously, body surface area and weight were found to be determinants of V1 of both irinotecan [71, 198] and topotecan [47]. In our study (Table 5-5), considering sex on V1 resulted in significant (~25 %) decrease in the intersubject variability. Since plasma volume is higher in men than in women and correlates with body-size measures [199], findings reported here are aligned with the aforementioned studies. Moreover, although the lactone is the predominant species in the plasma, it is anticipated that the pharmacokinetic behavior of total AR-67 carries attributes of both the lactone and the carboxylate form. Therefore, we reason that the importance of sex on the total AR-67 V1 reflects confinement of the carboxylate in the plasma compartment (V1) as a result of its hydrophilicity and charge.

AR-67 had displayed noteworthy lactone stability in blood *in vitro* [38] and was expected to partition in red blood cells due its lipophilicity. Moreover, Loos et al. demonstrated that

topotecan partitioning into the red blood cells resulted in lower clearance rates of the camptothecin from the plasma of women than men [200, 201]. However, contrary to the findings by Loos et al. [200, 201], in our study the hematocrit values did not differ between men and women (p=0.78) and the plasma lactone clearance was not found to be gender-dependent (p=0.36). Therefore, considering HCT as a covariate in the lactone population model did not decrease the CL intersubject variability.

The effect of smoking on AR-67 pharmacokinetics and toxicity profile was also of interest as tobacco exacerbates the activity of metabolic enzymes such as CYP1A1, CYP1A2 and UGTs [194, 202-204] that have been identified as potentially playing a role in the elimination of AR-67 in the liver and gut. Although van der Bol et al. showed that exposure to irinotecan and SN-38 was lower in smokers than patients that did not smoke [205], our analysis indicated that exposure to AR-67 did not differ significantly (p<0.05) between smokers and non-smokers (Figure 5-3).

Moreover, studies have demonstrated increased metabolic activity of CYP1A2 and UGTs, but not of CYP3A4 in obese individuals [195, 206]. We showed that normal-weight and obese patients cleared AR-67 at the same rate (Figure 5-4). *In vitro* studies on AR-67 metabolism indicated high affinity between AR-67 lactone and UGT1A7 and UGT1A8. In absence of any studies associating UGT1A7 or UGT1A8 metabolic activity with obesity, we speculate that UGT1A7/8 metabolic activity is unaffected in obese individuals or that the effect of the induced UGTs on the metabolic profile of AR-67 was negated by the decrease in the metabolic activity of CYP3A4 as a result of the considerable metabolic capacity of the latter. It is also possible that the iv administration of AR-67 masked the obesity-related induction of UGT activity as UGT1A7/8 are selectively expressed in the gut wall.

Performance status had been related to irinotecan, SN-38 and topotecan clearance in population covariate models developed previously (Table 1-1). Our analysis did not reveal statistically significant differences on the population parameter estimates when patients were sorted by performance status (data not shown, p=0.08). Moreover, Comella et al. reported that patients with PS≥1 ran a higher risk of experiencing grade 4 neutropenia after irinotecan administration [207]. Similarly, in our study, the patient group with the worst performance status (PS=2) appeared to be more susceptible to hematological toxicity in our study (Figure 5-5). This finding is of great significance for the frail population of cancer patients and needs to be verified in a larger population sample.

Despite the intensive study presented here on the factors that could have an impact on AR-67 clearance, intersubject variability of the pharmacokinetic parameters studied remained high in a final covariate model (Table 5-4 and 5.5). More specifically, intersubject variability of CL was 58.2 % and 25.1 % for lactone and total AR-67, respectively, in the developed covariate models. Preclinical studies have suggested that the liver-specific uptake transporters OATP1B1 and OATP1B3 and the efflux transporters MDR1 and BCRP could play an important role on the disposition and elimination of AR-67 (manuscript in preparation),[122]. Moreover, a plethora of metabolic enzymes have exhibited affinity for the lactone form [79]. Therefore, we reason that differences in the expression levels or function of the aforementioned transporters and metabolic enzymes as well as variability on the degree of induction or inhibition of those complex systems by co-administered drugs or by health conditions of the study participants could account for the unexplained variability we are reporting. Future studies should focus on exploring relationships between AR-67-induced toxicity and genetic

polymorphisms of the aforementioned transporters and metabolic enzymes [68, 69, 208-212].

In conclusion, population pharmacokinetic models were developed for AR-67 lactone and total AR-67 using the nonlinear mixed effects approach. The pharmacokinetic parameter estimates did not differ between the two models suggesting similar pharmacokinetic behavior for lactone and total AR-67. BUN, BSA and sex were identified as covariates explaining intersubject variability within the studied patient population and were incorporated into the lactone and total AR-67 covariate models. Patients with unfavorable performance status at study entry did seem to suffer high grade hematological toxicity and might require dose adjustments or incorporation of hematopoietic growth factors in their standard treatment. Finally, based on our analysis, flat or fixed dosing of AR-67 warrants further investigation as AR-67 clearance was found to be independent of body-size measures. As this is the first population pharmacokinetic analysis on AR-67, more extensive studies need to take place to identify individual predictors of AR-67 elimination and evaluate their clinical significance.

6. Chapter 6: Summary - Future Studies

AR-67 is a lipophilic 3rd generation camptothecin analogue with considerable stability of its pharmacologically active lactone form and its biological activity in animal models. Preclinical studies indicated noteworthy cytotoxicity *in vitro* [74] and promising antitumor activity using xenografts [76, 77]. In view of those results, AR-67 advanced to clinical trials. In the recently completed phase I clinical trial, stable disease and prolonged partial response were observed [78]. Therefore, the promising findings obtained in the preclinical and clinical level underlying the efficacy of this camptothecin analogue in cancer encourage further development of AR-67.

Transporter proteins localizing at the membrane of tumor cells have been implicated in resistance or chemosensitivity often observed with anticancer agents. Therefore, we designed studies to determine the effect of overexpression of efflux and uptake transporters would have on AR-67 cytotoxicity *in vitro*. Using cell lines over-expressing the efflux transporters BCRP and MDR1, we demonstrated that AR-67 is a substrate for both BCRP and MDR1. Our studies also indicated that over-expression of these efflux transporters conferred resistance to AR-67 *in vitro*.

Studies have shown that BCRP and MDR1 expression in human tumors could result in drug resistance and therapy failure [85, 97-103]. Therefore, it would be interesting to examine the effect of BCRP and MDR1 over-expression on the antitumor activity of AR-67 *in vivo* using xenograft models. Our hypothesis is that tumor-bearing animals that over-express BCRP or MDR1 will show lower response rate than animals with tumors that do not express the efflux transporter. To address this question, the development of a xenograft tumor model using mock- and BCRP/MDR1-transfected cell lines is required. To improve the predictability of the study, human tumor xenografts screened for BCRP or MDR1 expression should also be considered as an option as they represent more

accurately the heterogeneity of human tumors in regards to transporter expression [164]. Additionally, quantifying the amount of AR-67 at the tumor site would also be of interest. That way we will obtain a better understanding on the functional activity of the transporter *in vivo* and will be able to correlate that information with survival data.

Studies report increased expression of OATP1B3 in tumor tissues [110, 112, 113]. Based on our study results using OATP1B3 over-expressing cell lines, AR-67 cytotoxicity is mediated by the lactone form which is favored intracellularly potentially because of protein binding, partitioning into membranes and/or distribution in organelles with acidic environment such as the peroxisomes. Increased membrane expression of the OATP1B3 transporter did not sensitize cells to AR-67 treatment *in vitro*. Therefore, our study suggests no therapeutic advantage of AR-67 administration in patients that over-express OATP1B3 in their tumor tissue.

Previous studies on camptothecins using xenografts models have demonstrated that low-dose protracted dosing schedules are more efficacious than intense high-dose schedules [123, 125-128]. Similar results were obtained for AR-67 when dosed following varying dosing schedules. Further exploration of the underlying reasons for these findings using NSCLC xenografts allowed us to conclude that the pharmacokinetics of AR-67 at the tumor site were associated with lower elimination rates than the respective ones in the plasma. Moreover, Top1 kinetics was schedule-dependent. More specifically, groups that received low-doses of AR-67 for an extended period of time and responded better to AR-67 treatment showed detectable expression levels of Top1 in the tumor tissue. We concluded that low-dose protracted dosing schedules that do not deplete Top1 expression at the tumor site result in higher response rates than more intense dosing schedules.

Following, a pilot human trial was conducted to provide an insight on the safety and toxicity of AR-67 given following a protracted dosing schedule. Although the type of the toxicities observed during this pilot study were similar to the ones identified in the phase I clinical trial, dose de-escalation was necessary. Therefore, the recommended dose for future studies on AR-67 protracted dosing is 5.5 mg/m^2/day given as an 1-hr infusion on days 1, 4, 8, 12 and 15 every 21 days. Moreover, sampling the tumor in patients participating in the study twice within 24 hours after the drug administration on day 1 was proven feasible. Interestingly, similarly to the preclinical studies, drug accumulation in the tumor was observed in one of the study participants. Although this finding is encouraging, it is imperative to examine the AR-67 tumor pharmacokinetics in a larger group of patients with different cancer types as the physiology of the tumor could also play a role in the tumor distribution of the camptothecin at the site of action.

Finally, the experience obtained during this proof-of-concept study is one of the most important aspects of this study in terms of designing future trials. The amount of tumor tissue collected and limitations associated with the bioanalytical method used to quantify AR-67 in the tumor tissue were essential issues [137]. Moreover, although we were able to detect Top1 in the tumor, the enzyme kinetics in the presence of AR-67 requires further evaluation. Our work highlights the importance of acquiring a baseline measurement of Top1.

The first pharmacokinetic population model on AR-67 was presented here. It was developed by analyzing pharmacokinetic data collected in the AR-67 phase I clinical trial [78]. The analysis was performed using the nonlinear mixed effects theory [130]. Covariate analysis [192] did allow the incorporation of patient attributes into the population pharmacokinetic model. However, their clinical relevance needs to be evaluated further in a larger population.

More specifically, the phase I clinical trial data and *in vitro* studies have demonstrated that AR-67 is being metabolized in the liver and the gut while its renal elimination is limited [78, 79, 81]. However, no liver-specific covariates were identified as determinants of AR-67 clearance and smoking or obesity did not have any impact on drug clearance although they have been reported to interfere with the metabolic activity of enzymes [79, 194, 195, 205]. Future studies that compare the pharmacokinetic parameters such as clearance and AUC between cancer patients with normal liver function and cancer patients with impaired liver function will provide us with a definitive answer on whether or not patients with liver dysfunction run increased risk for toxicity when given AR-67. This finding could be of extreme importance as most of cancer types are associated with liver metastases that could result in liver impairment that render dose adjustments necessary.

Studies presented here have demonstrated the interaction between AR-67 and a number of uptake and efflux transporters and metabolic enzymes that allow us to obtain a better understanding of the disposition and elimination of AR-67 (Figure 6-1). More specifically, AR-67 carboxylate has been identified as a substrate for the liver-specific transporters OATP1B1 and OATP1B3 (Chapter 3). Preclinical work by Adane et al. [75] indicates that the carboxylate form is being eliminated 3.5-fold faster than the lactone form. Therefore, it is hypothesized that those two uptake transporters might play a fundamental role on the elimination of AR-67. Horn et al [79] demonstrated that AR-67 lactone can be biotransformed *in vitro* by the metabolic enzymes CYP3A4/5 and CYP1A1/2 and UGT1A1/3 that localize in the liver. We reason that the lactone that escaped metabolism and its metabolic products have the potential of being transferred in the bile by BCRP and MDR1. While in the gut, we reason that the lactone is being released from its glucuronide form as a result of the bacterial β-glucuronidase activity and passively diffuses into the enterocytes where it is being effectively metabolized by

UGT1A7/8 and CYP3A4/5 [79]. Alternatively, AR-67 and its metabolites have the potential of being effluxed back into the lumen by MDR1 and BCRP. In conclusion, the disposition and elimination AR-67 pathways are of great complexity.

Against this background, we reason that the pharmacogenetics of AR-67 warrant further study. We hypothesize that differences in the expression levels and in the functional activity of the previously mentioned transporters (Figure 6-1) could account for part of the unexplained variability observed with the developed population pharmacokinetic model. Additionally, similarly to other camptothecins [68, 69], polymorphisms of metabolic enzymes (Figure 6-1) localized in the liver or the gut could influence disposition and elimination of AR-67. For instance, findings by Horn et al [79] suggest that the intense metabolism that AR-67 undergoes in the gut is the reason why no diarrhea was reported by the phase I clinical trial patients [78]. Therefore, it would be interesting to monitor patients with genetic variations on UGT1A7 and UGT1A8 for gastrointestinal toxicity after AR-67 administration.

Additionally, early studies on the metabolism and transport of irinotecan and its metabolites showed that MRP2 plays a fundamental role on irinotecan and SN-38 elimination by mediating the transfer of their glucuronides into the bile [66, 213]. Therefore, potential interaction between MRP2 and AR-67 needs to be explored *in vitro* and the clinical relevance of known MRP2 polymorphisms on the disposition and elimination of AR-67 needs to be studied should there be an interaction identified *in vitro.*

Finally, AR-67 displayed noticeable antitumor activity in a mouse glioma model system [77]. Considering camptothecins have been used to treat patients with brain tumors with documented success [214, 215], AR-67 should be evaluated as an alternative option for patients with brain tumors not responding to available treatments. Additionally, studies

have shown that anticonvulsant agents received by cancer patients for seizure control interfere with the pharmacokinetics of camptothecins that undergo hepatic elimination [58, 214, 216-218]. Therefore, the potential for drug-drug interactions between AR-67 and anticonvulsants needs to be explored further.

In conclusion, the development of AR-67 has been proven to be challenging. Although the work presented here has contributed to the development of this camptothecin analogue, the later remains a work in progress.
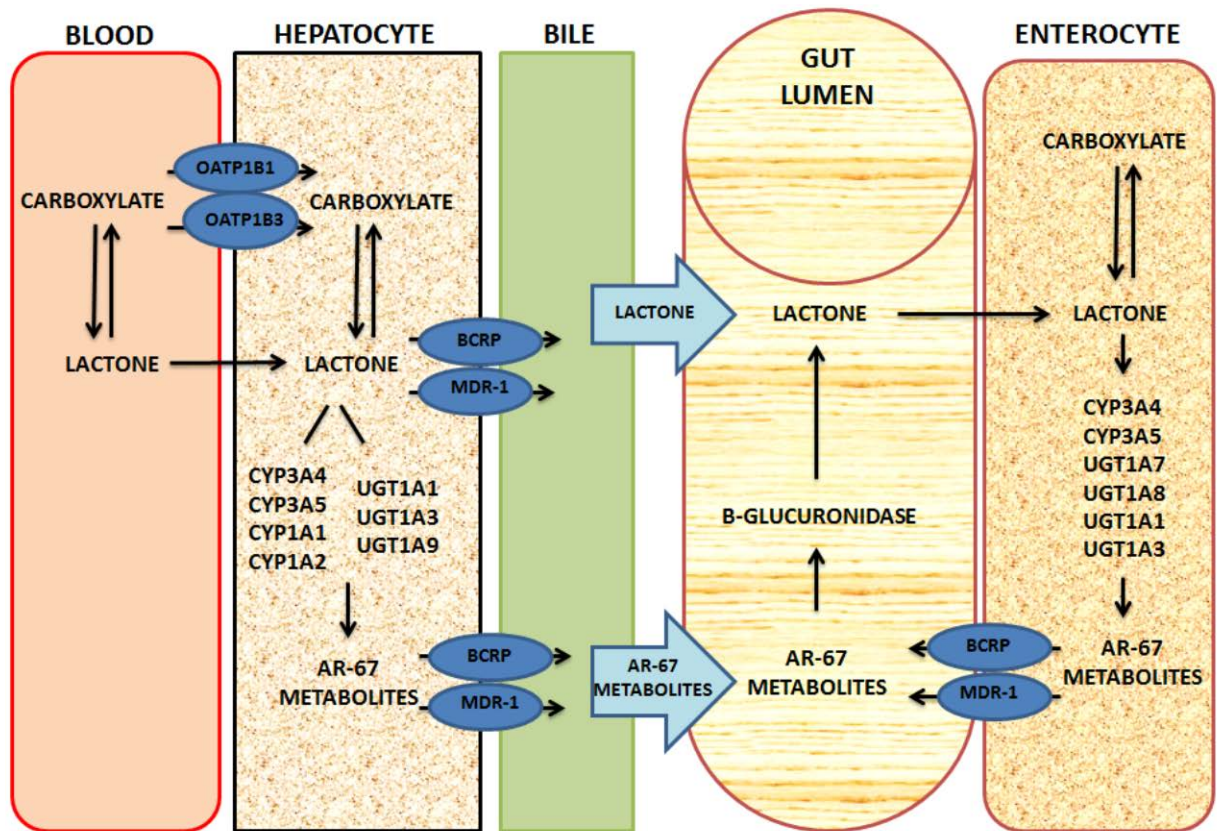
Figure 6-1. Hypothetical schematic including transporters and enzymes involved in the disposition and elimination of AR-67.

133

www.manaraa.com

7. Appendix
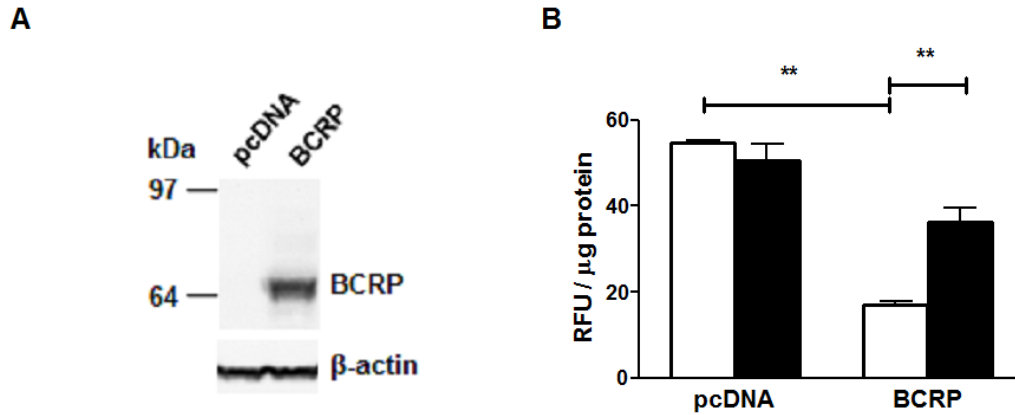
Figure 7-1: Expression and functional validation of BCRP transporter in MDCKII-pcDNA/BCRP cells.

Immunoblotting analysis of lysates prepared from (A) MDCKII-pcDNA/BCRP cells to evaluate the BCRP expression. Actin was used as a loading control. (B) MDCKII-pcDNA/BCRP cells were incubated with Hoechst 33342 (2 µM) for 45 min (open bars). The inhibitory effect of 4 µM of GF120918 in the transporter-mediated efflux of (B) Hoechst 33342 was also assessed (solid bars) as described in the Materials and Methods section. Data are represented as mean (n=3) ± SD. Statistical analysis was performed using unpaired and paired t-test, statistical significance for * $p < 0.05$ and ** $p < 0.01$.

134
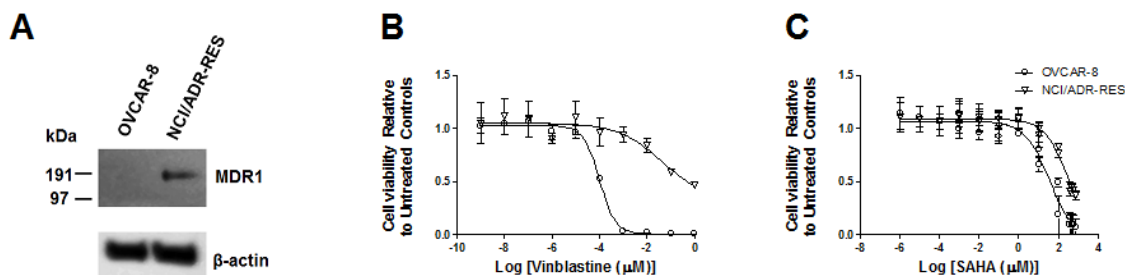
Figure 7-2: Expression and functional validation of MDR1 transporter in OVCAR-8/NCI/ADR-RES cells.

Immunoblotting analysis of lysates prepared from (A) OVCAR-8/NCI/ADR-RES cells to evaluate the MDR1 expression. Actin was used as a loading control. (B) Effect of Vinblastine on OVCAR-8 and NCI/ADR-RES cell lines. Cells were treated with Vinblastine for 72 hours before assessing cell viability as described in the Materials and Methods section. The estimated IC_{50} values were 0.099 nM (0.086-0.116) and 43.9 nM (0.75-2,563) for OVCAR-8 and NCI/ADR-RES cells, respectively. (C) Effect of SAHA on OVCAR-8 and NCI/ADR-RES cell lines. Cells were treated with SAHA for 72 hours before assessing cell viability as described in the Materials and Methods section. The estimated IC_{50} values were 40.79 µM (21.78-76.38) and 418.5 µM (59.61-2939) for OVCAR-8 and NCI/ADR-RES cells, respectively when exposed to SAHA. Data are represented as mean (n=3) ± SD. Data analysis to obtain IC_{50} values was performed using nonlinear regression. IC_{50} values (µM) are reported as mean (95 % confidence interval).

Table 7-1: P_{app} and efflux ratio values describing the efflux activity of BCRP for AR-67 lactone in polarized MDCKII cells, in the presence and absence of the BCRP inhibitor GF120918.

	Control		GF120918 (5µM)	
	MDCKII-pcDNA	MDCKII-BCRP	MDCKII-pcDNA	MDCKII-BCRP
$P_{app,A>B}$	2.18 ± 0.26	0.08 ± 0.02	1.33 ± 0.07	2.96 ± 0.12
$P_{app,B>A}$	2.85 ± 0.13	6.86 ± 0.7	1.31 ± 0.10	6.72 ± 1.81
Efflux ratio (B>A/A>B)	1.31 ± 0.17	90.82 ± 23.35	0.99 ± 0.09	2.27 ± 0.62
P_{app} is expressed in cm/sec x 10^5 Values are expressed as mean ± SD				
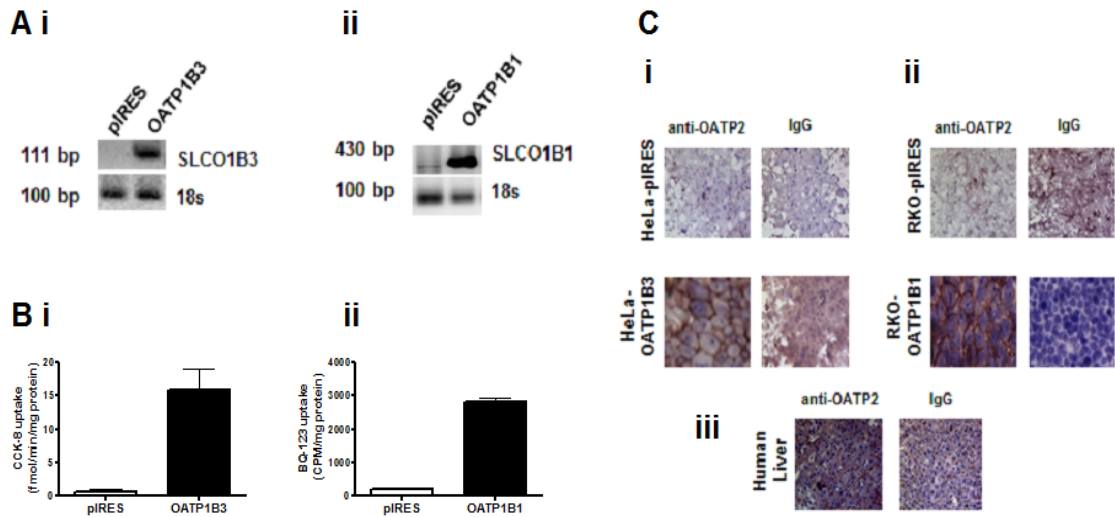
Figure 7-3: Expression and functional validation of OATP1B3 and OATP1B1 transporters in HeLa and RKO cell lines.

(A) Quantitative RT-PCR analysis was used to validate (i) OATP1B3 and (ii) OATP1B1 mRNA expression in the stably OATP-transfected HeLa and RKO cells, respectively. (B) (i) Hela-pIRES and Hela-OATP1B3 cells were incubated with 0.005 µM of ^{3}H-CCK-8 for 10 min. (ii) RKO-pIRES and RKO-OATP1B1 cells were incubated with 0.5 µM of ^{3}H-BQ-123 for 30 min. The scintillation counting was determined in the cell lysate and normalized with the cell lysate protein concentration as described in the Materials and Methods section. Data are represented as mean ± SD (n=8-10). (C) Immunohistochemical staining for OATP2 was used to validate OATP1B1 and OATP1B3 transporter expression in the OATP stably transfected cell lines (i) HeLa-pIRES and HeLa-OATP1B3 and (ii) RKO-pIRES and RKO-OATP1B1, respectively. (iii) Human liver was used as positive control to confirm the specificity of the OATP2 antibody for the OATP1B1 and OATP1B3 uptake transporters.
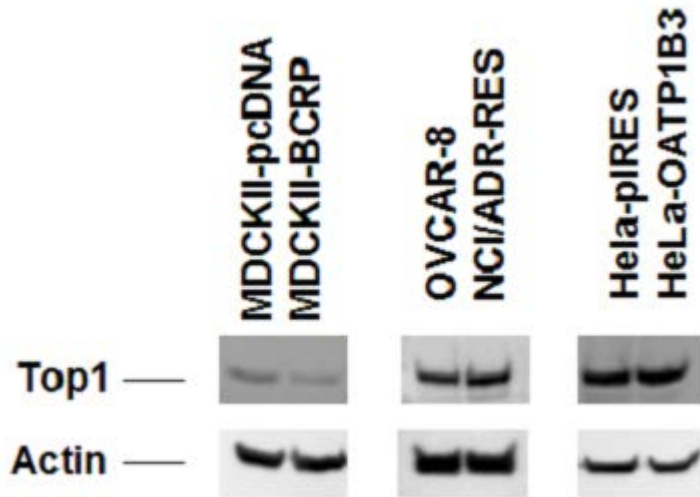
Figure 7-4: Expression of Top1 in MDCKII-pcDNA/BCRP, OVCAR-8/NCI/ADR-RES and HeLa-pIRES/OATP1B3 cell lines.

Immunoblotting analysis was employed to evaluate the expression of Top1 in lysates prepared from MDCKII-pcDNA/BCRP, OVCAR-8/NCI/ADR-RES and HeLa-pIRES/OATP1B3 cells. Actin was used as a loading control.
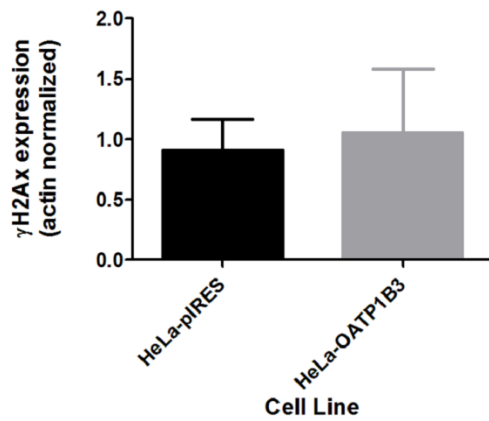
Figure 7-5: Expression of γH2AX in HeLa-pIRES/OATP1B3 cells lines.

Western blot analysis was used to evaluate γH2AX in lysates of mock- and OATP1B3-transfected cells treated with AR-67 carboxylate (20 µM) for 5 min. γH2AX to actin band intensity ratios were calculated and are presented as mean (n=3) ± SD. Statistical analysis was performed using unpaired t-test, p=0.669.
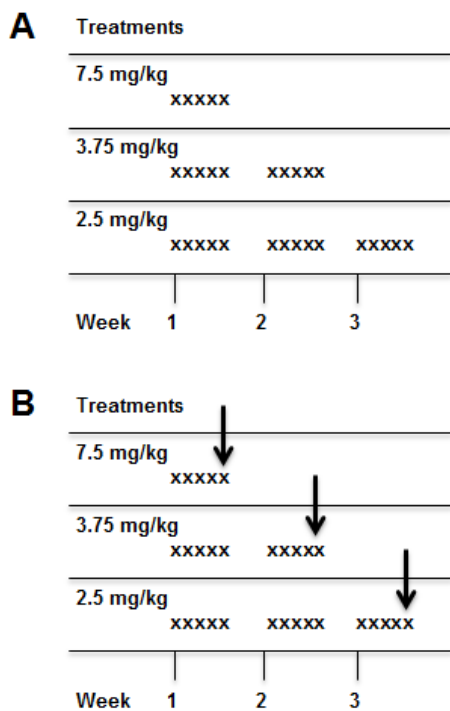
Figure 7-6: Schematic of AR-67 dosing schedules.

(A) The AR-67 antitumor effect was evaluated using NCI-H460 tumor-bearing nude mice. They received AR-67 lactone as an iv bolus at 3 dose levels on days designated with x. More specifically, the animals received lactone at doses equal to 7.5 mg/kg daily for 5 consecutive days (day 1-5) or 3.75 mg/kg daily for 5 consecutive days (day 1-5) a week for 2 weeks or 2.5 mg/kg daily for 5 consecutive days (day 1-5) a week for 3 weeks. (B) Biological activity of AR-67 lactone in NSCLC xenografts was studied in NSCLC xenografts. They received AR-67 lactone as an iv bolus at 3 dose levels on days designated with x. More specifically, the animals received lactone at doses equal to 7.5 mg/kg daily for 5 consecutive days (day 1-5) or 3.75 mg/kg daily for 5 consecutive days (day 1-5) a week for 2 weeks or 2.5 mg/kg daily for 5 consecutive days (day 1-5) a week for 3 weeks. They were sacrificed and had their tumor tissue collected on the last day of treatment, 6 hours after AR-67 administration, designated by arrows.
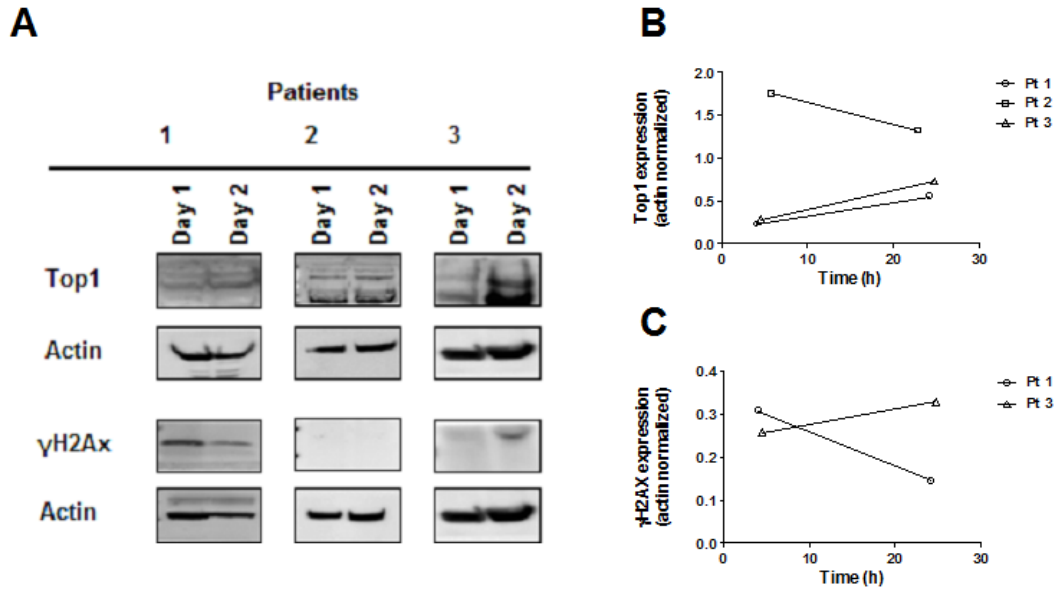
Figure 7-7: Biological activity of AR-67 lactone in cancer patients with metastatic or refractory solid tumors.

Western blotting was used to evaluate the expression level of Top1 and γH2AX in tumor tissue collected from study participants at two different time points, between 3 and 24 hours after the start of the infusion, designated as t=0 hours, on Day 1 of Cycle 1 (A). Actin was used as a loading control. (B and C) Graphical representation of the densitometry analysis results performed on the Top1 (B) and γH2AX (C) data presented on panel (A).
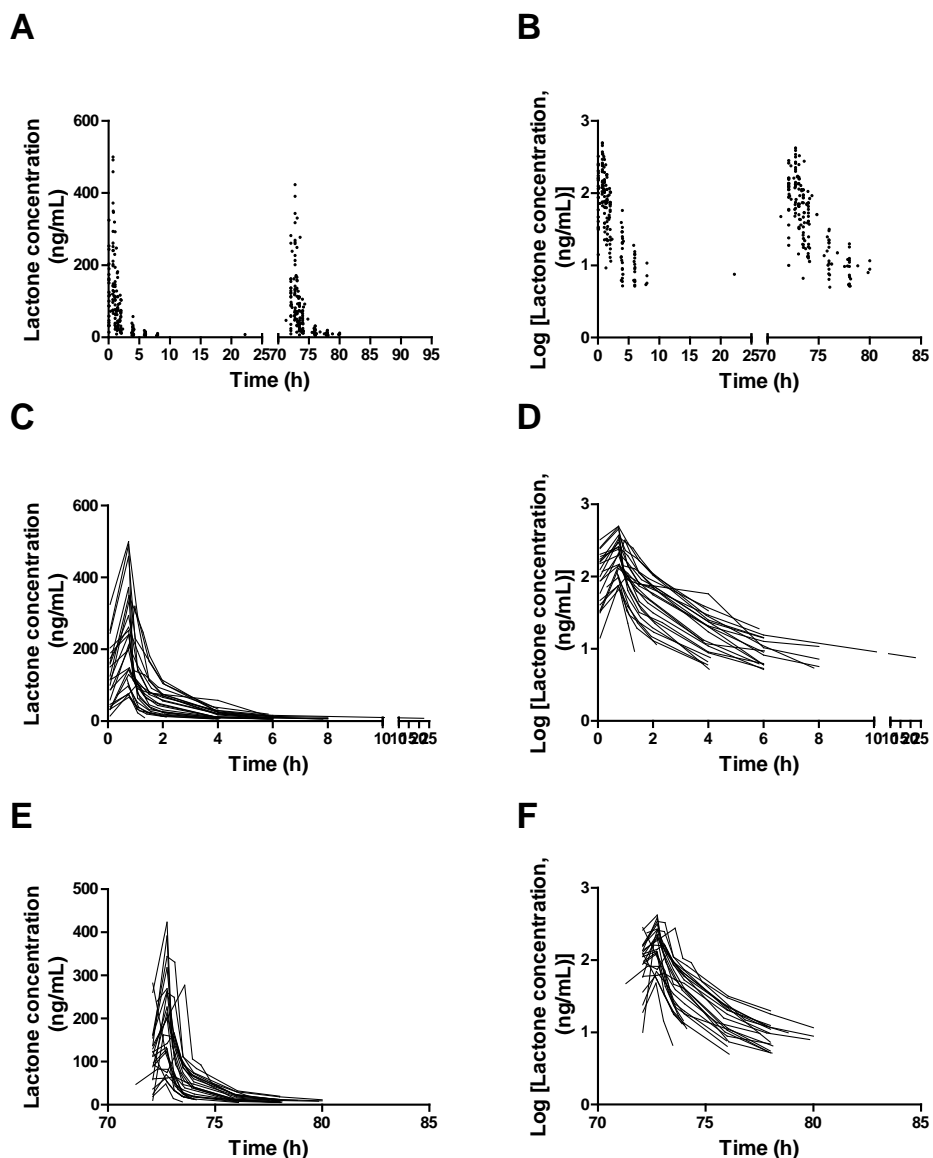
Figure 7-8: Pharmacokinetic profile of AR-67 lactone in plasma of phase I cancer patients after iv administration of AR-67 lactone.

AR-67 lactone was quantified using a validated bioanalytical method in plasma samples collected from patients (n=26) participating in a first-in-human phase I clinical trial. AR-67 lactone was administered at doses ranging from 1.2 to 12.4 mg/m^2/kg for 5 consecutive days as a 1-h infusion every 21 days and the pharmacokinetics of the agent were studied on days 1 (C, D) and 4 (E, F) of cycle 1 (A, B). Concentrations of lactone (A, C and E) and their logarithmic values ((B, D and F) are plotted agaist time (h).
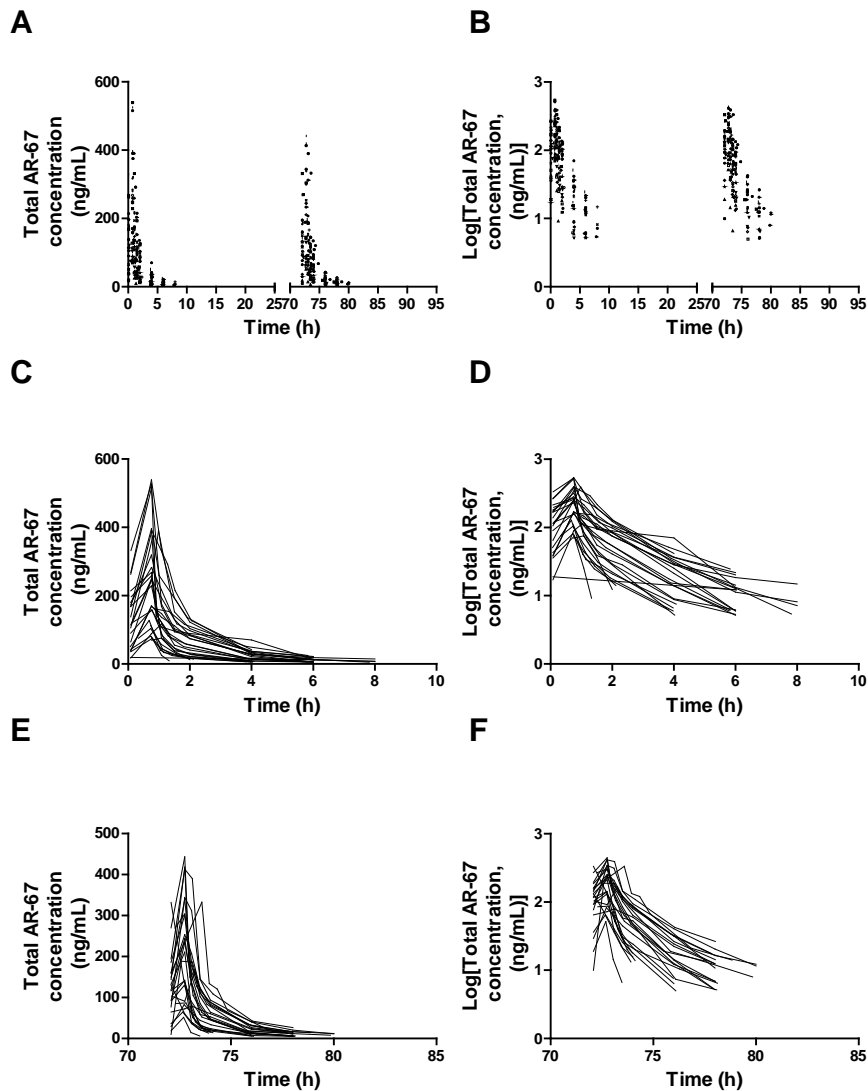
Figure 7-9: Pharmacokinetic profile of total AR-67 in plasma of phase I cancer patients after iv administration of AR-67 lactone.

Total AR-67 (lactone and carboxylate) was quantified using a validated bioanalytical method in plasma samples collected from patients (n=26) participating in a first-in-human phase I clinical trial. AR-67 lactone was administered at doses ranging from 1.2 to 12.4 mg/m^2/kg for 5 consecutive days as a 1-h infusion every 21 days and the pharmacokinetics of the agent were studied on days 1 (C, D) and 4 (E, F) of cycle 1 (A, B). Concentrations of Total AR-67 (A, C and E) and their logarithmic values ((B, D and F) are plotted agaist time (h).

143

Table 7-2: Evaluation of co-linearity between patient clinical characteristics used for covariate model development.

Covariate	CRCL	AGE	BUN	Alb	T_{bil}	ALP	ALT	AST	LDH	DOSELEV	HCT
BSA	0.01*	0.94	0.77	0.04*	0.56	0.19	0.25	0.41	0.36	0.63	0.63
CRCL		0.22	0.02*	0.31	0.32	0.06	0.48	0.32	0.04*	0.59	0.39
AGE			0.17	0.45	0.69	0.95	0.01*	0.02*	0.38	0.84	0.92
BUN				0.64	0.11	0.35	0.19	0.10	0.07	0.76	0.50
Alb					0.18	0.01*	0.74	0.88	0.04*	0.35	0.03*
T_{bil}						0.15	0.83	0.16	0.003*	0.44	0.03*
ALP							0.87	0.84	0.01*	0.85	0.06
ALT								0.0007*	0.62	0.36	0.85
AST									0.13	0.67	0.01*
LDH										0.96	0.01*
DOSELEV											0.24
p value: linear regression analysis where slope significantly different from zero for *p<0.05											
BSA: Body surface area, CRCL: creatinine clearance, BUN: blood urea nitrogen, Alb: albumin, T_{bil}: total bilirubin, ALP: alkaline phosphatase, ALT: alanine transaminase, AST: aspartate transaminase, LDH: liver dehydrogenase, DOSELEV: AR-67 dose level that patients were assigned to, HCT: hematocrit.											
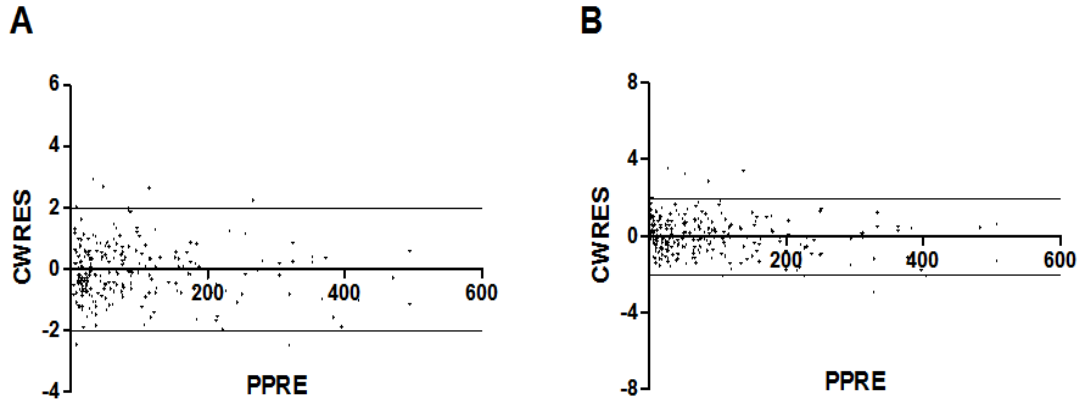
Figure 7-10: Diagnostic plots of conditional weighted residuals obtained from population pharmacokinetic models developed for AR-67 lactone and total AR-67.

Plots of conditional weighted residuals (CWRES) versus population predicted AR-67 lactone (A) and total AR-67 (B) plasma concentrations (PPRE). The population pharmacokinetics were studied after administration of AR-67 in cancer patients (n=19) with solid tumors using a two-compartment structural model to fit the data (panels A and B for lactone and total AR-67, respectively). Lines vertical to the X-axis at Y=-2 and 2 were included in the graph for evaluation of randomness. AR-67 PPRE plasma concentrations are given in ng/mL.
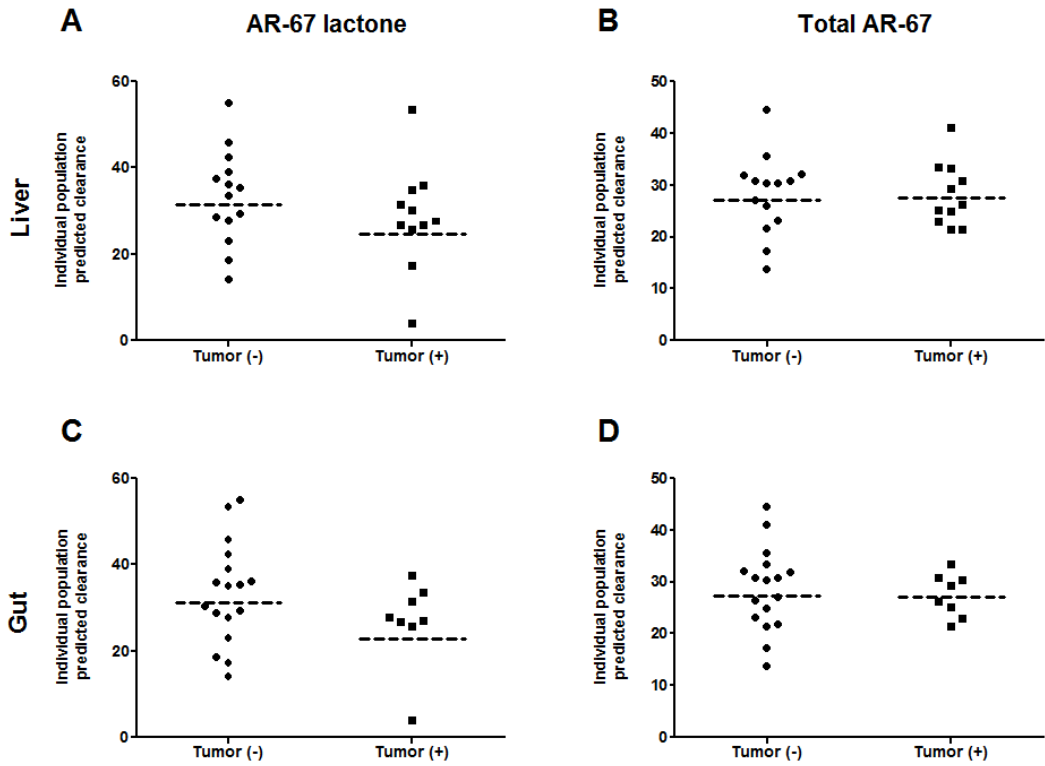
Figure 7-11: Scatter plots of the effect of tumor type on AR-67 clearance.

The relationship between AR-67 lactone (A, C) or total AR-67 (B, D) individual population predicted clearance estimates and tumor type (liver, gut) is depicted. The individual population clearance estimates for lactone and total AR-67 were obtained after performing population analysis on pharmacokinetic data (n=25) collected during the AR-67 phase I clinical trial as described in the materials and methods section. Statistically significant differences between subject groups were detected by performing the Unpaired t-test/Mann-Whitney test (Tumor (+) vs Tumor (-)). P<0.05 was considered statistically significant (*p<0.05). Only statistically significant differences are indicated. Clearance values are given as Liters/hour, L/h. Broken line, geometric mean.

Table 7-3: AR-67 individual population predicted clearance estimates normalized to body-size measures of patients that received AR-67 lactone.

Body-size measurements	AR-67 lactone		AR-67 total	
	Individual population predicted clearance (L/h)			
	mean ± SD	CV(%)	mean ± SD	CV(%)
None	31.1 ± 11.4	36.7	28.3 ± 6.9	24.5
BSA, m^2	16.1 ± 5.6	34.5	14.5 ± 3.2	22.0
LBW, kg	0.4 ± 0.1	37.2	0.3 ±0.1	26.8
IBW, kg	0.5 ± 0.2	36.5	0.4 ± 0.1	26.5
AIBW, kg	0.5 ± 0.2	34.5	0.4 ± 0.1	22.8
BMI, kg/m^2	1.1 ± 0.5	40.5	1.0 ± 0.3	29.8

8. Appendix 2: An HPLC Assay for the Lipophilic Camptothecin Analog AR-67 Carboxylate and Lactone in Human Whole Blood

Eleftheria Tsakalozou, Jamie Horn, Mark Leggas

8.1 Abstract.

AR-67 (7-t-butyldimethylsilyl-10-hydroxycamptothecin, DB-67) is a camptothecin analog currently in early stage clinical trials. The lactone moiety of camptothecins hydrolyzes readily in blood to yield the pharmacologically inactive carboxylate form. However the lactone form of third generation lipophilic congeners, such as AR-67, is more stable possibly due to partitioning into red cell membranes. This prompted us to develop a reverse phase HPLC method with fluorescence detection (excitation 380 nm / emission 560 nm), which could quantitate the concentration of AR-67 lactone and carboxylate in whole blood. Samples were prepared by red cell lysis, protein precipitation with methanol and centrifugation to remove denatured materials. Recovery was estimated to be >85%. Analytes were eluted isocratically with 0.15 M ammonium acetate buffer containing 10 mM TBAP (pH 6.5) and acetonitrile (65:35, v/v) on a Nova-Pak C18 column (4 μm; 3.9 mm × 150 mm). The assay was linear in the range of 0.5-300 ng/mL and 2.5-300 ng/mL for carboxylate and lactone, respectively. Accuracy and precision were acceptable. AR-67 forms were stable in whole blood and in methanolic supernatants. This assay has been successfully applied to measure AR-67 concentrations in whole blood of patients enrolled in a phase I study.

8.2 Introduction.

AR-67 is a novel 3rd generation camptothecin analog currently under clinical investigation for the treatment of cancer (Figure 8-1). Camptothecin analogs are anticancer agents that prevent relaxation of supercoiled DNA by interacting and "poisoning" the function of topoisomerase-I. During DNA transcription and replication, camptothecins can interfere with topoisomerase-I as it tries to religate nicked DNA strands. This ultimately leads to double strand DNA breaks and cell death [3, 5, 20]. In vitro and in vivo pharmacological studies have demonstrated that the E-ring lactone and 20-hydroxyl group of camptothecin and its analogs play a fundamental role in the topoisomerase-I mediated anticancer activity [219-221].

One limitation to the anticancer activity of all camptothecins is the labile nature of their α-hydroxy-δ-lactone ring (lactone form), which is reversibly hydrolyzed to yield a more hydrophilic and pharmacologically inactive carboxylate at physiological pH. Lactone hydrolysis is facilitated further by favorable protein binding of the carboxylate to the human serum albumin (HSA), which provides sink conditions and shifts the equilibrium toward carboxylate formation [16, 222].

To overcome this limitation, 2nd generation analogues were designed with substituent groups that decreased the lactone hydrolysis rates. Compared to camptothecin, the clinically available analogs topotecan and irinotecan as well as its active metabolite SN-38, bind to a lesser extent to HSA and the pharmacophore lactone ring is stabilized [17, 223]. However, the clinically reported ratios of lactone areas under the concentration-time curve (AUC) for those and other congeners in early clinical development are in the order of 30-70% of the total AUC [42, 224-226].

More recent efforts have focused on the development of highly lipophilic analogs, including AR-67, which have various silyl-hydrocarbon substituents that appear to minimize interaction with albumin and decrease hydrolysis rates [125, 227-229]. We have previously developed an analytical method for measuring AR-67 in plasma [137]. However, given its increased lipophilicity it is possible that in clinical situations AR-67 could partition into erythrocytes, which could effectively act as a drug depot [201]. This has led us to develop an assay for measuring AR-67 concentration in whole blood so that we can explore relationships between pharmacokinetic parameters obtained from blood and plasma. Strong correlations between such parameters would allow the use of a blood assay and minimize the methodological efforts associated with plasma extraction and procedures designed to ensure lactone stabilization at the bedside. In this study we sought to develop processing and analytical methods that would accurately quantitate the lactone and carboxylate forms of AR-67 in whole blood. This assay would be used to analyze samples obtained from the first-in-man clinical study of AR-67.
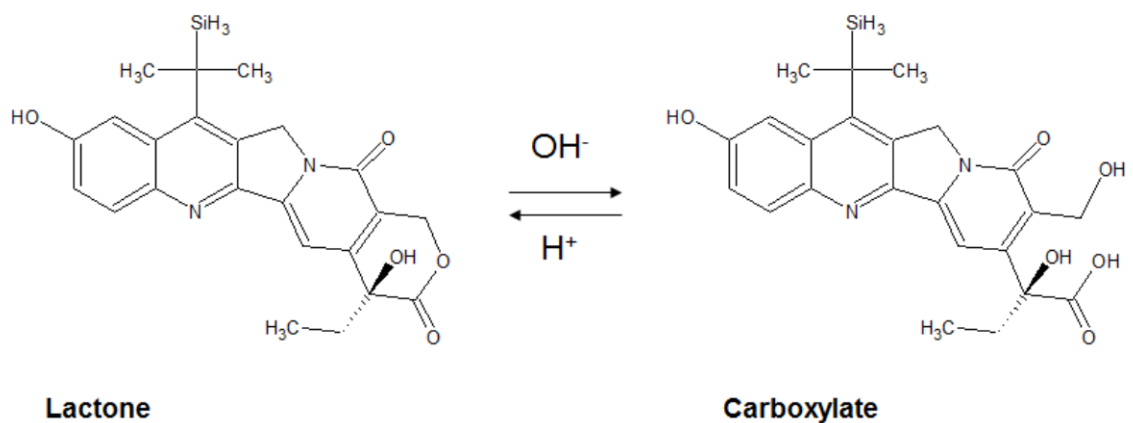
Figure 8-1: Chemical structure of the lactone and carboxylate form of the camptothecin analog, AR-67

8.3 Experimental.

8.3.1 Chemicals and Reagents.

Solvents including methanol and acetonitrile (from Mallinckrodt Baker, Philipsburg, NJ) were of HPLC grade and obtained from VWR (West Chester, PA). Ammonium acetate (Mallinckrodt Baker, Philipsburg, NJ) and sodium hydroxide (EM Science, Gibbstown, NJ) were purchased from VWR (West Chester, PA). Tetrabutylammonium dihydrogenphosphate (TBAP; 1.0 M aqueous solution) and dimethyl sulfoxide (DMSO) were obtained from Sigma-Aldrich (St. Louis, MO). Hydrochloric acid came from Fisher Scientific (Fair Lawn, NJ). Magnesium- and calcium-free Dulbecco's phosphate buffer saline (PBS) was from Gibco (Invitrogen Corp., Carlsbad, CA). Amber siliconized polypropylene micro centrifuge tubes were from Crystalgen Inc. (Plainview, NJ) and siliconized pipet tips were from VWR (West Chester, PA). AR-67 (7-t-butyldimethylsilyl-10-hydroxycamptothecin, DB-67) of high purity (>98%) was obtained from Novartis Pharmaceuticals Corporation. The solid compound was stored at -80°C. Blank human whole blood used during the validation procedure was obtained from the Central Kentucky Blood Bank (Lexington, KY), or from consenting patients enrolled in an AR-67 phase I clinical trial [78].

8.3.2 Instrumentation and Chromatographic Conditions.

Analysis was performed on a Shimadzu HPLC system (Shimadzu Inc., Atlanta, GA) controlled by Class-VP integrating software (Version 7.2.1). The system was equipped with an DGU-14A in-line degasser, a LC-10AD-$_{VP}$ pump, a Shimandzu SIL-10AD-$_{VP}$ refrigerated autoinjector with rack temperature stable at 4°C and an RF-10$_{XL}$ fluorescence detector. Separation of compounds was carried out at ambient temperature using a reverse-phase C18 analytical column (Waters Nova-Pak C18 4 μm; 3.9 mm ×

150 mm) and a C18 guard column (Waters Nova-Pak C18 4 µm; 3.9 mm × 20 mm). The mobile phase consisted of 0.15 M ammonium acetate buffer containing 10 mM TBAP (pH 6.5) and acetonitrile (65:35, v/v). These buffer concentrations were necessary to obtain optimal peak shape for the carboxylate analyte. In all analyses, the mobile phase was pumped at a flow rate of 1 mL/min, a 50-µL aliquot was injected onto the chromatographic system and the excitation wavelength was set at 380 nm while the emission wavelength was set at 560 nm [74]. Unless otherwise indicated, sample extracts were diluted with an equivalent volume of 0.15 M ammonium acetate buffer containing 10 mM TBAP (pH 6.5) prior to 50-µL injection. Once stability was characterized, all buffered diluted samples were analyzed within a 6-hour window to minimize analyte interconversion.

8.3.3 Validation Procedures.

The method was validated according to the FDA "Guidance for

Industry: Bioanalytical Method Validation" document [230]. Certain aspects of the validation process are presented below.

8.3.4 Specificity and Selectivity.

Whole blood samples from four different sources were spiked (0.5 - 5 ng/mL) with either lactone or carboxylate and were injected in triplicate. The lowest limit of quantification (LLOQ) was determined based upon analyte signal to noise ratio of ≥5, analyte accuracy of 80-120%, and precision of <20%.

8.3.5 Calibration, Quality Control and Experimental Sample Preparation.

During the preparation of calibrators and control samples, all aqueous diluents and solutions were kept on wet ice and all methanolic diluents and solutions were kept on dry ice. Amber containers were used throughout sample preparation to avoid photo

degradation while siliconized plastics and glass were used to prevent drug absorption. An accurately weighed amount of AR-67 was dissolved in DMSO to produce a stock solution of 1 mg/mL that was aliquoted (30 µL) for single-time use. These aliquots were stored at -80°C for up to one month [137]. Aqueous working solutions of 10, 1 and 0.1 µg/mL were freshly prepared from stock in 0.005 N sodium hydroxide solution or 0.005 N hydrochloric acid solutions for carboxylate or lactone, respectively. The carboxylate working solutions were prepared by serial dilutions whereas the lactone working solutions were prepared individually from the stock solution. Working solutions were equilibrated for one hour on ice (4°C). Whole blood calibrators containing 0, 0.5, 1, 5, 10, 20, 50, 100, 200 and 300 ng/mL of AR-67 carboxylate and 0, 2.5, 5, 10, 20, 50, 100, 200 and 300 ng/mL of AR-67 lactone were prepared by adding the appropriate volumes of the individual working solutions to 940 µL of whole blood and diluted to 1000 µL with 1x PBS (pH 7.4). The lactone form of AR-67 was generally added prior to the carboxylate form. After vortex mixing for 10 sec, the spiked whole blood samples were frozen at –80°C for 30 min to lyse the blood cells. Lysed samples were thawed at room temperature and deproteinated with 4 volumes of cold (-80°C) methanol. The methanolic mixture was vortexed for 10 min at room temperature and centrifuged at 13,000 × g (10 min, 4°C). The methanolic supernatants were decanted into amber tubes and analyzed immediately as indicated above or stored at -80°C until analysis. Finally, the methanolic extracts were diluted 1:1 with mobile phase buffer before being placed in the Shimandzu SIL-10AD-$_{VP}$ refrigerated autoinjector to be injected. Three quality control samples (QC) containing 1.5 ng/mL of carboxylate and 7.0 ng/mL of lactone (QC1), 150 ng/mL of each analyte (QC2) and 250 ng/mL of each analyte (QC3) were prepared following the same procedure as described for the calibrators. Quality control methanolic supernatants were used in assay validation and to confirm daily system suitability throughout the analysis of

experimental samples. The acceptance criterion for each back-calculated quality control sample concentration was 15% deviation from the nominal.

8.3.6   Interconversion and Stability Experiments.

Experiments were conducted to compare the interconversion of analytes in individually spiked whole blood samples (250 ng/mL carboxylate or lactone) and in purely basic (0.005 N NaOH) and acidic (0.005 N HCl) solutions diluted as necessary (250 ng/mL carboxylate or lactone).

Stability tests were performed on QC1 and QC3 whole blood samples and their methanolic supernatants. Samples were deemed stable if their assayed concentration remained within 15% of the initially measured concentration. When short term stability of methanolic supernatants was studied, either lactone or carboxylate supernatants were stored in the autosampler (4°C) for up to 24 hours after being diluted with an equal volume of mobile phase buffer. Samples were injected at 0, 1, 3, 6 and 24 hours and analytical HPLC runs were conducted based on the results regarding the stability of the methanolic extracts in mobile phase buffer. For long term stability of the methanolic supernatants, the supernatants containing both analytes were stored at -80°C and were mixed 1:1 with mobile phase buffer immediately before injection at predetermined time points (0, 1, 5 days, 1 and 2 weeks, 1 and 2 months). Moreover, short (0, 1, 3 and 6 hours at 4ºC) and long term (0, 1 and 3 days, 1 and 2 weeks, 1 and 2 months at -80°C) stability was evaluated in human whole blood. In those cases, the analytes were extracted from QC samples at the experimental time points and injected after being mixed 1:1 with mobile phase buffer. Single injections of triplicate samples were analyzed unless otherwise indicated.

8.3.7 Recovery.

Single injections of triplicate QC1 and QC3 methanolic supernatants were used to evaluate the recovery of both AR-67 forms. Recovery was estimated by comparing peak heights of whole blood methanolic supernatants to those of carboxylate and lactone methanol solutions freshly prepared and immediately injected after dilution with an equal volume of mobile phase buffer.

8.3.8 Statistical Analysis.

Data and regression analyses were performed with Shimadzu Class VP software (Version 7.2.1.). A linear regression model was used to fit the peak heights from the calibration solutions. Inverse or inverse square weighting schemes were used as needed to increase the correlation coefficient. Control and unknown sample concentrations were calculated using the resulting standard curve equations.

8.3.9 Pharmacokinetics in Humans.

The pharmacokinetic profile of AR-67 in whole blood samples was obtained from a consenting patient enrolled in a phase I clinical trial. The study was approved by institutional review boards and met all ethical and research standards. Design of that trial will be reported elsewhere [78]. The patient received a dose of 6.3 mg/m^2 AR-67 as an 1-hour intravenous infusion and blood samples were collected at 0, 10, 45 minutes, 1, 1.25, 1.5, 2, 4, 6 and 8 hours after the start of the infusion. Collected blood samples were transfered into amber siliconized microcentrifuge tubes, and stored on dry ice for later transfer to -80°C freezer. Within one month from the time of collection, blood samples were thawed and processed. Methanolic supernatants were analysed within 1 week from their preparation. Once processed and diluted with buffer, samples were analyzed within a 6-hour window to minimize analyte interconversion.

8.4 Results.

8.4.1 Sample Processing and Assay Development.

The conditions used for processing and quantitating AR-67 from human whole blood were adapted and developed from those used to quantify AR-67 in mouse plasma [137]. Due to the lipophilicity of the AR-67 lactone, we expected increased partitioning in red blood cell membranes. Thus, a lysis step was implemented to increase lactone recovery. In addition, the deproteinization time was increased from 10 sec to 10 min, while vortex mixing, and the resulting solution was centrifuged at 13,000x rpm for 10 min, rather than 2 min, in order to ensure complete removal of particulates.

8.4.2 Selectivity and Specificity.

The carboxylate and lactone of AR-67 were well separated from interfering matrix peaks and from each other (resolution $\geq$ 1.5; R_t = 3.2 and 9.7 min for carboxylate and lactone, respectively) at all concentrations. Four different human whole blood sources were analyzed and endogenous components did not interfere with any of the analytes at analyte LLOQ values (Figure 8-2).

8.4.3 Linearity, LLOQ, Accuracy and Precision.

Calibration curves prepared in whole blood were created in the range of 0.5-300 ng/mL for the carboxylate and 2.5-300 ng/mL for the lactone moiety. As shown in Table 1, three calibration curves were prepared from different healthy human volunteer whole blood sources, resulting in a mean correlation coefficient for both analyte curves of r^2 ≥0.999. The linearity between the detector response and the nominal concentration of the analytes, allows for accurate and precise estimations of AR-67 carboxylate and lactone concentrations in high, mid, and low quality control solutions, which were within 85-115% of the expected concentration value (Table 8-1). The LLOQ for carboxylate was determined to be 0.5 ng/mL while for lactone was found to be 2.5 ng/mL. The

reproducibility of the analytical method was evaluated by calculating the intra- and inter-day relative standard deviations (RSDs). The intraday variability for low, mid, and high QC concentrations was <5.2% and <3.4% for carboxylate and lactone, respectively. The interday variability for low, mid, and high QC concenttrations was <8.4% and 9.3% for carboxylate and lactone respectively. These results indicate that the assay method is reproducible within the same day as well as on different days (Table 8-1).
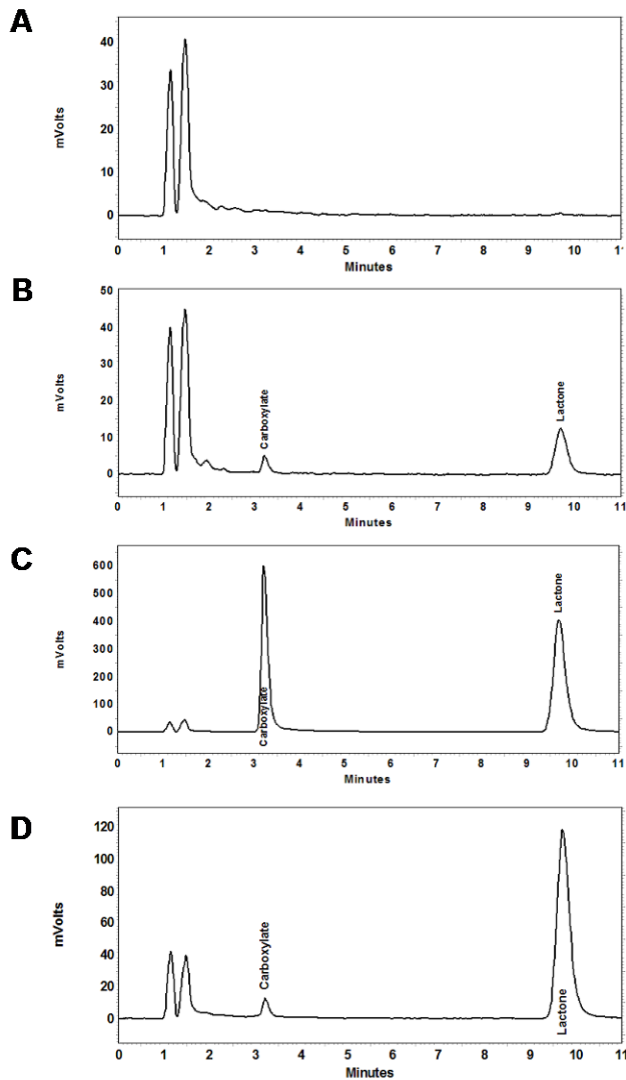
Figure 8-2: Chromatograms of AR-67 carboxylate and lactone in human blood.

Representative chromatographic traces of methanolic supernatants generated from (A) blank human whole blood, (B) low concentration quality control sample (QC1), (C) high concentration quality control sample (QC3), and (D) phase I patient sample collected 5 min after the start of a 1-hour intravenous infusion of AR-67 lactone.

Table 8-1: Assay regression, accuracy and precision.

Analyte Calibration Curves (n=3)	Average Regression Parameters* (± standard deviation)			
	Slope	y-intercept	R^2	Weighting
Carboxylate 0, 0.5-300 ng/mL	0.0003395 (±0.0000265)	0.2090 (±0.1490)	0.999 (±0.0016)	1/Amount^2
Lactone 0, 2.5-300 ng/mL	0.0005107 (±0.0000064)	0.4419 (±0.3239)	0.999 (±0.0002)	1/Response
Intra-day Accuracy and Precision (n=5)**	Average Percent Accuracy (Relative Standard Deviation)			
	QC-1		QC-2	QC-3
Carboxylate	99.6 (5.23 %)		105.0 (2.66 %)	104.3 (3.25 %)
Lactone	86.7 (1.26 %)		105.4 (2.13 %)	105.6 (3.43 %)
Inter-day Accuracy and Precision (n=10)**	Average Percent Accuracy (Relative Standard Deviation)			
	QC-1		QC-2	QC-3
Carboxylate	89.0 (1.87 %)		100.0 (8.36 %)	99.7 (5.92 %)
Lactone	113.7 (1.35 %)		97.5 (9.26 %)	103.2 (6.36 %)
*Regression with peak height as independent variable.** Accuracy was measured as the percent of nominal with quality control samples containing 1.5 ng/mL carboxylate and 7 ng/mL lactone (QC-1), 150 ng/mL each analyte (QC-2), or 250 ng/mL each analyte (QC-3).				

8.4.4   Interconversion and Stability of Analytes.

Experiments to determine the interconversion of analytes in whole blood spiked individually with 250 ng/mL carboxylate or lactone indicated that sample workup resulted in 6.1% conversion of carboxylate to lactone and 2.2% conversion of lactone to carboxylate (n=2-5). Analytes prepared in basic (pH 11.3; 0.005 N NaOH) and acidic (pH 3.4; 0.005 N HCl) solutions and processed the same as the whole blood samples yielded no interconversion for either analyte.

Short term stability of methanolic supernatants indicated that lactone and carboxylate, in low and high concentration (QC1and QC3), were stable for at least 6 hours in the autoinjector (4°C) after being and diluted (1:1, v/v) with mobile phase buffer (Table 8-2). Long term stability of the methanolic supernatants indicated that they were stable for up to 14 days if stored at -80°C (Table 8-3). Short term stability in whole blood indicated that analytes were stable for 6 hours at 4°C (Table 8-2). The lactone form of AR-67 in spiked whole blood samples proved to be stable after being stored at -80°C for at least 28 days. However, the carboxylate concentrations decreased to approximately 85% of the initial values by 1 week in storage at -80°C, but further decrease was not observed by the end of week 4 (Table 8-3). Freeze-thaw analysis of whole blood samples spiked with low (QC1) or high (QC3) concentrations of either lactone or carboxylate were stable after three freeze-thaw cycles (Table 8-4).

161

Table 8-2: Analyte short term stability in whole blood and in buffer diluted methanolic supernatants stored at 4°C.

Whole Blood		Average Percent Remaining at Given Time Point* (± standard deviation)			
		Time 0	1 hr	3 hr	6 hr
QC-1 (n=3)	Carboxylate	100.0	108.5 (±6.5)	104.5 (±8.6)	104.8 (±2.9)
	Lactone	100.0	101.7 (±5.8)	97.2 (±5.2)	96.3 (±2.8)
QC-3 (n=3)	Carboxylate	100.0	99.4 (±3.8)	99.1 (±6.9)	97.8 (±4.3)
	Lactone	100.0	102.5 (±2.1)	108.1 (±5.9)	109.8 (±5.1)

Buffer Diluted Methanolic Supernatants		Average Percent Remaining at Given Time Point (± standard deviation)				
		Time 0	1 hr	3 hr	6 hr	24 hr
QC-1 (n=3)	Carboxylate	100.0	101.3 (±2.4)	99.8 (±4.4)	102.3 (±2.6)	121.9 (±6.1)
	Lactone	100.0	99.9 (±3.4)	98.3 (±3.8)	95.8 (±2.6)	95.7 (±1.5)
QC-3 (n=3)	Carboxylate	100.0	96.8 (±1.2)	95.7 (±1.6)	91.0 (±3.2)	79.7 (±1.2)
	Lactone	100.0	101.3 (±3.1)	102.4 (±1.5)	107.4 (±3.0)	113.7 (±3.1)

*Analyte levels expressed as the average percent of average time zero values with quality control samples containing 1.5 ng/mL carboxylate and 7 ng/mL lactone (QC-1), or 250 ng/mL each analyte (QC-3).

Table 8-3: Analyte long term stability in whole blood and methanolic supernatants stored at -80°C.

Whole Blood		Average Percent Remaining at Given Time Point* (± standard deviation)						
		Time 0	1 Day	3 Days	1 Week	2 Weeks	1 Month	2 Months
QC-1 (n=3)	Carboxylate	100.0	101.11 (±6.7)	105.64 (±9.8)	99.08 (±10.0)	109.28 (±5.2)	77.49 (±3.0)	95.87 (±1.9)
QC-1 (n=3)	Lactone	100.0	103.41 (±2.3)	104.51 (±11.5)	98.77 (±7.8)	105.23 (±4.2)	87.57 (±1.3)	118.66 (±7.1)
QC-3 (n=3)	Carboxylate	100.0	89.03 (±8.0)	88.43 (±8.1)	85.05 (±7.1)	83.05 (±3.4)	79.95 (±5.3)	84.58 (±7.0)
QC-3 (n=3)	Lactone	100.0	97.64 (±8.0)	97.12 (±10.0)	84.28 (±7.9)	87.62 (±4.4)	90.74 (±6.4)	111.12 (±10.4)

Methanolic Supernatants		Average Percent Remaining at Given Time Point* (± standard deviation)						
		Time 0	1 Day	5 Days	1 Week	2 Weeks	1 Month	2 Months
QC-1 (n=3)	Carboxylate	100.0	107.4 (±1.8)	101.2 (±1.14)	93.4 (±8.3)	93.7 (±6.6)	82.4 (±3.6)	60.0 (±9.4)
QC-1 (n=3)	Lactone	100.0	109.9 (±3.1)	100.3 (±2.6)	94.4 (±0.8)	96.0 (±2.4)	86.7 (±2.7)	75.0 (±3.1)
QC-3 (n=3)	Carboxylate	100.0	102.1 (±0.3)	95.6 (±1.9)	90.0 (±3.2)	86.7 (±1.5)	81.4 (±2.4)	71.8 (±2.2)
QC-3 (n=3)	Lactone	100.0	107.1 (±1.8)	98.9 (±2.1)	94.1 (±2.8)	93.3 (±1.7)	88.2 (±2.4)	77.5 (±1.7)

*Analyte levels expressed as the average percent of average time zero values with quality control samples containing 1.5 ng/mL carboxylate and 7 ng/mL lactone (QC-1), or 250 ng/mL each analyte (QC-3).

163

Table 8-4: Analyte recovery and freeze-thaw (F-T) stability.

Recovery*		Percent of Methanolic Analyte Solutions (± standard deviation)			
		QC-1 (n=3)		QC-3 (n=3)	
Carboxylate		94.76 (±2.99)		86.6 (±0.99)	
Lactone		109.66 (±5.30)		99.83 (±1.40)	
Freeze-Thaw Stability**		Average Percent Remaining at Given Cycle (± standard deviation)			
		Cycle 0	1	2	3
QC-1 (n=5)	Carboxylate	100	119.52 (±9.19)	97.73 (±6.32)	94.02 (±6.08)
	Lactone	100	120.24 (±16.00)	109.25 (±21.02)	98.58 (±7.15)
QC-3 (n=5)	Carboxylate	100	108.56 (±14.83)	108.67 (±10.28)	91.41 (±12.47)
	Lactone	100	113.43 (±10.14)	115.95 (±11.50)	99.23 (±6.82)

*Recovery was measured as percent peak height of individually spiked methanolic supernatants to individually spiked methanolic solutions. ** Stability given as their percentage of Cycle 0 averages.

8.4.5 Recovery.

Recovery was similar at low and high concentrations of each analyte (Table 8-4). In whole blood samples spiked with low concentrations (QC1), average recovery was 94.8% (±3.0) and 109.7% (±5.3) for carboxylate and lactone, respectively. Recovery in samples spiked with high concentrations (QC3), average recovery was 86.6% (±1.0) and 99.8% (±1.4) for carboxylate and lactone, respectively.

8.4.6 Clinical application.

This method enabled us to determine the pharmacokinetic profile of AR-67 following intravenous administration to patients with solid malignancies. Blood concentrations for AR-67 carboxylate and lactone versus time are shown in Figure 8-3 for one of the patients participating in the study.

165
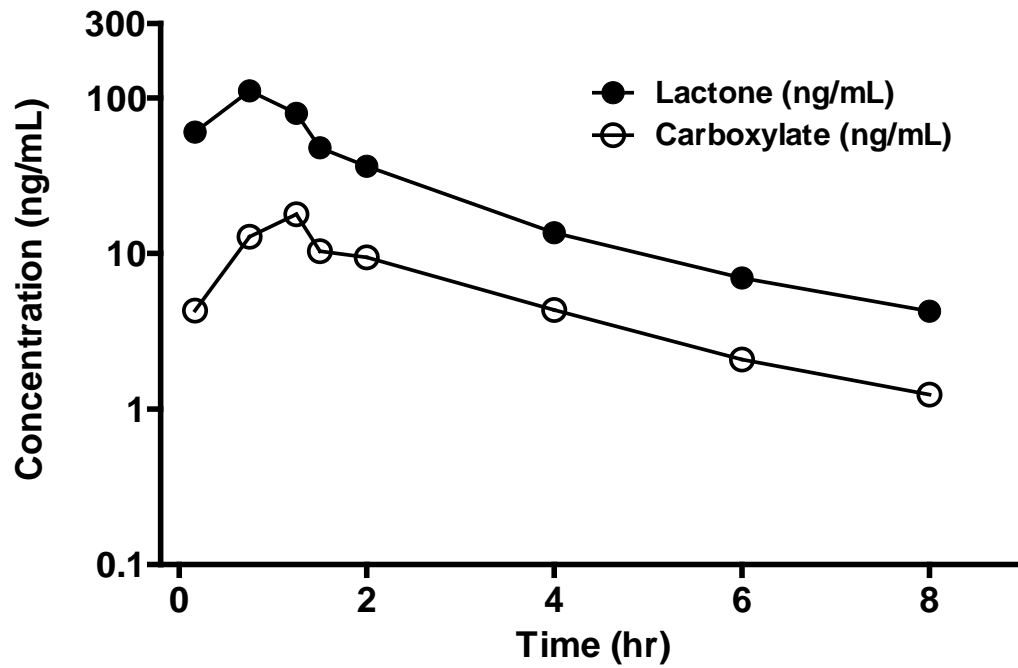
Figure 8-3: Pharmacokinetic profile of AR-67 in whole blood from a patient after administration of AR-67 (6.3 mg/m^2) as an intravenous infusion for 60 min.

8.5 Discussion.

An assay to quantitate carboxylate and lactone AR-67 forms in human whole blood has been developed and validated. The analysis was performed using reversed-phase high performance liquid chromatography coupled with fluorescence detection. Sample processing included a red cell lysis step by storage on dry ice or -80°C to ensure efficient recovery of both the hydrophilic carboxylate and, in particular, the highly lipophilic lactone, followed by a simple methanolic protein precipitation step.

Although numerous analytical methods using HPLC [137, 231, 232] have been developed for the quantification of camptothecin analogs in biological matrices, the challenge of their chemical instability remains. Our method demonstrates that protein precipitation with cold (-80°C) methanol efficiently releases protein bound analytes and provides adequate stability for accurate analysis in the laboratory setting, provided that methanolic supernatants are stored at -80°C and analyzed at 4°C within 2 weeks of sample processing. The present assay allows for the accurate and precise quantitation of AR-67 carboxylate and lactone forms in human whole blood making it a valid assay for future clinical studies. Its linearity in the range of 0.5-300 ng/mL for the carboxylate and 2.5-300 ng/mL for the lactone was found satisfactory and allows quantitation of both analytes in biological samples within this concentration range. In contrast to other methods, acidification of the blood samples is not necessary since complete separation between both analytes and endogenous compounds was achieved under the chromatographic conditions described above. Red cell lysis followed by the methanolic protein precipitation appears to efficiently recover both the carboxylate and lactone from the biological matrix. The LLOQ for carboxylate and lactone (0.5 and 2.5 ng/mL, respectively) allows for its application to future pharmacokinetic studies. Stability tests

have shown that both AR-67 forms are stable after 3 freeze-thaw cycles. Most importantly, although both carboxylate and lactone forms are stable in their methanolic extracts for up to two weeks, they seem to be stable in whole blood for a longer period. The lactone form appears to be more stable in the biological matrix compared to the carboxylate form. This apparent stability could also be because the highly lipophilic lactone may absorb onto surfaces but is replenished via conversion from the carboxylate. This was prevented to a large extent by pretreating all consumables with a siliconizing solution. However, absorption of the highly lipophilic lactone may continue, albeit at a much reduced rate, over time. Under our processing and chromatography conditions, analysis of experimental samples with high lactone concentrations is likely to overestimate the carboxylate concentration. However, given the relatively high lactone concentatrations (Figure 8-3), this is insignificant in relative terms.

Previous clinical work has demonstrated that camptothecins interact with red cells. It has been reported that irinotecan is selectively partitions into red blood cells, while its metabolite SN-38 distributes preferentially in the plasma compartment [231]. Interestingly, differences on the pharmacokinetic profile of topotecan between the two sexes were noted, but ultimately they were attributed to hematocrit differences between males and females [49, 201, 232]. Finally, studies have shown that red blood cells serve as a depot compartment for the lactone 9-amino-20(S)-campothecin [233]. Consequently, pharmacokinetic parameters such as the volume of distribution and the clearance depend greatly on the biological matrix from which the sample was collected [234]. The development of the current analytical method for assaying AR-67 in whole blood will allow us to study the pharmacokinetics of AR-67 in the blood compartment.

The assay was successfully applied to determine the concentrations of AR-67 in cancer patients enrolled in a phase I clinical trial [78]. As demonstrated in Figure 8-3, the

lactone concentration was higher than the carboxylate at all time points. This was consistent with the expected behavior of the lactone partitioning in red cell membranes. Interestingly, the pharmacokinetic profiles of AR-67 in blood and in plasma appeared to mirror each other indicating that the red cells were not acting as a depot for AR-67 (data not shown). Further studies are in progress to assess whether patient dependent covariates, such as hematocrit, age and weight play a role in the disposition of AR-67.

8.6 Conclusions.

A high-performance liquid chromatography method for simultaneous determination of AR-67 carboxylate and lactone in whole blood has been developed and validated. The method has been shown to be sensitive, accurate and precise. Lactone stability during sample processing remains a concern if temperature is not controlled and consumables are not siliconized, but AR-67 is stable in whole blood stored under the proper conditions (-80°C). This is the first reported method for the analysis of AR-67 in whole blood matrix and will be used for the analysis of samples obtained from patients treated in clinical studies.

9. Appendix 3: A Phase 1 Study of 7-t-butyldimethylsilyl-10-hydroxycamptothecin (AR-67) in Adult Patients with Refractory or Metastatic Solid Malignancies

Susanne M. Arnold[1], John J. Rinehart[1], Eleftheria Tsakalozou[1], John R. Eckardt[2], Scott Z. Fields[3], Brent J. Shelton[1], Philip A. DeSimone[1]; Bryan K. Kee[1], Jeffrey A. Moscow[1], Markos Leggas[1,4]

[1]Markey Cancer Center, University of Kentucky, Lexington, KY 40536

[2]The Center for Cancer Care and Research, St. Louis, MO 63141

[3]Arno Therapeutics, Inc. Parsippany, NJ 07054

9.1   Translational Relevance.

Topoisomerase I interacting agents have shown antineoplastic activity that is closely associated with the stability of their α-hydroxy-δ-lactone pharmacophore. 7-t-Butyldimethylsilyl-10-hydroxycamptothecin (AR-67) is a novel third generation camptothecin analogue with increased lipophilicity and blood stability, relative to the clinically approved analogues topotecan and irinotecan. This phase I study was conducted to determine the maximum tolerated dose, dose limiting toxicities, and pharmacokinetics of AR-67 given daily for 5 days during a 21-day cycle to patients with advanced solid tumors. Four patients experienced stable disease and one patient had prolonged partial response (>16 months), indicating preliminary evidence of antitumor activity. Hematologic toxicities were manageable and notably none of the patients experienced diarrhea. AR-67 exhibited increased blood stability, and compared with other lipophilic investigational analogues, it did not seem to accumulate in plasma with repeat dosing. AR-67 warrants further evaluation to assess its efficacy alone or in combination with other agents.

9.2 Abstract.

Purpose: 7-t-Butyldimethylsilyl-10-hydroxycamptothecin (AR-67) is a novel third generation camptothecin selected for development based on the blood stability of its pharmacologically active lactone form and its high potency in preclinical models. Here, we report the initial phase I experience with i.v. AR-67 in adults with refractory solid tumors.

Experimental Design and Methods: AR-67 was infused over 1 hour daily five times, every 21 days, using an accelerated titration trial design. Plasma was collected on the 1st and 4th day of cycle 1 to determine pharmacokinetic parameters.

Results: Twenty-six patients were treated at nine dosage levels (1.2-12.4 mg/m2/d). Dose-limiting toxicities were observed in five patients and consisted of grade 4 febrile neutropenia, grade 3 fatigue, and grade 4 thrombocytopenia. Common toxicities included leukopenia (23%), thrombocytopenia (15.4%), fatigue (15.4%), neutropenia (11.5%), and anemia (11.5%). No diarrhea was observed. The maximum tolerated dosage was 7.5 mg/m2/d. The lactone form was the predominant species in plasma (>87% of area under the plasma concentration-time curve) at all dosages. No drug accumulation was observed on day 4. Clearance was constant with increasing dosage and hematologic toxicities correlated with exposure ($P < 0.001$). A prolonged partial response was observed in one subject with non–small cell lung cancer. Stable disease was noted in patients with small cell lung cancer, non–small cell lung cancer, and duodenal cancer.

Conclusions: AR-67 is a novel, blood-stable camptothecin with a predictable toxicity profile and linear pharmacokinetics. The recommended phase II dosage is 7.5 mg/m2/d five times every 21 days.

9.3 Introduction.

Camptothecins are potent DNA/topoisomerase-I interacting agents and combine the merits of both cytotoxic and molecularly targeted agents [4, 20, 235]. Their potency is controlled by their α-hydroxy-δ-lactone pharmacophore, which hydrolyses to the open ring or carboxylate form in a pH dependent, but reversible manner. Although both the lactone and carboxylate forms have been shown to interact with the DNA/Topoisomerase-I complex, the lactone moiety is considered the active one [4, 20, 29]. This may be attributed to the higher lipophilicity of the lactone form that could facilitate cell penetration as compared to the charged carboxylate [236]. In addition to the intrinsic hydrolysis rate of each analog, the carboxylate binds human serum albumin with high affinity and facilitates an equilibrium shift toward hydrolysis, thus further compromising the lactone form by creating sink conditions [16, 27, 179, 222].

Given that camptothecin pharmacokinetics present a significant challenge to achieving lactone exposure, there has been a tremendous effort to create novel analogs with improved stability and potency [237]. One such effort was initiated by the research groups of Drs. Thomas Burke and Dennis Curran that successfully achieved lactone stabilization by introducing substituents that promote lipid bilayer partitioning (hence protecting the drug from hydrolysis) and minimized albumin binding [16, 17, 222]. Several silatecans and homosilatecans were synthesized and tested for their blood stability and potency [37, 38, 227, 238]. Among those, AR-67 (7-*t*-butyldimethylsilyl-10-hydroxycamptothecin, also known as DB-67, emerged as the most blood stable and potent analog and was chosen for further preclinical and clinical development [37, 38, 74].

We initiated this phase I trial to determine the maximum tolerated dosage (MTD), and describe the dose limiting toxicities (DLT) of intravenous AR-67 administered once daily

174

for 5 days of an every 21 day schedule to adults with refractory and metastatic solid tumors. In addition, we evaluated antitumor activity, PK and explored correlations between AR-67 exposure and toxicity.

9.4 Experimental Design and methods.

9.4.1 Patient Eligibility.

Patients (>18 years) with refractory solid malignancies were eligible if their disease was metastatic or unresectable and standard curative or palliative measures no longer existed or were no longer effective. Other eligibility requirements included Eastern Cooperative Group (ECOG) performance status ≤ 2, adequate hematologic (leukocytes >3,000/µL, absolute neutrophil count (ANC) > 1,500/µL, platelet count > 100,000/µL), hepatic, and renal function. Objective measurable disease was not required. No prior chemotherapy, molecularly targeted agents or radiation therapy was allowed within 2 weeks (6 weeks for mitomycin C or nitrosoureas), and no major surgery was allowed within 3 weeks; all therapy-related toxicity should have resolved to less than grade 1. Prior camptothecin therapy was allowed, but patients with allergic reactions attributed to compounds of similar chemical or biologic composition to AR-67 or subjects with prior grade 3 or 4 anaphylactic reaction to any product formulated with cremophor (i.e., paclitaxel) were excluded. Patients with known brain metastases that had been treated and were clinically stable were eligible for this clinical trial. Other exclusions included subjects with: uncontrolled intercurrent illness that would limit study compliance, HIV disease, QTc prolongation over 450 msec, evidence of ongoing and significant consumptive coagulopathy, or pregnant or nursing females.

9.4.2 Study Drug.

AR-67 was supplied by the NCI (RAID program) in vials that contained 10mg/2mL in cremophor ethanol diluent. After reconstitution with 5% dextrose for injection in non-PVC bags (0.05 – 0.5 mg/mL), the drug was administered at a constant rate over one hour into a free flowing intravenous (iv) line (non-PVC tubing) of 5% dextrose via a

standard infusion pump. The drug was given within 4 hours of reconstitution to ensure lactone stability.

9.4.3 Study Treatments and Dose Escalation.

Since it is established that 25 - 30% of those receiving cremophor-formulated compounds will experience grade 3 or 4 allergic infusion reactions [239], all patients were premedicated to prevent potential cremophor toxicities as follows: dexamethasone 20 mg orally (PO), 12 hr prior to the first dose of AR-67 and 30 min prior to each dose on days 1-5, ondansetron 8 mg PO, loratidine 10 mg PO, famotidine 20 mg PO, and diphenhydramine 25 mg PO. Institutional equivalents were allowed. Investigators could reduce the dose of dexamethasone if no allergic reactions were noted in the previous cycle.

The phase-I starting dose was 1.67 mg/m^2/day, iv, daily x 5. The first patient (prostate cancer) at dose level 1 developed grade 4 thrombocytopenia and consumptive coagulopathy, and his dose was reduced to level -1 (1.2 mg/m^2) for safety. Ultimately, toxicities were attributed to a disease progression with extensive bone metastasis and myelophthisic marrow changes and consumptive coagulopathy. This phase I trial was designed to have an accelerated dose escalation followed by a modified Fibonacci design when certain parameters were met. Accordingly, after two subjects developed grade 2 toxicity early in the study, the study reverted to a modified Fibonacci design, as required by protocol. After 8 more subjects were accrued and demonstrated no grade 2 or greater toxicities, a secondary accelerated phase design was proposed and approved by the IRB in order to expose the minimal number of subjects to potentially sub-therapeutic dosage levels. Two dosage level escalations occurred during this secondary accelerated phase (at 4.5 mg/m^2 and 6.3 mg/m^2), with subsequent expansion to a

modified Fibonacci design at dosage level 5.5 (7.5 mg/m^2). All dosage levels are described in Table 9-1.

Table 9-1: Dose – escalation scheme and dose limiting toxicities.

Dose Level	Dose daily x 5	n	DLT per Cohort	Type of DLT
Level -1	1.2 mg/m2/day	2*	0	
Level 1	1.67 mg/m2/day	3	0	
Level 2	2.34 mg/m2/day	3	0	
Level 3	3.2 mg/m2/day	3	0	
Level 4	4.5 mg/m2/day	1	0	
Level 5	6.3 mg/m2/day	1	0	
Level 5.5	7.5 mg/m2/day	7	1/7	Grade 4 thrombocytopenia
Level 6	8.9 mg/m2/day	4	2/4	Grade 4 thrombocytopenia (2)
Level 7	12.4 mg/m2/day	2	2/2	Grade 4 febrile neutropenia Grade 3 fatigue
* One subject did not receive 5 days of therapy and was replaced				

9.4.4 Assessments, Follow-Up, and Monitoring.

Toxicities were defined using the National Cancer Institute Common Toxicity Criteria 3.0 (CTCAE 3.0). The toxicity of a given AR-67 dosage level was considered a dose limiting toxicity (DLT) if any of the following were observed during cycle 1: (1) any Grade 5 toxicity, (2) ANC < 500/μL for longer than seven days or associated with fever or infection of any duration, (3) platelet < 25,000/μL of any duration, (4) grade 3 or 4 non-hematopoietic toxicity according to the CTCAE version 3.0 with the exception of grade 3 nausea and/or vomiting, grade 3 diarrhea of less than 3 days after treatment with loperamide or grade 3 fever (with or without neutropenia). The recommended phase II dose and the MTD were defined as the dosage level below the dosage that induced a DLT in two or more patients during cycle 1. Routine use of colony stimulating factors were not permitted during cycle one. Treatment was resumed once the ANC had recovered to ≥ 1,500/μL and a platelet > 100,000/μL (measured within 1 day of treatment) and resolution of all non-hematologic toxicity to less than grade 2. If these parameters were not met, therapy was delayed for up to 3 weeks for recovery. AR-67 dosage reductions by one dosage level were made for any DLT, any grade 4 neutropenia or thrombocytopenia or grade 3 or 4 non-hematologic toxicity in the previous cycle. A maximum of two dose reductions were allowed per subject and no dosage escalations were allowed. In the absence of treatment delays due to adverse events, treatment continued until one of the following occurred: disease progression, unacceptable adverse event(s), request of patient to withdraw from study, general or specific changes in the patient's condition that rendered further treatment unacceptable or treatment delay of greater than 3 weeks. Tumor measurements were performed by computer tomography (CT) scan or magnetic resonance imaging (MRI) every two cycles of therapy. Disease was assessed according to the response evaluation criteria in solid tumors (RECIST v1.0) [240]. Treatment was continued for 6 cycles in the absence of

disease progression, provided all toxicities remained acceptable and patients were willing to continue on study.

9.4.5 Pharmacokinetic and Pharmacodynamic Methods.

Blood was collected from all patients in heparinized tubes at pre-dose, 5 min, 45 min, 65 min and 1.5, 2, 4, 6, 8, and 24 hrs after the start of infusion on days 1 and 4. Day 4 samples were collected to determine if repeat dosing of AR-67 would result in drug accumulation as previously noted with other 3rd generation lipophilic camptothecin analogs [241].   AR-67 lactone and carboxylate concentrations were determined in plasma by a validated high-performance liquid chromatography method with fluorescence detection based on a previously published assay [137]. Plasma PK parameters were estimated by noncompartmental methods with WinNonlin (version5.2; Pharsight, Mountain View, CA). Clearance values were compared by the Wilcoxon signed rank paired test to assess differences between days 1 and 4. Relationships between drug exposure and toxicity were explored using sigmoid E-max and logistic regression models (Graph-Pad Prism V5, La Jolla, CA). Spearman correlation was used to evaluate relationships between hematologic toxicities and exposure in terms of AUC, dosage level, and absolute dose.

9.5 Results.

9.5.1 Patient characteristics.

Between November 2, 2006 and December 15, 2008, 26 subjects were enrolled and all were assessable for toxicity. Patient demographics are listed in Table 9-2. Overall, 61 courses of AR-67 over 9 dosage levels were delivered. One patient at dose level 1 received only 2 days of drug administration prior to progressive disease manifested by bowel obstruction that required hospitalization, and was removed from study. This subject was not evaluable for response, but was evaluable for toxicity.

Table 9-2: Patient characteristics.

Characteristic	No of Patients (N = 26)
Median age, years	62
Range	30-79
Performance Status	
0	13
1	12
2	1
Male/Female	15/11
Median prior chemotherapy regimens	3
Range	(1-6)
Race	
Caucasian	25
African-American	1
Tumor types	
Colon	8
Non-Small Cell Lung	4
Small Cell Lung	3
Soft Tissue Sarcoma	3
Head and Neck	2
Prostate	2
Bladder	1
Duodenal	1
Esophageal	1
Pancreas	1

9.5.2 Toxicity.

Dose limiting toxicities were observed in 5 patients: two of two subjects at 12.4mg/m^2/day (highest dosage level) experienced DLTs; one grade 4 febrile neutropenia and one grade 3 fatigue; two of four subjects at 8.9 mg/m^2/day exhibited grade 4 thrombocytopenia and one of seven subjects at 7.5 mg/m^2/day manifested grade 4 thrombocytopenia. All DLTs resolved without permanent sequellae. Table 9-3 summarizes all CTCAE toxicities at least possibly related to AR-67. Common Grade 3 and 4 toxicities included: leukocytopenia (23%), thrombocytopenia (15.4%), fatigue (15.4%), neutropenia (11.5%), and anemia (11.5%). Notably, none of the patients experienced infusion related allergic reactions or diarrhea.

Table 9-3: CTCAE toxicities possibly, probably or definitely related to AR-67.

Category	Adverse Event	Grade 1	2	3	4	Total
BLOOD/BONE MARROW	Hemoglobin	8	12	6	0	26
	Leukocytes (total WBC)	18	15	8	0	41
	Monocytopenia	0	0	0	1	1
	Neutrophils/granulocytes (ANC/AGC)	3	10	5	1	19
	Platelets	13	8	9	7	37
CARDIAC GENERAL	Hypotension	0	1	0	0	1
CONSTITUTIONAL SYMPTOMS	Fatigue (asthenia, lethargy, malaise)	4	14	8	0	26
	Fever (in the absence of neutropenia)	0	1	0	0	1
	Insomnia	2	5	0	0	7
	Weight loss	2	0	0	0	2
DERMATOLOGY/SKIN	Pruritus/itching/Dry skin/Flushing	7	0	0	0	7
	Nail changes	1	0	0	0	1
	Rash/desquamation	2	1	0	0	3
GASTROINTESTINAL	Anorexia/Taste Alteration	4	7	1	0	12
	Constipation/Dehydration	6	8	0	0	14
	Mucositis/stomatitis	2	0	0	0	2
	Nausea	14	0	0	0	14
HEMORRHAGE/BLEEDING	Hemorrhage, GI - Duodenum	0	0	1	0	1
INFECTION	Febrile neutropenia	0	0	1	2	3
	Infection - ANC grade 0-2	3	4	0	2	9
	Infection with unknown ANC	2	1	0	0	3
METABOLIC/LABORATORY	ALT, SGPT, Alkaline Phosphatase	8	0	0	0	8
	Electrolyte abnormalities	8	0	0	0	8
Extremity-lower (gait/walking)		1	0	0	0	1
	Muscle weakness - Lower extremity	0	3	1	0	4
NEUROLOGY	Dizziness	0	1	0	0	1
	Neuropathy: sensory	1	0	0	0	1
Dyspnea		1	0	0	0	1
	Hiccoughs (hiccups, singultus)	2	1	0	0	3
TOTAL		112	92	40	13	257

9.5.3 Efficacy.

The secondary endpoint of response per RECIST v1.0 was evaluable in 22 subjects. One subject with squamous cell carcinoma of the lung received ten cycles of therapy and had a prolonged partial response at dosage level 5.5. This response continues as of this writing, seven months after cessation of therapy (Figure 9-1). Four subjects had stable disease: one patient at dosage level 7 with duodenal cancer (82 days), two patients at dosage levels 5.5 and 6 with small cell lung cancer (refractory disease, 91 days; sensitive relapse, 112 days) and one patient with non small cell lung cancer at dose level 5.5 (74 days).
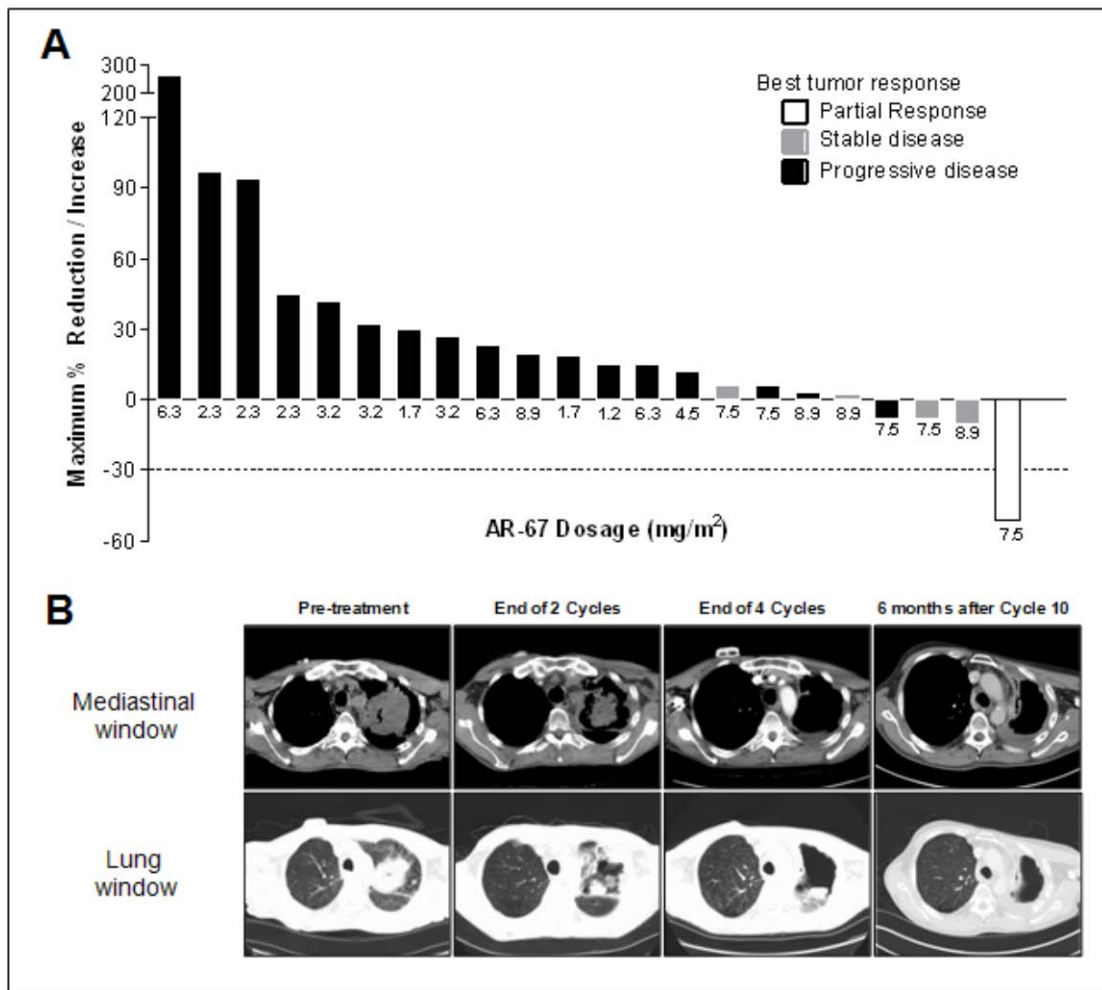
Figure 9-1: Antitumor efficacy of AR-67.

(A) Best response of target lesions measured by using Response Evaluation Criteria in Solid Tumors (best response does not include longest dimensions of new lesions). (B) Reduction in tumor burden in a patient with recurrent non-small cell lung cancer who received 10 cycles of AR67 therapy (7.5 mg/m2/day for 4 cycles, 6.3 mg/m2/day for 5 cycles and 4.5 mg/m2/day for 1 cycle). The patient achieved partial response at the end of cycle 4, which was maintained as of this writing (7 months after the end of cycle 10).

9.5.4 Pharmacokinetics.

This compound was designed to promote lactone stability in-vivo with the presumption that high lactone stability would lead to improved efficacy. Our results demonstrate that in human plasma the AR-67 lactone form accounts for 87.5% (±8.5%, SD) of the total AR-67 AUC (lactone + carboxylate). Summary PK parameters of total AR-67 at each dosage level and lactone AUCs are presented in Table 9-4 and Table 9-5. Mean plasma concentrations for the MTD cohort are presented in Figure 9-2A. The drug is eliminated with a bi-exponential profile and there is no evidence of accumulation on day 4. Greater than 80% of the total concentration is in the lactone form (Figure 9-2B) at each time point. The values of the lactone and total AUC (Figure 9-2C) were highly correlated (Spearman correlation: r=0.99, p<0.0001 and r=0.99, p<0.0001 for day 1 and 4, respectively). Given this strong correlation and the high lactone to total AR-67 ratio, further analysis was done based on the total AR-67 concentrations. Linear regression and correlation analysis demonstrated that the increase in C_{max} (data not shown) and AUC were dose dependent, while clearance was constant. As shown in Figure 9-2D no correlation was observed between dosage and clearance suggesting that clearance was constant across dosage levels. However, the mean clearance of total AR-67 increased 20% (p=0.0031, Wilcoxon signed rank two-tailed t-test) from day 1 (14.5 ±4.1L/hr/m2, N=26))
to day 4 (17.4 ±5.2 L/hr/m2, SD, N=25). It should be noted that the non-compartmental analysis may slightly overestimate the clearance since the true C_{max} may not have been captured by the 45-minute sample, which was collected during the infusion.

Table 9-4: Total AR-67 pharmacokinetic parameters on day 1 of cycle 1.

Day	Dosage Level (mg/m^2)	Total AUC$_{(0-\infty)}$ (ng x hr/mL) Mean	SD	Lactone AUC$_{(0-\infty)}$ (ng x hr/mL) Mean	SD	C$_{max, total}$[#] (ng/mL) Mean	SD	V$_{ss, total}$ (L/m^2) Mean	SD	T(1/2)$_{total}$[*] (hr) Mean	SD	Clearance$_{total}$ (L/hr/m^2) Mean	SD
1	1.2 (n=2)	88	11	81	8	77.6	2.9	7.4	2.2			13.8	1.8
	1.67 (n=3)	128	19	117	21	96.9	20.1	13.1	4			13.2	2
	2.34 (n=3)	201	118	186	110	158.9	97.3	13.5	6.9			14.1	6.3
	3.23 (n=3)	290	72	269	64	221.9	55.9	9.6	0.7			11.6	3
	4.5 (n=1)	214		179		117.8		32.7				21	
	6.3 (n=1)	490		334		168.5		51.6				12.9	
	7.5 (n=7)	581	82	498	66	349.7	114	18.7	7.3	1.4	0.3	13.1	1.8
	8.9 (n=4)	502	158	471	270	290.6	153.5	30.1	9.6	1.6	0.2	18.9	5.1
	12.4 (n=2)	786	64	686	77	464.7	105.4	18.1	3.8	1.1	0.1	15.8	1.3
	All dosage levels									1.4	0.1	14.5	4.1

Abbreviations: AUC area under the plasma concentration-time curve; SD, standard deviation; V$_{ss}$, volume of distribution at steady-state.

*Half-life estimates are reported for dosage levels at which estimation of terminal slopes could be obtained by at least 3 data points in the elimination phase.

[#]C$_{max}$ values are the observed values at 45 minutes during the 1-hr infusion.

Table 9-5: Total AR-67 pharmacokinetic parameters day 4 of cycle 1.

Day	Dosage Level (mg/m^2)	Total AUC$_{(0-\infty)}$ (ng x hr/mL) Mean	SD	Lactone AUC$_{(0-\infty)}$ (ng x hr/mL) Mean	SD	C$_{max, total}$[#] (ng/mL) Mean	SD	V$_{ss, total}$ (L/m^2) Mean	SD	T(1/2)$_{total}$* (hr) Mean	SD	Clearance $_{total}$ (L/hr/m^2) Mean	SD
4	1.2 (n=1)	51		49		51.6		15.6				23.6	
	1.67 (n=3)	115	57	109	58	74.6	11.3	16.3	4.4			16.7	6.5
	2.34 (n=3)	154	10	137	9	137.8	6.1	7.9	3.4			15.3	1
	3.23 (n=3)	255	70	236	61	195	58.8	10.6	4.3			13.3	3.5
	4.5 (n=1)	186		149		82.5		45.3				24.2	
	6.3 (n=1)	429		327		166.4		35.3				14.7	
	7.5 (n=7)	478	127	411	104	308.6	122.9	25.6	16.3	1.8	0.7	16.8	5
	8.9 (n=4)	507	145	397	119	276.7	69.5	27.5	6.7	1.4	0	18.6	4.9
	12.4 (n=2)	663	216	551	146	358.5	77.5	28.9	5.4	1.7	0.1	19.8	6.5
	All dosage levels									1.6	0.4	17.4	5.2

Abbreviations: AUC area under the plasma concentration-time curve; SD, standard deviation; V$_{ss}$, volume of distribution at steady-state.

*Half-life estimates are reported for dosage levels at which estimation of terminal slopes could be obtained by at least 3 data points in the elimination phase.
[#]C$_{max}$ values are the observed values at 45 minutes during the 1-hr infusion.
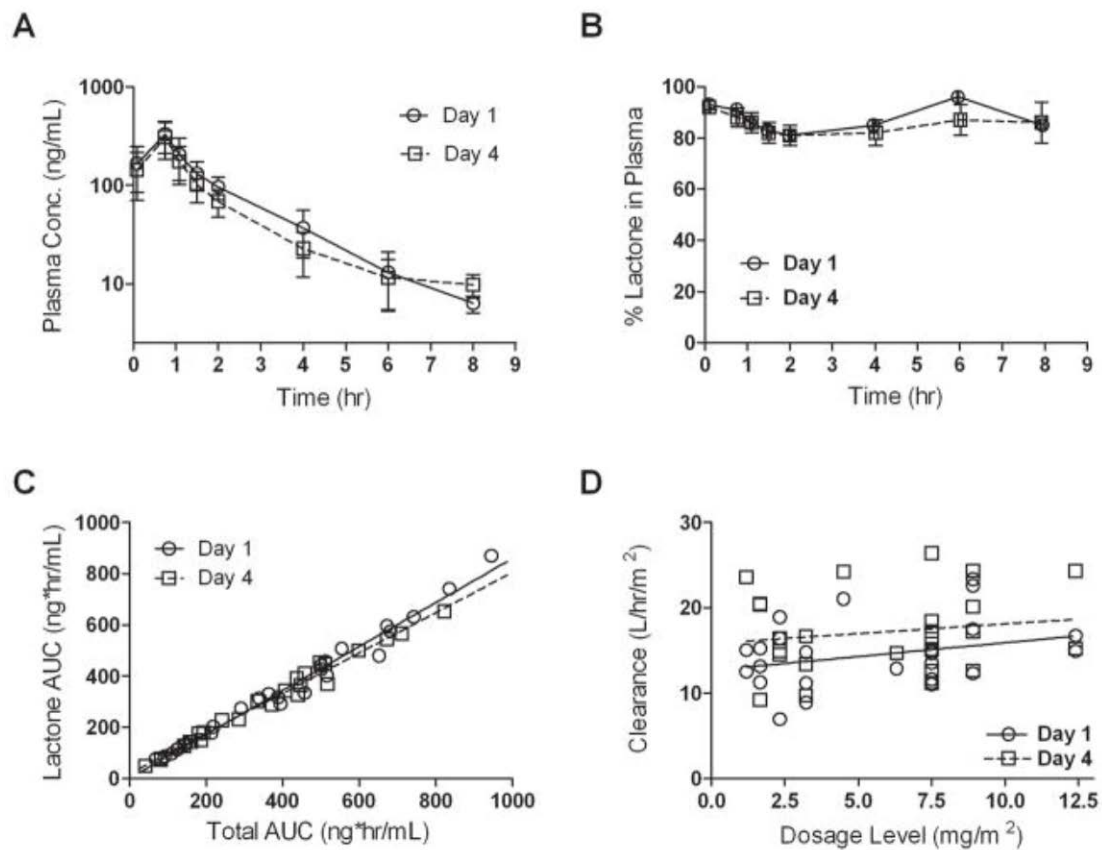
Figure 9-2: Pharmacokinetic analysis.

(A) Mean plasma concentration-time profiles of total AR-67 in the MTD cohort (n=7). (B) The mean percent lactone in plasma at each time point for all patients. (C) Correlation plot of total and lactone AUC. (D) Relationship of administered AR-67 dosage with clearance. Solid lines in panels C and D represent linear regression lines.

9.5.5   Pharmacodynamics.

Given the high correlation and low variability in the lactone to total AR-67 ratio in all subjects, we used the total AR-67 PK parameters to explore relationship between exposure and toxicity. Total AR-67 exposure and the observed hematologic DLTs were examined using a sigmoid E-max model (Equation 1). Where E(d) is the effect as a function of AUC or dosage, H is the curve shape factor (i.e., Hill coefficient), and ED_{50} is the AUC or dosage at which 50% of the effect is observed.

$$E(d) = \frac{E_{max} \cdot d^H}{ED_{50} + d^H}$$ Equation 1

Figure 9-3 depicts the relationship between dosage level (panel A) or AUC (panel B) and the % decrease in ANC and platelets from baseline. The dosage level ED_{50} (95% CI) of 6.1 (4.3 – 8.7), and 4.9 (3.2 – 7.6) mg/m^2 were estimated for the % decrease in ANC and platelets, respectively. The estimated AUC ED_{50} (95% CI) values were 323.6 (231.9 - 451.6) and 364.2 (249.4 - 531.9) hr*ng/mL for ANC and platelets, respectively.

To determine the probability for the occurrence of each toxicity during cycle 1, we performed logistic regression (Equation 2), where P is the probability, X (values of 1 or 0) denotes the presence or absence, respectively, of toxicity determined by a nadir value below the respective lower limit set for ANC (<1500/mm^3) and platelets (<100,000/mm^3), and α and β are model parameters (α representing the log-odds of toxicity occurrence when X=0 and β is the increment in the log-odds of toxicity when X=1. Furthermore, the

parameter β describes the steepness of the s-shaped curved or the rate of change in probability with increasing drug exposure.

$$P = \frac{1}{1 + \exp^{-(\alpha + \beta \cdot X)}}$$ Equation 2

As depicted in Figure 9-3 (panel C), during cycle 1 the occurrence of neutropenia was more likely than thrombocytopenia at exposures resulting from the MTD dosage level. Strong correlations could also be demonstrated between exposure and nadir values of ANC and platelets (Figure 9-4). This analysis demonstrates that the correlations were similar when considering exposure in terms of AUC and dosage level (mg/m^2). Similar correlations were also observed with leucopenia and the probability for observing leucopenia was similar to that for neutropenia (data not shown). At the MTD level ANC and platelet nadir levels were observed on days 10-14 during cycle 1 but patients recovered prior to day 22 (day 1 of cycle 2).
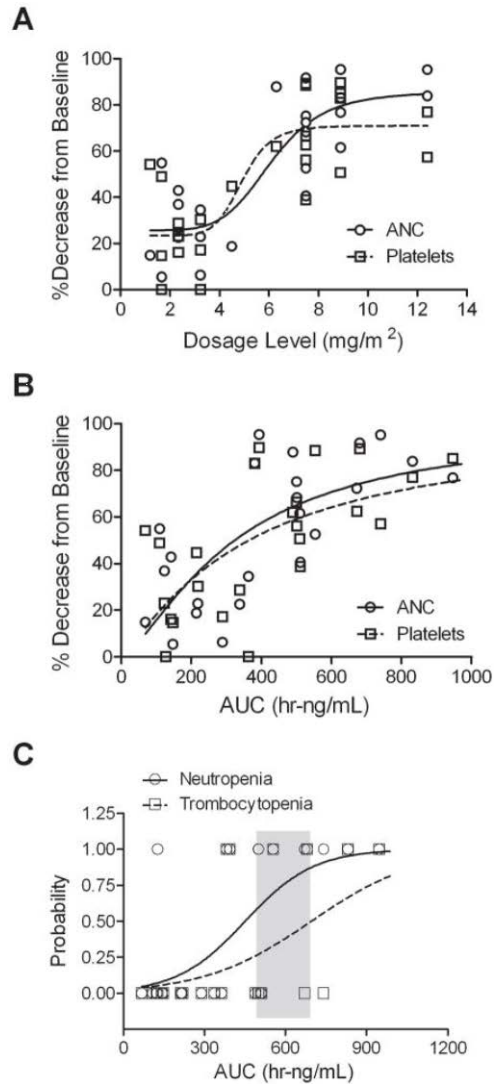
Figure 9-3: Pharmacodynamic analysis of neutropenia and thrombocytopenia during cycle 1 in all patients.

Percent decrease from baseline as a result of (A) increasing dosage level and (B) AUC (day 1 of cycle 1). Lines represent fit of a sigmoid Emax model to the data. (C) Logistic regression analysis demonstrating the probabilities of manifesting neutropenia and thrombocytopenia with increasing AR-67 exposure. The gray area encompasses the range of AR-67 AUC achieved at the MTD during day 1 of cycle 1.
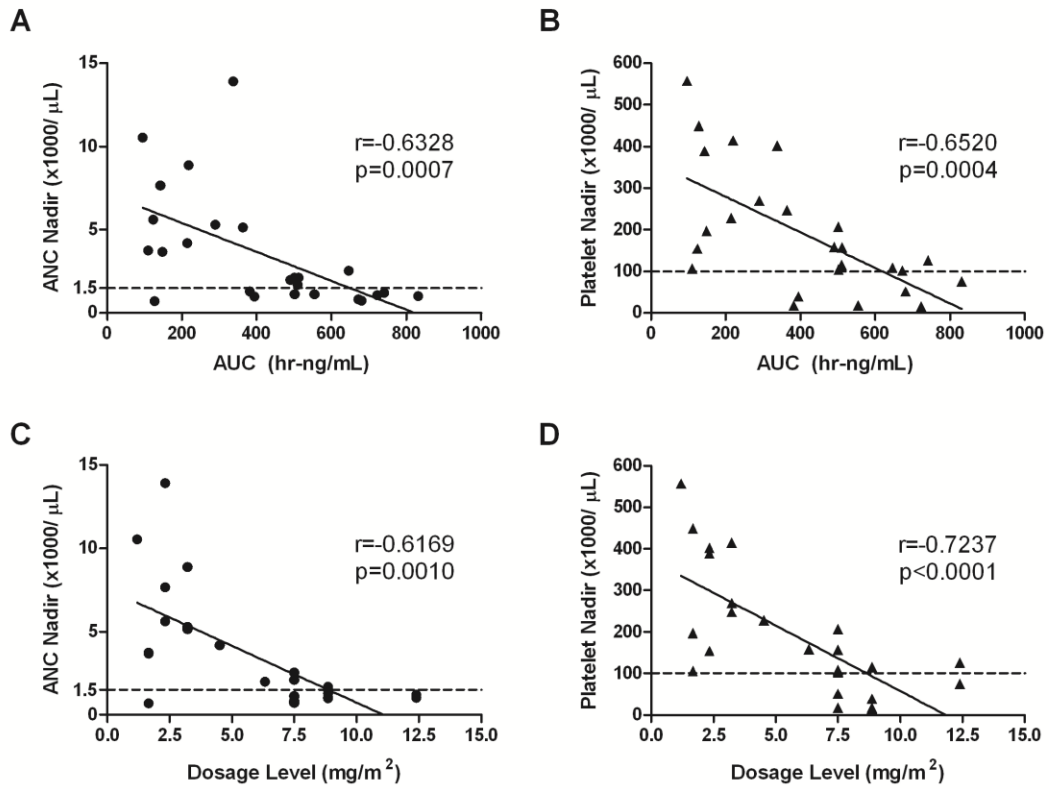
Figure 9-4: AR-67 exposure – toxicity relationships.

Increased drug exposure determined by AUC (day 1 of cycle 1) and dosage level correlated with neutrophil (A, C) and platelet (B, D) nadir values (cycle 1).

9.6   Discussion.

AR-67 administered daily for five days of an every 21-day cycle was well tolerated in this study. DLTs were thrombocytopenia, febrile neutropenia and fatigue and the MTD was defined as 7.5 mg/m^2/day. Notably, no diarrhea or allergic infusional reactions occurred in the 26 people exposed to this compound. At the recommended phase II dose of 7.5 mg/m^2/day (n=7), the regimen produced only modest and manageable side effects. While fatigue and hematologic toxicities are hallmarks of camptothecins, the lack of diarrhea seen in the present trial is notable compared to other drugs of this class, particularly irinotecan. Interestingly, although AR-67 is lipophilic and shares some structural characteristics with the active metabolite of irinotecan (i.e., SN-38), it does not undergo UGT1A1 mediated glucuronidation, but is extensively metabolized by UGT1A8, which is primarily expressed in the gastrointestinal tract [242, 243]. This may partly explain the lack of diarrhea observed in this study. Complete studies related to the metabolism and transport pathways of this compound are underway and will be presented elsewhere.

Pharmacokinetic studies demonstrated that 87.5% (±8.5%) of the drug is in the lactone form. This represents a significant improvement in effective drug delivery from other clinically approved camptothecins with reported lactone AUC ratios of 30~76% for irinotecan and irinotecan derived SN-38 [54, 225, 226] and for topotecan [42]. With respect to 3rd generation analogs, the AR-67 lactone ratio is lower than the reported values for gimatecan and karenitecin, both in early clinical trials, which exist in plasma as 90-98% [229, 241] and ~90-95% [244, 245] in the lactone form, respectively [229, 244, 245]. However, the AR-67 elimination half-life (~1.4 hr) may explain the lack of accumulation observed with gimatecan and karenitecin, which have documented half-lives of 77 hr and 15 hr, respectively. Interestingly, despite their long half-lives, these

analogs have not proven more effective than the clinically approved camptothecins, which exhibit shorter half-lives. Thus, the prolonged exposures required for efficacy in rapidly growing preclinical models are not necessarily important for improved clinical efficacy.

AR-67 clearance is linear and correlates with hematologic toxicity. Interestingly, AR-67 clearance increased on day 4 of cycle 1 suggesting that this may be due to dexamethasone co-treatment inducing CYP3A4 activity. This is consistent with our *in-vitro* data demonstrating that AR-67 is a substrate for CYP3A4 and with previous clinical evidence demonstrating that dexamethasone treatment for 5 days induces CYP3A4 activity [193, 242]. However, CYP3A4 induction was highly variable in that study [193] as compared to our data that demonstrates a consistent ~20% decrease in AUC between days 1 and 4 in all patients. Thus, it is possible that the drug is also inducing its own metabolism to some extent.

The use of the cremophor-ethanol excipient is known to be associated with hypersensitivity reactions and has the potential to cause non-linear pharmacokinetics [239, 246]. However, the amount of cremophor at the MTD is less that 4% of that administered to a patient receiving a typical paclitaxel dose of 200 mg/m^2 and no patients exhibited hypersensitivity reactions. Nonetheless, patients treated in upcoming Phase II studies will continue to receive prophylactic premedication to prevent potential hypersensitivity reactions.

The partial response seen in NSCLC is notable because of the rapid tumor regression demonstrated by CT scan (Figure 9-1). This subject continued to benefit, despite two dose reductions for a total of 10 cycles, and ultimately stopped treatment due to grade 3 fatigue. The partial response was ongoing seven months after cessation

of therapy. In addition, stable disease was noted in two patients with SCLC (refractory and sensitive relapse for over three months) and one patient each with NSCLC and duodenal cancer. Camptothecins as a class have been proven effective in each of these cancer types, and further exploration of AR-67 in these groups is warranted [237].

In conclusion, AR-67 given daily for 5 days in an every-21-day cycle is well tolerated, with acceptable myelosuppression and fatigue as DLTs. At the MTD, toxicities were manageable and no diarrhea or hypersensitivity reactions were seen. Critically important was the demonstration of high lactone stability (~87.5% of total AR-67) in human plasma. Interestingly, a confirmed partial response was noted in a patient with non-small cell lung cancer, who remained on therapy for ten cycles.   We also demonstrated linear PK and correlation of AUC and dosage with toxicity. Further clinical testing of AR-67 is warranted and ongoing.

10. References

1. Wall, M.E., M.C. Wani, and H. Taylor, *Isolation and chemical characterization of antitumor agents from plants.* Cancer Treat Rep, 1976. **60**(8): p. 1011-30.
2. Gallo, R.C., J. Whang-Peng, and R.H. Adamson, *Studies on the antitumor activity, mechanism of action, and cell cycle effects of camptothecin.* J Natl Cancer Inst, 1971. **46**(4): p. 789-95.
3. Hsiang, Y.H., et al., *DNA topoisomerase I-mediated DNA cleavage and cytotoxicity of camptothecin analogues.* Cancer Res, 1989. **49**(16): p. 4385-9.
4. Hsiang, Y.H., et al., *Camptothecin induces protein-linked DNA breaks via mammalian DNA topoisomerase I.* J Biol Chem, 1985. **260**(27): p. 14873-8.
5. Jaxel, C., et al., *Structure-activity study of the actions of camptothecin derivatives on mammalian topoisomerase I: evidence for a specific receptor site and a relation to antitumor activity.* Cancer Res, 1989. **49**(6): p. 1465-9.
6. Fan, Y., et al., *Molecular modeling studies of the DNA-topoisomerase I ternary cleavable complex with camptothecin.* J Med Chem, 1998. **41**(13): p. 2216-26.
7. Redinbo, M.R., et al., *Crystal structures of human topoisomerase I in covalent and noncovalent complexes with DNA.* Science, 1998. **279**(5356): p. 1504-13.
8. D'Arpa, P. and L.F. Liu, *Topoisomerase-targeting antitumor drugs.* Biochim Biophys Acta, 1989. **989**(2): p. 163-77.
9. Bence, A.K., et al., *The effect of DB-67, a lipophilic camptothecin derivative, on topoisomerase I levels in non-small-cell lung cancer cells.* Cancer Chemother Pharmacol, 2004. **54**(4): p. 354-60.
10. Hochster, H., et al., *Activity and pharmacodynamics of 21-Day topotecan infusion in patients with ovarian cancer previously treated with platinum-based chemotherapy. New York Gynecologic Oncology Group.* J Clin Oncol, 1999. **17**(8): p. 2553-61.
11. Desai, S.D., et al., *Ubiquitin-dependent destruction of topoisomerase I is stimulated by the antitumor drug camptothecin.* J Biol Chem, 1997. **272**(39): p. 24159-64.
12. Gongora, C., et al., *New Topoisomerase I mutations are associated with resistance to camptothecin.* Mol Cancer, 2011. **10**: p. 64.
13. Wang, L.F., et al., *Identification of mutations at DNA topoisomerase I responsible for camptothecin resistance.* Cancer Res, 1997. **57**(8): p. 1516-22.
14. Chrencik, J.E., et al., *Mechanisms of camptothecin resistance by human topoisomerase I mutations.* J Mol Biol, 2004. **339**(4): p. 773-84.
15. Gottesman, M.M., T. Fojo, and S.E. Bates, *Multidrug resistance in cancer: role of ATP-dependent transporters.* Nat Rev Cancer, 2002. **2**(1): p. 48-58.
16. Burke, T.G. and Z. Mi, *Preferential binding of the carboxylate form of camptothecin by human serum albumin.* Anal Biochem, 1993. **212**(1): p. 285-7.
17. Mi, Z., H. Malak, and T.G. Burke, *Reduced albumin binding promotes the stability and activity of topotecan in human blood.* Biochemistry, 1995. **34**(42): p. 13722-8.
18. Fassberg, J. and V.J. Stella, *A kinetic and mechanistic study of the hydrolysis of camptothecin and some analogues.* J Pharm Sci, 1992. **81**(7): p. 676-84.
19. Chourpa, I., et al., *Kinetics of lactone hydrolysis in antitumor drugs of camptothecin series as studied by fluorescence spectroscopy.* Biochim Biophys Acta, 1998. **1379**(3): p. 353-66.

20. Hertzberg, R.P., et al., *Modification of the hydroxy lactone ring of camptothecin: inhibition of mammalian topoisomerase I and biological activity.* J Med Chem, 1989. **32**(3): p. 715-20.

21. Nicholas, A.W., et al., *Plant antitumor agents. 29. Synthesis and biological activity of ring D and ring E modified analogues of camptothecin.* J Med Chem, 1990. **33**(3): p. 972-8.

22. Holden, J.A., et al., *Human DNA topoisomerase I: quantitative analysis of the effects of camptothecin analogs and the benzophenanthridine alkaloids nitidine and 6-ethoxydihydronitidine on DNA topoisomerase I-induced DNA strand breakage.* Arch Biochem Biophys, 1999. **370**(1): p. 66-76.

23. Uehling, D.E., et al., *Synthesis, topoisomerase I inhibitory activity, and in vivo evaluation of 11-azacamptothecin analogs.* J Med Chem, 1995. **38**(7): p. 1106-18.

24. Luzzio, M.J., et al., *Synthesis and antitumor activity of novel water soluble derivatives of camptothecin as specific inhibitors of topoisomerase I.* J Med Chem, 1995. **38**(3): p. 395-401.

25. Vladu, B., et al., *7- and 10-substituted camptothecins: dependence of topoisomerase I-DNA cleavable complex formation and stability on the 7- and 10-substituents.* Mol Pharmacol, 2000. **57**(2): p. 243-51.

26. Burke, T.G., et al., *The important role of albumin in determining the relative human blood stabilities of the camptothecin anticancer drugs.* J Pharm Sci, 1995. **84**(4): p. 518-9.

27. Burke, T.G. and Z. Mi, *Ethyl substitution at the 7 position extends the half-life of 10-hydroxycamptothecin in the presence of human serum albumin.* J Med Chem, 1993. **36**(17): p. 2580-2.

28. Wani, M.C., A.W. Nicholas, and M.E. Wall, *Plant antitumor agents. 23. Synthesis and antileukemic activity of camptothecin analogues.* J Med Chem, 1986. **29**(11): p. 2358-63.

29. Staker, B.L., et al., *The mechanism of topoisomerase I poisoning by a camptothecin analog.* Proc Natl Acad Sci U S A, 2002. **99**(24): p. 15387-92.

30. Kunimoto, T., et al., *Antitumor activity of 7-ethyl-10-[4-(1-piperidino)-1-piperidino]carbonyloxy-camptothec in, a novel water-soluble derivative of camptothecin, against murine tumors.* Cancer Res, 1987. **47**(22): p. 5944-7.

31. Kingsbury, W.D., et al., *Synthesis of water-soluble (aminoalkyl)camptothecin analogues: inhibition of topoisomerase I and antitumor activity.* J Med Chem, 1991. **34**(1): p. 98-107.

32. Ulukan, H. and P.W. Swaan, *Camptothecins: a review of their chemotherapeutic potential.* Drugs, 2002. **62**(14): p. 2039-57.

33. Venditto, V.J. and E.E. Simanek, *Cancer therapies utilizing the camptothecins: a review of the in vivo literature.* Mol Pharm, 2010. **7**(2): p. 307-49.

34. Lavergne, O., et al., *Homocamptothecins: synthesis and antitumor activity of novel E-ring-modified camptothecin analogues.* J Med Chem, 1998. **41**(27): p. 5410-9.

35. Bailly, C., et al., *Homocamptothecin, an E-ring-modified camptothecin analogue, generates new topoisomerase I-mediated DNA breaks.* Biochemistry, 1999. **38**(47): p. 15556-63.

36. Kroep, J.R. and H. Gelderblom, *Diflomotecan, a promising homocamptothecin for cancer therapy.* Expert Opin Investig Drugs, 2009. **18**(1): p. 69-75.

37. Curran, D.P., et al., *The cascade radical annulation approach to new analogues of camptothecins. Combinatorial synthesis of silatecans and homosilatecans.* Ann N Y Acad Sci, 2000. **922**: p. 112-21.

38.   Bom, D., et al., *The novel silatecan 7-tert-butyldimethylsilyl-10-hydroxycamptothecin displays high lipophilicity, improved human blood stability, and potent anticancer activity.* J Med Chem, 2000. **43**(21): p. 3970-80.

39.   Moertel, C.G., et al., *Phase II study of camptothecin (NSC-100880) in the treatment of advanced gastrointestinal cancer.* Cancer Chemother Rep, 1972. **56**(1): p. 95-101.

40.   Creemers, G.J., et al., *Topotecan, an active drug in the second-line treatment of epithelial ovarian cancer: results of a large European phase II study.* J Clin Oncol, 1996. **14**(12): p. 3056-61.

41.   Ardizzoni, A., et al., *Topotecan, a new active drug in the second-line treatment of small-cell lung cancer: a phase II study in patients with refractory and sensitive disease. The European Organization for Research and Treatment of Cancer Early Clinical Studies Group and New Drug Development Office, and the Lung Cancer Cooperative Group.* J Clin Oncol, 1997. **15**(5): p. 2090-6.

42.   Zamboni, W.C., et al., *Interpatient variability in bioavailability of the intravenous formulation of topotecan given orally to children with recurrent solid tumors.* Cancer Chemother Pharmacol, 1999. **43**(6): p. 454-60.

43.   Herben, V.M., W.W. ten Bokkel Huinink, and J.H. Beijnen, *Clinical pharmacokinetics of topotecan.* Clin Pharmacokinet, 1996. **31**(2): p. 85-102.

44.   Schellens, J.H., et al., *Bioavailability and pharmacokinetics of oral topotecan: a new topoisomerase I inhibitor.* Br J Cancer, 1996. **73**(10): p. 1268-71.

45.   Grochow, L.B., et al., *Pharmacokinetics and pharmacodynamics of topotecan in patients with advanced cancer.* Drug Metab Dispos, 1992. **20**(5): p. 706-13.

46.   Schaiquevich, P., et al., *Population pharmacokinetic analysis of topotecan in pediatric cancer patients.* Clin Cancer Res, 2007. **13**(22 Pt 1): p. 6703-11.

47.   Leger, F., et al., *Factors affecting pharmacokinetic variability of oral topotecan: a population analysis.* Br J Cancer, 2004. **90**(2): p. 343-7.

48.   Mould, D.R., et al., *Population pharmacokinetic and adverse event analysis of topotecan in patients with solid tumors.* Clin Pharmacol Ther, 2002. **71**(5): p. 334-48.

49.   Gallo, J.M., et al., *Population pharmacokinetic model for topotecan derived from phase I clinical trials.* J Clin Oncol, 2000. **18**(12): p. 2459-67.

50.   Montazeri, A., et al., *Population pharmacokinetics of topotecan: intraindividual variability in total drug.* Cancer Chemother Pharmacol, 2000. **46**(5): p. 375-81.

51.   Armstrong, D. and S. O'Reilly, *Clinical Guidelines for Managing Topotecan-Related Hematologic Toxicity.* Oncologist, 1998. **3**(1): p. 4-10.

52.   O'Reilly, S., D.K. Armstrong, and L.B. Grochow, *Life-threatening myelosuppression in patients with occult renal impairment receiving topotecan.* Gynecol Oncol, 1997. **67**(3): p. 329-30.

53.   Shimada, Y., et al., *Phase II study of CPT-11, a new camptothecin derivative, in metastatic colorectal cancer. CPT-11 Gastrointestinal Cancer Study Group.* J Clin Oncol, 1993. **11**(5): p. 909-13.

54.   Drengler, R.L., et al., *Phase I and pharmacokinetic trial of oral irinotecan administered daily for 5 days every 3 weeks in patients with solid tumors.* J Clin Oncol, 1999. **17**(2): p. 685-96.

55.   Sasaki, Y., et al., *Pharmacological correlation between total drug concentration and lactones of CPT-11 and SN-38 in patients treated with CPT-11.* Jpn J Cancer Res, 1995. **86**(1): p. 111-6.

56.   Humerickhouse, R., et al., *Characterization of CPT-11 hydrolysis by human liver carboxylesterase isoforms hCE-1 and hCE-2.* Cancer Res, 2000. **60**(5): p. 1189-92.

57. Slatter, J.G., et al., *Pharmacokinetics, metabolism, and excretion of irinotecan (CPT-11) following I.V. infusion of [(14)C]CPT-11 in cancer patients.* Drug Metab Dispos, 2000. **28**(4): p. 423-33.

58. Mathijssen, R.H., et al., *Clinical pharmacokinetics and metabolism of irinotecan (CPT-11).* Clin Cancer Res, 2001. **7**(8): p. 2182-94.

59. Chabot, G.G., et al., *Population pharmacokinetics and pharmacodynamics of irinotecan (CPT-11) and active metabolite SN-38 during phase I trials.* Ann Oncol, 1995. **6**(2): p. 141-51.

60. Gupta, E., et al., *Metabolic fate of irinotecan in humans: correlation of glucuronidation with diarrhea.* Cancer Res, 1994. **54**(14): p. 3723-5.

61. Raymond, E., et al., *Dosage adjustment and pharmacokinetic profile of irinotecan in cancer patients with hepatic dysfunction.* J Clin Oncol, 2002. **20**(21): p. 4303-12.

62. Ramchandani, R.P., et al., *The role of SN-38 exposure, UGT1A1*28 polymorphism, and baseline bilirubin level in predicting severe irinotecan toxicity.* J Clin Pharmacol, 2007. **47**(1): p. 78-86.

63. Schaaf, L.J., et al., *Phase 1 and pharmacokinetic study of intravenous irinotecan in refractory solid tumor patients with hepatic dysfunction.* Clin Cancer Res, 2006. **12**(12): p. 3782-91.

64. Ho, R.H. and R.B. Kim, *Transporters and drug therapy: implications for drug disposition and disease.* Clin Pharmacol Ther, 2005. **78**(3): p. 260-77.

65. Kalliokoski, A. and M. Niemi, *Impact of OATP transporters on pharmacokinetics.* Br J Pharmacol, 2009. **158**(3): p. 693-705.

66. Sugiyama, Y., Y. Kato, and X. Chu, *Multiplicity of biliary excretion mechanisms for the camptothecin derivative irinotecan (CPT-11), its metabolite SN-38, and its glucuronide: role of canalicular multispecific organic anion transporter and P-glycoprotein.* Cancer Chemother Pharmacol, 1998. **42 Suppl**: p. S44-9.

67. Sharom, F.J., *ABC multidrug transporters: structure, function and role in chemoresistance.* Pharmacogenomics, 2008. **9**(1): p. 105-27.

68. Han, J.Y., et al., *Associations of ABCB1, ABCC2, and ABCG2 polymorphisms with irinotecan-pharmacokinetics and clinical outcome in patients with advanced non-small cell lung cancer.* Cancer, 2007. **110**(1): p. 138-47.

69. Innocenti, F., et al., *Comprehensive pharmacogenetic analysis of irinotecan neutropenia and pharmacokinetics.* J Clin Oncol, 2009. **27**(16): p. 2604-14.

70. Xie, R., et al., *Clinical pharmacokinetics of irinotecan and its metabolites in relation with diarrhea.* Clin Pharmacol Ther, 2002. **72**(3): p. 265-75.

71. Klein, C.E., et al., *Population pharmacokinetic model for irinotecan and two of its metabolites, SN-38 and SN-38 glucuronide.* Clin Pharmacol Ther, 2002. **72**(6): p. 638-47.

72. Xie, R., et al., *Clinical pharmacokinetics of irinotecan and its metabolites: a population analysis.* J Clin Oncol, 2002. **20**(15): p. 3293-301.

73. Burke, T.G. and D. Bom, *Camptothecin design and delivery approaches for elevating anti-topoisomerase I activities in vivo.* Ann N Y Acad Sci, 2000. **922**: p. 36-45.

74. Bom, D., et al., *The highly lipophilic DNA topoisomerase I inhibitor DB-67 displays elevated lactone levels in human blood and potent anticancer activity.* J Control Release, 2001. **74**(1-3): p. 325-33.

75. Adane, E.D., et al., *Factors affecting the in vivo lactone stability and systemic clearance of the lipophilic camptothecin analogue AR-67.* Pharm Res, 2010. **27**(7): p. 1416-25.

76. Lopez-Barcons, L.A., et al., *The novel highly lipophilic topoisomerase I inhibitor DB67 is effective in the treatment of liver metastases of murine CT-26 colon carcinoma.* Neoplasia, 2004. **6**(5): p. 457-67.

77. Pollack, I.F., et al., *Potent topoisomerase I inhibition by novel silatecans eliminates glioma proliferation in vitro and in vivo.* Cancer Res, 1999. **59**(19): p. 4898-905.

78. Arnold, S.M., et al., *A phase I study of 7-t-butyldimethylsilyl-10-hydroxycamptothecin in adult patients with refractory or metastatic solid malignancies.* Clin Cancer Res, 2010. **16**(2): p. 673-80.

79. Horn, J., et al., *Metabolic pathways of the camptothecin analog AR-67.* Drug Metab Dispos, 2011. **39**(4): p. 683-92.

80. Desai, A.A., F. Innocenti, and M.J. Ratain, *UGT pharmacogenomics: implications for cancer risk and cancer therapeutics.* Pharmacogenetics, 2003. **13**(8): p. 517-23.

81. Leggas, M., et al., *Pharmacokinetics (PK) of the Highly Lipophilic and Blood Stable Camptothecin AR-67 (7-t-butyldimethylsilyl-10-hydroxycamptothecin) in Adult Patients with Solid Malignancies*, in *American Society of Clinical Oncology*2009: Florida, USA.

82. Doyle, L.A., et al., *A multidrug resistance transporter from human MCF-7 breast cancer cells.* Proc Natl Acad Sci U S A, 1998. **95**(26): p. 15665-70.

83. Lee, J.S., et al., *Reduced drug accumulation and multidrug resistance in human breast cancer cells without associated P-glycoprotein or MRP overexpression.* J Cell Biochem, 1997. **65**(4): p. 513-26.

84. McDevitt, C.A., et al., *Purification and 3D structural analysis of oligomeric human multidrug transporter ABCG2.* Structure, 2006. **14**(11): p. 1623-32.

85. Doyle, L.A. and D.D. Ross, *Multidrug resistance mediated by the breast cancer resistance protein BCRP (ABCG2).* Oncogene, 2003. **22**(47): p. 7340-58.

86. Jonker, J.W., et al., *Role of breast cancer resistance protein in the bioavailability and fetal penetration of topotecan.* J Natl Cancer Inst, 2000. **92**(20): p. 1651-6.

87. Wang, L., et al., *N-(4-[2-(1,2,3,4-tetrahydro-6,7-dimethoxy-2-isoquinolinyl)ethyl]-phenyl)-9,10-dih ydro-5-methoxy-9-oxo-4-acridine carboxamide (GF120918) as a chemical ATP-binding cassette transporter family G member 2 (Abcg2) knockout model to study nitrofurantoin transfer into milk.* Drug Metab Dispos, 2008. **36**(12): p. 2591-6.

88. Fojo, A.T., et al., *Expression of a multidrug-resistance gene in human tumors and tissues.* Proc Natl Acad Sci U S A, 1987. **84**(1): p. 265-9.

89. Cordon-Cardo, C., et al., *Expression of the multidrug resistance gene product (P-glycoprotein) in human normal and tumor tissues.* J Histochem Cytochem, 1990. **38**(9): p. 1277-87.

90. Vavricka, S.R., et al., *The human organic anion transporting polypeptide 8 (SLCO1B3) gene is transcriptionally repressed by hepatocyte nuclear factor 3beta in hepatocellular carcinoma.* J Hepatol, 2004. **40**(2): p. 212-8.

91. Obaidat, A., M. Roth, and B. Hagenbuch, *The expression and function of organic anion transporting polypeptides in normal tissues and in cancer.* Annu Rev Pharmacol Toxicol, 2012. **52**: p. 135-51.

92. Abe, T., et al., *Identification of a novel gene family encoding human liver-specific organic anion transporter LST-1.* J Biol Chem, 1999. **274**(24): p. 17159-63.

93. Konig, J., et al., *A novel human organic anion transporting polypeptide localized to the basolateral hepatocyte membrane.* Am J Physiol Gastrointest Liver Physiol, 2000. **278**(1): p. G156-64.

94.   Abe, T., et al., *LST-2, a human liver-specific organic anion transporter, determines methotrexate sensitivity in gastrointestinal cancers.* Gastroenterology, 2001. **120**(7): p. 1689-99.

95.   Konig, J., et al., *Localization and genomic organization of a new hepatocellular organic anion transporting polypeptide.* J Biol Chem, 2000. **275**(30): p. 23161-8.

96.   Fahrmayr, C., M.F. Fromm, and J. Konig, *Hepatic OATP and OCT uptake transporters: their role for drug-drug interactions and pharmacogenetic aspects.* Drug Metab Rev, 2010. **42**(3): p. 380-401.

97.   Nakanishi, T. and D.D. Ross, *Breast cancer resistance protein (BCRP/ABCG2): its role in multidrug resistance and regulation of its gene expression.* Chin J Cancer, 2012. **31**(2): p. 73-99.

98.   Ross, D.D., et al., *Expression of breast cancer resistance protein in blast cells from patients with acute leukemia.* Blood, 2000. **96**(1): p. 365-8.

99.   Diestra, J.E., et al., *Frequent expression of the multi-drug resistance-associated protein BCRP/MXR/ABCP/ABCG2 in human tumours detected by the BXP-21 monoclonal antibody in paraffin-embedded material.* J Pathol, 2002. **198**(2): p. 213-9.

100.   Kawabata, S., et al., *Expression and functional analyses of breast cancer resistance protein in lung cancer.* Clin Cancer Res, 2003. **9**(8): p. 3052-7.

101.   Candeil, L., et al., *ABCG2 overexpression in colon cancer cells resistant to SN38 and in irinotecan-treated metastases.* Int J Cancer, 2004. **109**(6): p. 848-54.

102.   Smeets, M., et al., *A low but functionally significant MDR1 expression protects primitive haemopoietic progenitor cells from anthracycline toxicity.* Br J Haematol, 1997. **96**(2): p. 346-55.

103.   Guerci, A., et al., *Predictive value for treatment outcome in acute myeloid leukemia of cellular daunorubicin accumulation and P-glycoprotein expression simultaneously determined by flow cytometry.* Blood, 1995. **85**(8): p. 2147-53.

104.   Leith, C.P., et al., *Frequency and clinical significance of the expression of the multidrug resistance proteins MDR1/P-glycoprotein, MRP1, and LRP in acute myeloid leukemia: a Southwest Oncology Group Study.* Blood, 1999. **94**(3): p. 1086-99.

105.   Damiani, D., et al., *The prognostic value of P-glycoprotein (ABCB) and breast cancer resistance protein (ABCG2) in adults with de novo acute myeloid leukemia with normal karyotype.* Haematologica, 2006. **91**(6): p. 825-8.

106.   Ho, M.M., D.E. Hogge, and V. Ling, *MDR1 and BCRP1 expression in leukemic progenitors correlates with chemotherapy response in acute myeloid leukemia.* Exp Hematol, 2008. **36**(4): p. 433-42.

107.   Benderra, Z., et al., *MRP3, BCRP, and P-glycoprotein activities are prognostic factors in adult acute myeloid leukemia.* Clin Cancer Res, 2005. **11**(21): p. 7764-72.

108.   Monks, N.R., et al., *Potent cytotoxicity of the phosphatase inhibitor microcystin LR and microcystin analogues in OATP1B1- and OATP1B3-expressing HeLa cells.* Mol Cancer Ther, 2007. **6**(2): p. 587-98.

109.   Wright, J.L., et al., *Expression of SLCO transport genes in castration-resistant prostate cancer and impact of genetic variation in SLCO1B3 and SLCO2B1 on prostate cancer outcomes.* Cancer Epidemiol Biomarkers Prev, 2011. **20**(4): p. 619-27.

110.   Muto, M., et al., *Human liver-specific organic anion transporter-2 is a potent prognostic factor for human breast carcinoma.* Cancer Sci, 2007. **98**(10): p. 1570-6.

111.   Lee, W., et al., *Overexpression of OATP1B3 confers apoptotic resistance in colon cancer.* Cancer Res, 2008. **68**(24): p. 10315-23.

112. Lockhart, A.C., et al., *Organic anion transporting polypeptide 1B3 (OATP1B3) is overexpressed in colorectal tumors and is a predictor of clinical outcome.* Clin Exp Gastroenterol, 2008. **1**: p. 1-7.

113. Pressler, H., et al., *Expression of OATP family members in hormone-related cancers: potential markers of progression.* PLoS One, 2011. **6**(5): p. e20372.

114. Smith, N.F., et al., *Identification of OATP1B3 as a high-affinity hepatocellular transporter of paclitaxel.* Cancer Biol Ther, 2005. **4**(8): p. 815-8.

115. Katayama, R., et al., *Dofequidar fumarate sensitizes cancer stem-like side population cells to chemotherapeutic drugs by inhibiting ABCG2/BCRP-mediated drug export.* Cancer Sci, 2009. **100**(11): p. 2060-8.

116. de Vries, N.A., et al., *P-glycoprotein and breast cancer resistance protein: two dominant transporters working together in limiting the brain penetration of topotecan.* Clin Cancer Res, 2007. **13**(21): p. 6440-9.

117. Luo, F.R., et al., *Intestinal transport of irinotecan in Caco-2 cells and MDCK II cells overexpressing efflux transporters Pgp, cMOAT, and MRP1.* Drug Metab Dispos, 2002. **30**(7): p. 763-70.

118. Nakatomi, K., et al., *Transport of 7-ethyl-10-hydroxycamptothecin (SN-38) by breast cancer resistance protein ABCG2 in human lung cancer cells.* Biochem Biophys Res Commun, 2001. **288**(4): p. 827-32.

119. Nozawa, T., et al., *Role of organic anion transporter OATP1B1 (OATP-C) in hepatic uptake of irinotecan and its active metabolite, 7-ethyl-10-hydroxycamptothecin: in vitro evidence and effect of single nucleotide polymorphisms.* Drug Metab Dispos, 2005. **33**(3): p. 434-9.

120. Oostendorp, R.L., et al., *Organic anion-transporting polypeptide 1B1 mediates transport of Gimatecan and BNP1350 and can be inhibited by several classic ATP-binding cassette (ABC) B1 and/or ABCG2 inhibitors.* Drug Metab Dispos, 2009. **37**(4): p. 917-23.

121. Yamaguchi, H., et al., *Rapid screening of antineoplastic candidates for the human organic anion transporter OATP1B3 substrates using fluorescent probes.* Cancer Lett, 2008. **260**(1-2): p. 163-9.

122. Adane, E.D., et al., *Pharmacokinetic modeling to assess factors affecting the oral bioavailability of the lactone and carboxylate forms of the lipophilic camptothecin analogue AR-67 in rats.* Pharm Res, 2012. **29**(7): p. 1722-36.

123. Houghton, P.J., et al., *Extending principles learned in model systems to clinical trials design.* Oncology (Williston Park), 1998. **12**(8 Suppl 6): p. 84-93.

124. Gerrits, C.J., et al., *Topoisomerase I inhibitors: the relevance of prolonged exposure for present clinical development.* Br J Cancer, 1997. **76**(7): p. 952-62.

125. De Cesare, M., et al., *Efficacy of the novel camptothecin gimatecan against orthotopic and metastatic human tumor xenograft models.* Clin Cancer Res, 2004. **10**(21): p. 7357-64.

126. Houghton, P.J., et al., *Therapeutic efficacy of the topoisomerase I inhibitor 7-ethyl-10-(4-[1-piperidino]-1-piperidino)-carbonyloxy-camptothecin against human tumor xenografts: lack of cross-resistance in vivo in tumors with acquired resistance to the topoisomerase I inhibitor 9-dimethylaminomethyl-10-hydroxycamptothecin.* Cancer Res, 1993. **53**(12): p. 2823-9.

127. Thompson, J., et al., *Efficacy of systemic administration of irinotecan against neuroblastoma xenografts.* Clin Cancer Res, 1997. **3**(3): p. 423-31.

128. Vassal, G., et al., *Therapeutic activity of CPT-11, a DNA-topoisomerase I inhibitor, against peripheral primitive neuroectodermal tumour and neuroblastoma xenografts.* Br J Cancer, 1996. **74**(4): p. 537-45.

129. Bauer, R.J., S. Guzy, and C. Ng, *A survey of population analysis methods and software for complex pharmacokinetic and pharmacodynamic models with examples.* AAPS J, 2007. **9**(1): p. E60-83.

130. Pillai, G.C., F. Mentre, and J.L. Steimer, *Non-linear mixed effects modeling - from methodology and software development to driving implementation in drug development science.* J Pharmacokinet Pharmacodyn, 2005. **32**(2): p. 161-83.

131. Wang, L., et al., *Stereoselective interaction of pantoprazole with ABCG2. II. In vitro flux analysis.* Drug Metab Dispos, 2012. **40**(5): p. 1024-31.

132. Daily, A., et al., *Abrogation of microcystin cytotoxicity by MAP kinase inhibitors and N-acetyl cysteine is confounded by OATPIB1 uptake activity inhibition.* Toxicon, 2010. **55**(4): p. 827-37.

133. de Bruin, M., et al., *Reversal of resistance by GF120918 in cell lines expressing the ABC half-transporter, MXR.* Cancer Lett, 1999. **146**(2): p. 117-26.

134. Evers, R., et al., *Inhibitory effect of the reversal agents V-104, GF120918 and Pluronic L61 on MDR1 Pgp-, MRP1- and MRP2-mediated transport.* Br J Cancer, 2000. **83**(3): p. 366-74.

135. Kullak-Ublick, G.A., et al., *Organic anion-transporting polypeptide B (OATP-B) and its functional comparison with three other OATPs of human liver.* Gastroenterology, 2001. **120**(2): p. 525-33.

136. Ismair, M.G., et al., *Hepatic uptake of cholecystokinin octapeptide by organic anion-transporting polypeptides OATP4 and OATP8 of rat and human liver.* Gastroenterology, 2001. **121**(5): p. 1185-90.

137. Horn, J., et al., *Validation of an HPLC method for analysis of DB-67 and its water soluble prodrug in mouse plasma.* J Chromatogr B Analyt Technol Biomed Life Sci, 2006. **844**(1): p. 15-22.

138. Sun, H. and K.S. Pang, *Permeability, transport, and metabolism of solutes in Caco-2 cell monolayers: a theoretical study.* Drug metabolism and disposition: the biological fate of chemicals, 2008. **36**(1): p. 102-23.

139. Kalvass, J.C. and G.M. Pollack, *Kinetic considerations for the quantitative assessment of efflux activity and inhibition: implications for understanding and predicting the effects of efflux inhibition.* Pharmaceutical research, 2007. **24**(2): p. 265-76.

140. Seithel, A., et al., *The influence of macrolide antibiotics on the uptake of organic anions and drugs mediated by OATP1B1 and OATP1B3.* Drug Metab Dispos, 2007. **35**(5): p. 779-86.

141. Furuta, T., et al., *Phosphorylation of histone H2AX and activation of Mre11, Rad50, and Nbs1 in response to replication-dependent DNA double-strand breaks induced by mammalian DNA topoisomerase I cleavage complexes.* J Biol Chem, 2003. **278**(22): p. 20303-12.

142. Wang, L.H., et al., *Monitoring drug-induced gammaH2AX as a pharmacodynamic biomarker in individual circulating tumor cells.* Clin Cancer Res, 2010. **16**(3): p. 1073-84.

143. Huang, X., et al., *Assessment of histone H2AX phosphorylation induced by DNA topoisomerase I and II inhibitors topotecan and mitoxantrone and by the DNA cross-linking agent cisplatin.* Cytometry A, 2004. **58**(2): p. 99-110.

144. Maliepaard, M., et al., *Overexpression of the BCRP/MXR/ABCP gene in a topotecan-selected ovarian tumor cell line.* Cancer Res, 1999. **59**(18): p. 4559-63.

145. Kawabata, S., et al., *Breast cancer resistance protein directly confers SN-38 resistance of lung cancer cells.* Biochemical and biophysical research communications, 2001. **280**(5): p. 1216-23.

146. Smith, N.F., et al., *Variants in the SLCO1B3 gene: interethnic distribution and association with paclitaxel pharmacokinetics.* Clin Pharmacol Ther, 2007. **81**(1): p. 76-82.

147. Svoboda, M., et al., *Expression of organic anion-transporting polypeptides 1B1 and 1B3 in ovarian cancer cells: relevance for paclitaxel transport.* Biomed Pharmacother, 2011. **65**(6): p. 417-26.

148. Croce, A.C., et al., *Subcellular localization of the camptothecin analogues, topotecan and gimatecan.* Biochem Pharmacol, 2004. **67**(6): p. 1035-45.

149. Gillies, R.J., et al., *MRI of the tumor microenvironment.* J Magn Reson Imaging, 2002. **16**(4): p. 430-50.

150. Cardone, R.A., V. Casavola, and S.J. Reshkin, *The role of disturbed pH dynamics and the Na+/H+ exchanger in metastasis.* Nat Rev Cancer, 2005. **5**(10): p. 786-95.

151. Breedveld, P., et al., *The effect of low pH on breast cancer resistance protein (ABCG2)-mediated transport of methotrexate, 7-hydroxymethotrexate, methotrexate diglutamate, folic acid, mitoxantrone, topotecan, and resveratrol in in vitro drug transport models.* Molecular pharmacology, 2007. **71**(1): p. 240-9.

152. Thews, O., et al., *Impact of extracellular acidity on the activity of P-glycoprotein and the cytotoxicity of chemotherapeutic drugs.* Neoplasia, 2006. **8**(2): p. 143-52.

153. Leuthold, S., et al., *Mechanisms of pH-gradient driven transport mediated by organic anion polypeptide transporters.* American journal of physiology. Cell physiology, 2009. **296**(3): p. C570-82.

154. Sparreboom, A., et al., *Diflomotecan pharmacokinetics in relation to ABCG2 421C>A genotype.* Clinical pharmacology and therapeutics, 2004. **76**(1): p. 38-44.

155. de Jong, F.A., et al., *ABCG2 pharmacogenetics: ethnic differences in allele frequency and assessment of influence on irinotecan disposition.* Clinical cancer research : an official journal of the American Association for Cancer Research, 2004. **10**(17): p. 5889-94.

156. Zhou, Q., et al., *Pharmacogenetic profiling across the irinotecan pathway in Asian patients with cancer.* British journal of clinical pharmacology, 2005. **59**(4): p. 415-24.

157. Sai, K., et al., *Haplotype analysis of ABCB1/MDR1 blocks in a Japanese population reveals genotype-dependent renal clearance of irinotecan.* Pharmacogenetics, 2003. **13**(12): p. 741-57.

158. Han, J.Y., et al., *Influence of the organic anion-transporting polypeptide 1B1 (OATP1B1) polymorphisms on irinotecan-pharmacokinetics and clinical outcome of patients with advanced non-small cell lung cancer.* Lung Cancer, 2008. **59**(1): p. 69-75.

159. Xiang, X., et al., *Pharmacogenetics of SLCO1B1 gene and the impact of *1b and *15 haplotypes on irinotecan disposition in Asian cancer patients.* Pharmacogenet Genomics, 2006. **16**(9): p. 683-91.

160. Letschert, K., D. Keppler, and J. Konig, *Mutations in the SLCO1B3 gene affecting the substrate specificity of the hepatocellular uptake transporter OATP1B3 (OATP8).* Pharmacogenetics, 2004. **14**(7): p. 441-52.

161. Hsiang, Y.H., M.G. Lihou, and L.F. Liu, *Arrest of replication forks by drug-stabilized topoisomerase I-DNA cleavable complexes as a mechanism of cell killing by camptothecin.* Cancer Res, 1989. **49**(18): p. 5077-82.

162. Gandia, D., et al., *CPT-11-induced cholinergic effects in cancer patients.* J Clin Oncol, 1993. **11**(1): p. 196-7.

163. Saliba, F., et al., *Pathophysiology and therapy of irinotecan-induced delayed-onset diarrhea in patients with advanced colorectal cancer: a prospective assessment.* J Clin Oncol, 1998. **16**(8): p. 2745-51.

164. Thompson, J., C.F. Stewart, and P.J. Houghton, *Animal models for studying the action of topoisomerase I targeted drugs.* Biochim Biophys Acta, 1998. **1400**(1-3): p. 301-19.

165. Erickson-Miller, C.L., et al., *Differential toxicity of camptothecin, topotecan and 9-aminocamptothecin to human, canine, and murine myeloid progenitors (CFU-GM) in vitro.* Cancer Chemother Pharmacol, 1997. **39**(5): p. 467-72.

166. Zamboni, W.C., et al., *Relationship between topotecan systemic exposure and tumor response in human neuroblastoma xenografts.* J Natl Cancer Inst, 1998. **90**(7): p. 505-11.

167. Eisenhauer, E.A., et al., *New response evaluation criteria in solid tumours: revised RECIST guideline (version 1.1).* Eur J Cancer, 2009. **45**(2): p. 228-47.

168. Rasheed, Z.A. and E.H. Rubin, *Mechanisms of resistance to topoisomerase I-targeting drugs.* Oncogene, 2003. **22**(47): p. 7296-304.

169. Shah, G.M., R.G. Shah, and G.G. Poirier, *Different cleavage pattern for poly(ADP-ribose) polymerase during necrosis and apoptosis in HL-60 cells.* Biochemical and biophysical research communications, 1996. **229**(3): p. 838-44.

170. Kaufmann, S.H., et al., *Specific proteolytic cleavage of poly(ADP-ribose) polymerase: an early marker of chemotherapy-induced apoptosis.* Cancer Res, 1993. **53**(17): p. 3976-85.

171. Nicholson, D.W., et al., *Identification and inhibition of the ICE/CED-3 protease necessary for mammalian apoptosis.* Nature, 1995. **376**(6535): p. 37-43.

172. Whitacre, C.M., et al., *Detection of poly(ADP-ribose) polymerase cleavage in response to treatment with topoisomerase I inhibitors: a potential surrogate end point to assess treatment effectiveness.* Clin Cancer Res, 1999. **5**(3): p. 665-72.

173. Cairns, R., I. Papandreou, and N. Denko, *Overcoming physiologic barriers to cancer treatment by molecularly targeting the tumor microenvironment.* Molecular cancer research : MCR, 2006. **4**(2): p. 61-70.

174. Mayer, L.D. and A.S. Janoff, *Optimizing combination chemotherapy by controlling drug ratios.* Molecular interventions, 2007. **7**(4): p. 216-23.

175. Fujimori, A., et al., *Mutation at the catalytic site of topoisomerase I in CEM/C2, a human leukemia cell line resistant to camptothecin.* Cancer Res, 1995. **55**(6): p. 1339-46.

176. Reckamp, K.L., et al., *A phase I trial to determine the optimal biological dose of celecoxib when combined with erlotinib in advanced non-small cell lung cancer.* Clin Cancer Res, 2006. **12**(11 Pt 1): p. 3381-8.

177. Kummar, S., et al., *Phase 0 clinical trial of the poly (ADP-ribose) polymerase inhibitor ABT-888 in patients with advanced malignancies.* J Clin Oncol, 2009. **27**(16): p. 2705-11.

178. Kummar, S., et al., *Phase I study of PARP inhibitor ABT-888 in combination with topotecan in adults with refractory solid tumors and lymphomas.* Cancer Res, 2011. **71**(17): p. 5626-34.

179. Burke, T.G., et al., *Lipid bilayer partitioning and stability of camptothecin drugs.* Biochemistry, 1993. **32**(20): p. 5352-64.

180. Vaupel, P., *Metabolic microenvironment of tumor cells: a key factor in malignant progression.* Exp Oncol, 2010. **32**(3): p. 125-7.

181. Gurney, H., *Dose calculation of anticancer drugs: a review of the current practice and introduction of an alternative.* J Clin Oncol, 1996. **14**(9): p. 2590-611.

182. de Jong, F.A., et al., *Flat-fixed dosing of irinotecan: influence on pharmacokinetic and pharmacodynamic variability.* Clin Cancer Res, 2004. **10**(12 Pt 1): p. 4068-71.

183. Freyer, G., et al., *Prognostic factors for tumour response, progression-free survival and toxicity in metastatic colorectal cancer patients given irinotecan (CPT-11) as second-line chemotherapy after 5FU failure. CPT-11 F205, F220, F221 and V222 study groups.* Br J Cancer, 2000. **83**(4): p. 431-7.

184. Rougier, P., et al., *Phase II study of irinotecan in the treatment of advanced colorectal cancer in chemotherapy-naive patients and patients pretreated with fluorouracil-based chemotherapy.* J Clin Oncol, 1997. **15**(1): p. 251-60.

185. Mathijssen, R.H., et al., *Impact of body-size measures on irinotecan clearance: alternative dosing recommendations.* J Clin Oncol, 2002. **20**(1): p. 81-7.

186. Du Bois, D. and E.F. Du Bois, *A formula to estimate the approximate surface area if height and weight be known. 1916.* Nutrition, 1989. **5**(5): p. 303-11; discussion 312-3.

187. Bonate, P.L., *Pharmacokinetic-Pharmacodynamic Modeling and Simulation*2011: Springer New York Dordrecht Heidelberg London.

188. Beal, S., Sheiner, L.B., Boeckmann, A., & Bauer, R.J., *NONMEM User's Guides (1989-2009)*2009: Icon Development Solutions, Ellicott City, MD, USA.

189. Karlsson, M.O. and L.B. Sheiner, *The importance of modeling interoccasion variability in population pharmacokinetic analyses.* J Pharmacokinet Biopharm, 1993. **21**(6): p. 735-50.

190. Cockcroft, D.W. and M.H. Gault, *Prediction of creatinine clearance from serum creatinine.* Nephron, 1976. **16**(1): p. 31-41.

191. Joerger, M., *Covariate pharmacokinetic model building in oncology and its potential clinical relevance.* AAPS J, 2012. **14**(1): p. 119-32.

192. Mandema, J.W., D. Verotta, and L.B. Sheiner, *Building population pharmacokinetic--pharmacodynamic models. I. Models for covariate effects.* J Pharmacokinet Biopharm, 1992. **20**(5): p. 511-28.

193. McCune, J.S., et al., *In vivo and in vitro induction of human cytochrome P4503A4 by dexamethasone.* Clin Pharmacol Ther, 2000. **68**(4): p. 356-66.

194. Zevin, S. and N.L. Benowitz, *Drug interactions with tobacco smoking. An update.* Clin Pharmacokinet, 1999. **36**(6): p. 425-38.

195. Brill, M.J., et al., *Impact of obesity on drug metabolism and elimination in adults and children.* Clin Pharmacokinet, 2012. **51**(5): p. 277-304.

196. Nawaratne, S., et al., *Relationships among liver and kidney volumes, lean body mass and drug clearance.* Br J Clin Pharmacol, 1998. **46**(5): p. 447-52.

197. Kratzer, W., et al., *Factors affecting liver size: a sonographic survey of 2080 subjects.* J Ultrasound Med, 2003. **22**(11): p. 1155-61.

198. Miya, T., et al., *Factors affecting the pharmacokinetics of CPT-11: the body mass index, age and sex are independent predictors of pharmacokinetic parameters of CPT-11.* Invest New Drugs, 2001. **19**(1): p. 61-7.

199. Hurley, P.J., *Red cell and plasma volumes in normal adults.* J Nucl Med, 1975. **16**(1): p. 46-52.

200. Loos, W.J., et al., *Gender-dependent pharmacokinetics of topotecan in adult patients.* Anticancer Drugs, 2000. **11**(9): p. 673-80.

201. Loos, W.J., et al., *Red blood cells: a neglected compartment in topotecan pharmacokinetic analysis.* Anticancer Drugs, 2003. **14**(3): p. 227-32.

202. Court, M.H., *Interindividual variability in hepatic drug glucuronidation: studies into the role of age, sex, enzyme inducers, and genetic polymorphism using the human liver bank as a model system.* Drug Metab Rev, 2010. **42**(1): p. 209-24.

203. Buchthal, J., et al., *Induction of cytochrome P4501A by smoking or omeprazole in comparison with UDP-glucuronosyltransferase in biopsies of human duodenal mucosa.* Eur J Clin Pharmacol, 1995. **47**(5): p. 431-5.

204. Walle, T., et al., *Selective induction of propranolol metabolism by smoking: additional effects on renal clearance of metabolites.* J Pharmacol Exp Ther, 1987. **241**(3): p. 928-33.

205. van der Bol, J.M., et al., *Cigarette smoking and irinotecan treatment: pharmacokinetic interaction and effects on neutropenia.* J Clin Oncol, 2007. **25**(19): p. 2719-26.

206. Abernethy, D.R., et al., *Obesity, sex, and acetaminophen disposition.* Clin Pharmacol Ther, 1982. **31**(6): p. 783-90.

207. Comella, P., et al., *Safety and efficacy of irinotecan plus high-dose leucovorin and intravenous bolus 5-fluorouracil for metastatic colorectal cancer: pooled analysis of two consecutive southern Italy cooperative oncology group trials.* Clin Colorectal Cancer, 2005. **5**(3): p. 203-10.

208. Huang, Y.H., et al., *Identification and functional characterization of UDP-glucuronosyltransferases UGT1A8*1, UGT1A8*2 and UGT1A8*3.* Pharmacogenetics, 2002. **12**(4): p. 287-97.

209. Cecchin, E., et al., *Predictive role of the UGT1A1, UGT1A7, and UGT1A9 genetic variants and their haplotypes on the outcome of metastatic colorectal cancer patients treated with fluorouracil, leucovorin, and irinotecan.* J Clin Oncol, 2009. **27**(15): p. 2457-65.

210. Guillemette, C., et al., *Structural heterogeneity at the UDP-glucuronosyltransferase 1 locus: functional consequences of three novel missense mutations in the human UGT1A7 gene.* Pharmacogenetics, 2000. **10**(7): p. 629-44.

211. Woillard, J.B., et al., *Risk of diarrhoea in a long-term cohort of renal transplant patients given mycophenolate mofetil: the significant role of the UGT1A8 2 variant allele.* Br J Clin Pharmacol, 2010. **69**(6): p. 675-83.

212. Johnson, L.A., et al., *Pharmacogenetic effect of the UGT polymorphisms on mycophenolate is modified by calcineurin inhibitors.* Eur J Clin Pharmacol, 2008. **64**(11): p. 1047-56.

213. Vlaming, M.L., et al., *Carcinogen and anticancer drug transport by Mrp2 in vivo: studies using Mrp2 (Abcc2) knockout mice.* J Pharmacol Exp Ther, 2006. **318**(1): p. 319-27.

214. Grossman, S.A., et al., *Phase I and pharmacokinetic study of karenitecin in patients with recurrent malignant gliomas.* Neuro Oncol, 2008. **10**(4): p. 608-16.

215. Gil, M.J., et al., *Bevacizumab plus irinotecan in recurrent malignant glioma shows high overall survival in a multicenter retrospective pooled series of the Spanish Neuro-Oncology Research Group (GEINO).* Anticancer Drugs, 2012. **23**(6): p. 659-65.

216. Santisteban, M., et al., *Phase II trial of two different irinotecan schedules with pharmacokinetic analysis in patients with recurrent glioma: North Central Cancer Treatment Group results.* J Neurooncol, 2009. **92**(2): p. 165-75.

217. Kiang, T.K., M.H. Ensom, and T.K. Chang, *UDP-glucuronosyltransferases and clinical drug-drug interactions.* Pharmacol Ther, 2005. **106**(1): p. 97-132.

218. Friedman, H.S., et al., *Irinotecan therapy in adults with recurrent or progressive malignant glioma.* J Clin Oncol, 1999. **17**(5): p. 1516-25.

219. Giovanella, B.C., et al., *Dependence of anticancer activity of camptothecins on maintaining their lactone function.* Ann N Y Acad Sci, 2000. **922**: p. 27-35.

220. Oguma, T., *Antitumor drugs possessing topoisomerase I inhibition: applicable separation methods.* J Chromatogr B Biomed Sci Appl, 2001. **764**(1-2): p. 49-58.

221. Li, Q.Y., et al., *Review camptothecin: current perspectives.* Curr Med Chem, 2006. **13**(17): p. 2021-39.

222. Mi, Z. and T.G. Burke, *Differential interactions of camptothecin lactone and carboxylate forms with human blood components.* Biochemistry, 1994. **33**(34): p. 10325-36.

223. Burke, T.G. and Z. Mi, *The structural basis of camptothecin interactions with human serum albumin: impact on drug stability.* J Med Chem, 1994. **37**(1): p. 40-6.

224. Rothenberg, M.L., et al., *Alternative dosing schedules for irinotecan.* Oncology (Williston Park), 1998. **12**(8 Suppl 6): p. 68-71.

225. Crews, K.R., et al., *Altered irinotecan pharmacokinetics in pediatric high-grade glioma patients receiving enzyme-inducing anticonvulsant therapy.* Clin Cancer Res, 2002. **8**(7): p. 2202-9.

226. van Riel, J.M., et al., *Continuous administration of irinotecan by hepatic arterial infusion: a phase I and pharmacokinetic study.* Clin Cancer Res, 2002. **8**(2): p. 405-12.

227. Bom, D., et al., *Novel A,B,E-ring-modified camptothecins displaying high lipophilicity and markedly improved human blood stabilities.* J Med Chem, 1999. **42**(16): p. 3018-22.

228. Keir, S.T., et al., *Therapeutic activity of 7-[(2-trimethylsilyl)ethyl)]-20 (S)-camptothecin against central nervous system tumor-derived xenografts in athymic mice.* Cancer Chemother Pharmacol, 2001. **48**(1): p. 83-7.

229. Sessa, C., et al., *Concerted escalation of dose and dosing duration in a phase I study of the oral camptothecin gimatecan (ST1481) in patients with advanced solid tumors.* Ann Oncol, 2007. **18**(3): p. 561-8.

230. (FDA), U.S.D.o.H.a.H.S.F.a.D.A. 2001 June 1, 2007]; Guidance for Industry: Bioanalytical Method Validation]. Available from: http://www.fda.gov/cder/guidance/4252fnl.htm

231. de Jong, F.A., et al., *Determination of irinotecan (CPT-11) and SN-38 in human whole blood and red blood cells by liquid chromatography with fluorescence detection.* J Chromatogr B Analyt Technol Biomed Life Sci, 2003. **795**(2): p. 383-8.

232. Hubbard, K.E., et al., *Application of a highly specific and sensitive fluorescent HPLC method for topotecan lactone in whole blood.* Biomed Chromatogr, 2009. **23**(7): p. 707-13.

233. Loos, W.J., et al., *Role of erythrocytes and serum proteins in the kinetic profile of total 9-amino-20(S)-camptothecin in humans.* Anticancer Drugs, 1999. **10**(8): p. 705-10.

234. Peck, C.C., et al., *Opportunities for integration of pharmacokinetics, pharmacodynamics, and toxicokinetics in rational drug development.* Pharm Res, 1992. **9**(6): p. 826-33.

235. Hsiang, Y.H. and L.F. Liu, *Identification of mammalian DNA topoisomerase I as an intracellular target of the anticancer drug camptothecin.* Cancer Res, 1988. **48**(7): p. 1722-6.

236. Ziomkowska, B., M. Cyrankiewicz, and S. Kruszewski, *Determination of hydroxycamptothecin affinities to albumin and membranes by steady-state fluorescence anisotropy measurements.* Comb Chem High Throughput Screen, 2007. **10**(6): p. 486-92.

237. Basili, S. and S. Moro, *Novel camptothecin derivatives as topoisomerase I inhibitors.* Expert Opin Ther Pat, 2009. **19**(5): p. 555-74.

238. Du, W., et al., *Semisynthesis of DB-67 and other silatecans from camptothecin by thiol-promoted addition of silyl radicals.* Bioorg Med Chem, 2003. **11**(3): p. 451-8.

239. Rowinsky, E.K. and R.C. Donehower, *Paclitaxel (taxol).* N Engl J Med, 1995. **332**(15): p. 1004-14.

240. Therasse, P., et al., *New guidelines to evaluate the response to treatment in solid tumors. European Organization for Research and Treatment of Cancer, National Cancer Institute of the United States, National Cancer Institute of Canada.* J Natl Cancer Inst, 2000. **92**(3): p. 205-16.

241.   Zhu, A.X., et al., *Phase I and pharmacokinetic study of gimatecan given orally once a week for 3 of 4 weeks in patients with advanced solid tumors.* Clin Cancer Res, 2009. **15**(1): p. 374-81.

242.   Milewska, M., Monks, N., Moscow, J.A., Arnold, S.M., Leggas, M., *Metabolism and transport pathways of the blood stable camptothecin AR-67 (7-t-butyldimethylsilyl-10-hydroxycamptothecin). , in *American Society of Clinical Oncology*2009: Orlando, FL.

243.   Strassburg, C.P., M.P. Manns, and R.H. Tukey, *Expression of the UDP-glucuronosyltransferase 1A locus in human colon. Identification and characterization of the novel extrahepatic UGT1A8.* J Biol Chem, 1998. **273**(15): p. 8719-26.

244.   Miller, A.A., et al., *Phase II trial of karenitecin in patients with relapsed or refractory non-small cell lung cancer (CALGB 30004).* Lung Cancer, 2005. **48**(3): p. 399-407.

245.   Thompson, P.A., et al., *Plasma and cerebrospinal fluid pharmacokinetic study of BNP1350 in nonhuman primates.* Cancer Chemother Pharmacol, 2004. **53**(6): p. 527-32.

246.   Sparreboom, A., et al., *Nonlinear pharmacokinetics of paclitaxel in mice results from the pharmaceutical vehicle Cremophor EL.* Cancer Res, 1996. **56**(9): p. 2112-5.

VITA

Eleftheria Tsakalozou

Place of birth: Astakos, Aitoloakarnania, Greece

Education:

2003-2006 – MSc in Clinical Pharmacy, Department of Pharmaceutical Technology, Biopharmaceutics and Pharmacokinetics, Faculty of Pharmacy, University of Athens, Greece

1998-2003 – BS in Pharmacy, Department of Pharmaceutical Technology, Biopharmaceutics and Pharmacokinetics, Faculty of Pharmacy, University of Athens, Greece

Professional Experience:

Pharmacist intern - UKHealthCare-Kentucky Clinic Pharmacy, 740 S. Limestone, Lexington, 40536-0284, Kentucky (January 2013 - present)

Teaching assistant - Patient Care Lab and Advanced Pharmacotherapy, College of Pharmacy, University of Kentucky, 789 S. Limestone, Lexington 40536, Kentucky (August 2007 - June 2011)

Pharmacist - Pharmacy, Riga Feraiou 110-112, Patras, Greece (July 2006 – July 2007)

Teaching assistant - Laboratory of Pharmaceutical Technology and Quality Control of Pharmaceutical Products - School of Pharmacy, University of Athens, Zografou Panepistimiopolis, Athens, Greece (February 2005 – April 2005)

Pharmacist intern - Pharmacy, Riga Feraiou 110-112, Patras, Greece (June 2002 – February 2003)

Pharmacist intern - Evangellismos General Hospital of Athens, Ypsilantou 45-47, Athens, Greece (February 2003 – June 2003)

Publications:

Fassoulaki, A. Paraskeva, G. Kostopanagiotou, E. Tsakalozou, S. Markantonis. "Acupressure on the Extra 1 Acupoint: Effect on BIS, Serum Melatonin, Plasma Beta-Endorphin and Stress", Anesthesia Analgesia, 2007;104 (2):312-317.

SL. Markantonis, E. Tsakalozou, A. Paraskeva, C. Staikou, A. Fassoulaki. Melatonin pharmacokinetics in premenopausal and postmenopausal healthy female volunteers. Journal of Clinical Pharmacology, 2008;48(2):240-245.

S.M. Arnold, J.J. Rinehart, E. Tsakalozou, J.R. Eckardt, S.Z. Fields, B.J. Shelton, P.A. DeSimone, B.K. Kee, J.A. Moscow, M. Leggas. A phase 1 Study of 7-t-butyldimethylsilyl-10-hydroxycamptothecin (AR-67) in Adult Patients with Refractory or Metastatic Solid Malignancies. Clinical Cancer Research 2010 Jan 15;16(2):673-80.

E. Tsakalozou, J. Horn, M. Leggas. A High-Performance Liquid Chromatography Method for Determination of AR-67 Carboxylate and Lactone in Human Whole Blood. Biomedical Chromatography 2010 Oct 24(10):1045-51.

M. Eckman, E. Tsakalozou, N. Y. Kang, A. Ponta, and Y. Bae. Effects of Drug Release Patterns of PEG-poly(aspartate) Block Copolymer Micelles on Cytotoxicity and Intracellular Drug Uptake in Cancer Cells. Pharm Res. 2012 Jul;29(7):1755-67.

E. Tsakalozou, A. M. Eckman, and Y. Bae. Combination Effects of Docetaxel and Doxorubicin in Hormone-Refractory Prostate Cancer Cells. Biochem Res Int. 2012;2012:832059.

E. Tsakalozou, E. D. Adane, K. Kuo, A. Daily, J. A. Moscow and M. Leggas. The effect of BCRP and OATP1B3 on the antitumor efficacy of the lipophilic camptothecin AR-67 *in vitro.* Drug Metab Dispos. 2013 Apri 25. Epub ahead of print.

Posters:

M. Leggas, J. Horn, E. Tsakalozou, J. Moscow, S. Z. Fields, J. R. Eckardt, P. DeSimone, B. K. Kee, J. J. Rinehart, S. M. Arnold. Clinical and pharmacokinetic (PK) findings in a phase I study of 7-t-butyldimethylsilyl-10-hydroxycamptothecin (AR-67) in patients with refractory solid tumors. ASCO, May 2009, Orlando FL.

E. Tsakalozou, A. Ponta, M. Leggas, Y. Bae. Heat Shock Protein 90 Mediated Chemotherapeutic Synergy in Prostate Cancer. Markey Cancer Center Research Day, April 2010, Lexington, KY.

E. Tsakalozou, K-L Kuo, E. D. Adane, A. Daily, J. A. Moscow and M. Leggas. The effect of efflux and uptake transporters on the in-vitro efficacy of the lipophilic camptothecin analogue AR-67. Markey Cancer Center Research Day, March 2011, Lexington KY.

E. Tsakalozou, D. S. Howard, M. Leggas. In vitro and ex vivo anti-leukemia activity of AR-67, a novel lipophilic and blood stable camptothecin analogue. AACR, April 2011, Orlando FL.

E. Tsakalozou, S. Arnold, M. Leggas. Population pharmacokinetic analysis of the lipophilic camptothecin analogue AR-67 in Phase I oncology patients. ACoP 2013, Fort Lauderdale, FL

Eleftheria Tsakalozou

Student's Signature

5/10/13

Date